Alkylation of Asphaltenes

by

Xiaohui Mao

A thesis submitted in partial fulfillment of the requirements for the degree of

Master of Science
in
Chemical Engineering

Department of Chemical and Materials Engineering
University of Alberta

Abstract

This work investigated different acid catalysts and olefinic alkylating agents for the alkylation of an industrial asphaltenes feed. The working hypothesis was that alkylation would change the solubility parameter and increase the H/C ratio of asphaltenes sufficiently to cause some asphaltenes to maltenes conversion.

The acid catalysts that were investigated were phosphoric acid, aluminium chloride, hydrochloric acid and amorphous silica alumina (Siral40). The olefins employed for alkylation were ethylene, propylene and hexene. These model olefins were used for experimental convenience; industrial applications would typically employ olefins in cracked naphtha. The products from reaction were characterized by determining the n-pentane precipitated asphaltenes content, H/C ratio, aliphatic/aromatic hydrogen ratio, micro-carbon residue and infrared spectroscopy.

The most successful combination of catalyst and olefin for alkylating asphaltenes was the amorphous silica-alumina catalyst (Siral40) and propylene. Propylene reacted with asphaltenes over Siral40 to generate an increase in maltenes content. It was postulated that success of alkylation of asphaltenes by propylene over Siral40 could be attributed to the ability to cause scission of bridging carbon-sulfur bonds. This was further investigated by model compound reactions. It was found that Siral40 in combination with propylene resulted in complete conversion of dibenzyl sulfide and benzyl phenyl sulfide, as well as near complete desulfurization of the reaction products from dibenzyl sulfide. It was also determined that 40 % of the sulfur of the industrial asphaltenes feed was aliphatic sulfur, of which at least some would be present in bridging sulfide (thioether) groups.

Conversion of asphaltenes with propylene over Siral40 at 325 °C resulted in ~20% asphaltenes into maltenes conversion.

Acknowledgement

First of all, I would like to express my sincere gratitude to my supervisor Dr. Arno De Klerk for all guidance and support. It was your patience, trust, encouragement and remarkable direction that lead me to overcome challenges in MSc study. You made me to think more and deeper about not only master study but also life and career in the view of philosophy. I will always be grateful and keep your valuable advice.

Secondly, I would like to thank Dr. Shaofeng Yang, Dr. Cibele Melo Halmenschlager and Dr. Glaucia Carvalho Do Prado for all the help and suggestions. I'd also like to thank all my colleagues especially Ms. Natalia Montoya Sanchez and Mr. Ivor Martin Do Prado for all encouragement, useful communications and sharing of lab experiences.

Thirdly, I'd like to thank my family for unconditional love and support during my research life in Canada. And thanks to all my friends.

Last but not least, I'd like to thank my boyfriend Weida for your love and support, being always with me, taking care of me and making me feel at home.

Table of Contents

List of Tables

List of Figures

1. Introduction

1.1 Background

In the past decades, the rate of discovery of high quality petroleum resources has lagged behind the rate of world consumption. As a result, the less desirable bitumen and heavy oil resources have become important resources.[1] Crude oil is classified based on its gravity, which is known as API (American Petroleum Institute) gravity. The API gravity for crude oil is an inverse density scale, with a gravity of 10 corresponding to a density of 1000 kg/m^3.

In Canada, the Cold Lake, Athabasca and Peace River deposits are grouped together as oil sands bitumens, all having a density of less than 10 °API, or more than 1000 kg/m^3.[1] Though it costs more to upgrade oil sands bitumen than conventional lighter crude oils, the bitumen is abundant. Canadian production is about 0.41 m^3/s and studying oil sands bitumen upgrading is therefore a topic of economic relevance.

Crude oil composition is often expressed in terms of four parts saturates, aromatics, resins and asphaltenes (SARA). This work investigates the upgrading of the asphaltenes fraction, which is a fraction with limited applications.

The asphaltenes are defined as a solubility class; it is soluble in aromatic solvents such as toluene but insoluble in light paraffins, such as n-pentane or n-heptane. The saturates, aromatics and resins are collectively referred to as maltenes. The asphaltenes fraction is the fraction that contains the higher molecular weight and more polar and aromatic molecules.[2] As depicted in **Figure 1-1**,[3] solubility is correlated with both the molecular weight and the hydrogen content.

The exact structure of asphaltenes is uncertain. Currently, two models, islands and archipelago, have been proposed.[4] The discussion of these two models have been ongoing for many years, but a confident conclusion is yet to be made.[5] The structure in **Figure 1-2** represents possible groups and interactions in asphaltenes, such as heteroatom containing functional groups, aromatic rings and intermolecular forces. The molar mass distribution of asphaltenes is estimated at 400-2000 g/mol.[6]
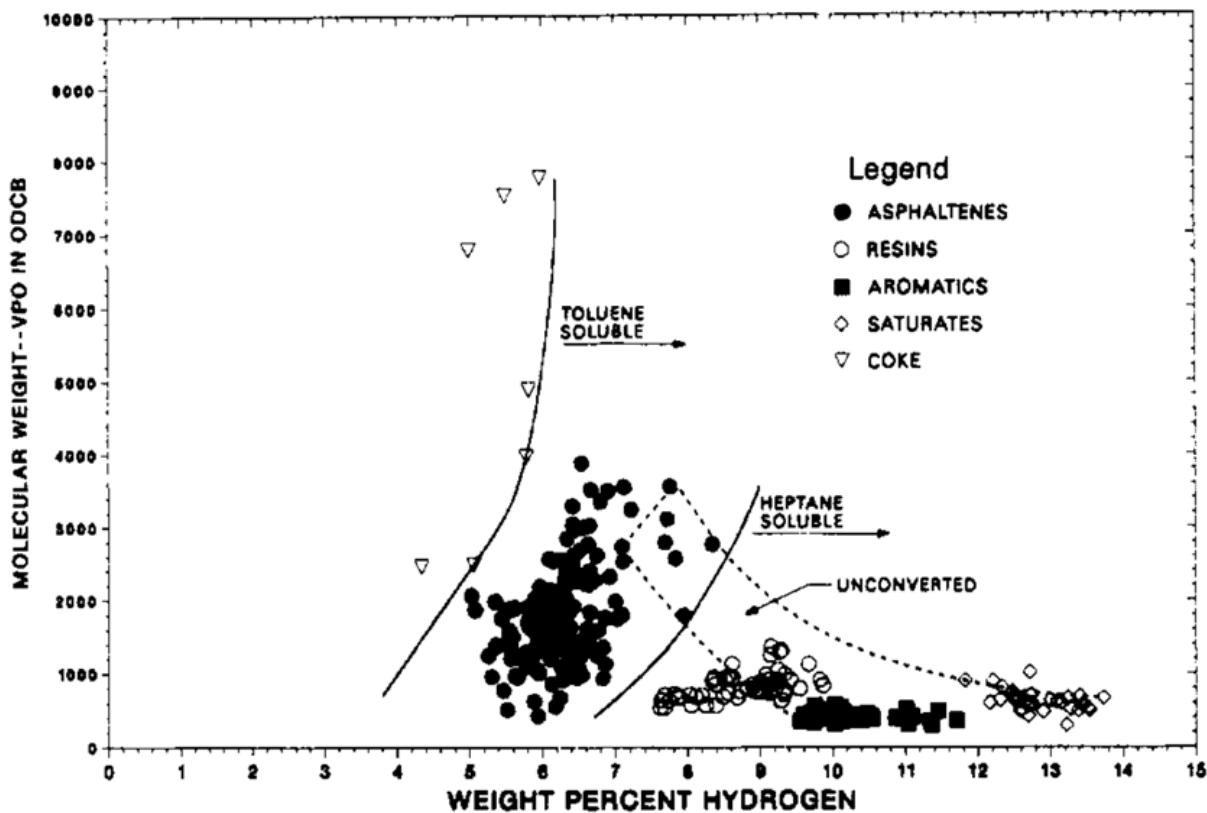
Figure 1-1. Solubility class of asphaltenes (from Wiehe, I. A. et al)
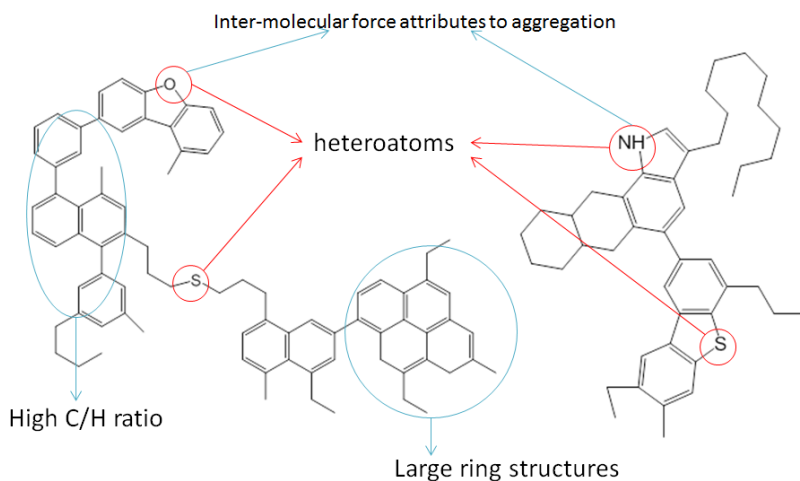
Figure 1-2. Possible groups and intermolecular forces in asphaltenes.

Many industrial problems such as wellbore or pipeline plugging, formation of stable water-in-oil emulsions, alteration of wettability of solids, and sedimentation during crude blending are all

attributed, at least partly, to molecular aggregation of asphaltenes upon exposure to an unfavorable liquid environment or to an oil/water interface or hydrophilic surfaces.[7] These problems associated with asphaltenes provide additional justification for the present study.

To make asphaltenes become less problematic and turn it into a higher value product, the solubility characteristics of the molecules in the asphaltenes fraction must be changed. One of the main contributors to the solubility behavior asphaltenes is its low hydrogen content (**Figure 1-1**). Although the contribution of molecular weight is also important, the present study focuses only on manipulating the hydrogen content, or H/C ratio, as means of changing solubility.

Different methods to increase the H/C ratio of asphaltenes are practised, such as hydrotreating to increase hydrogen content, or coking to decrease carbon content. In this thesis the alkylation of asphaltenes is investigated as potential strategy to increase the H/C ratio.

The hypothesis is that by alkylating asphaltenes with olefins that are more hydrogen-rich than the asphaltenes, the overall H/C ratio of the asphaltenes is increased. This comes at the expense of only a minor increase in molecular weight, so that at least some of the molecules in the asphaltenes fraction may have increased solubility in paraffinic solvents, i.e. they are no longer asphaltenes, but maltenes. Alkylation of asphaltenes with light olefins, typically from streams like cracked naphtha, may makes the conversion from asphaltenes to maltenes possible. A few catalysts and different olefinic alkylating agents have been selected to perform alkylation of asphaltenes. The mechanisms are explained in Chapter 2 and the experimental investigation is presented in Chapters 3 to 9.

1.2 Objectives
Evaluate different catalysts and alkylating agents for the alkylation of asphaltenes and conditions appropriate for each catalyst and determine the outcome in terms of asphaltenes to maltenes conversion. Specific sub-objectives were:

- Verify whether the alkylating agent reacted with the asphaltenes or not.
- Determine the extent of asphaltenes to maltenes conversion.
- Evaluate changes in the characteristics of the reaction products.
- When possible explain the observations.

1.3 Scope of work

Most of the work focused on alkylation reactions and was of an applied nature. The alkylation study is reported with the following topics being covered:

Chapter 2: Literature review of topics relevant to this study.

Chapter 3: Phosphoric acid (H_3PO_4) catalyzed alkylation of asphaltenes with hexene.

Chapter 4: Aluminium chloride ($AlCl_3$) and hydrochloric acid (HCl) catalyzed alkylation of asphaltenes with hexene.

Chapter 5: Amorphous silica alumina catalyzed alkylation of asphaltenes with ethylene.

Chapter 6: Amorphous silica alumina catalyzed alkylation of asphaltenes with propylene.

Chapter 7: Amorphous silica alumina catalyzed alkylation of model compounds to elucidate the observations with asphaltenes.

Chapter 8: Ligand formation as an alternative to Friedel–Crafts alkylation to target heteroatom functionality.

Chapter 9: Quantification of different sulfur species in support of observations made during the alkylation study in Chapters 6 and further probed with model compounds in Chapter 7.

Chapter 10: Final conclusions

Reference

1.   Gray, M. R., *Upgrading oilsands bitumen and heavy oil*. First ed.; The University of Alberta Press Ring House 2: 2015.

2.   Sirota, E. B.; Lin, M. Y., Physical behavior of asphaltenes. *Energy & Fuels* **2007,** *21* (5), 2809-2815.

3.   Wiehe, I. A., A Solvent Resid Phase-Diagram for Tracking Resid Conversion. *Ind Eng Chem Res* **1992,** *31* (2), 530-536.

4.   Alvarez-Ramirez, F.; Ruiz-Morales, Y., Island versus Archipelago Architecture for Asphaltenes: Polycyclic Aromatic Hydrocarbon Dimer Theoretical Studies. *Energy & Fuels* **2013,** *27* (4), 1791-1808.

5.   Sabbah, H.; Morrow, A. L.; Pomerantz, A. E.; Zare, R. N., Evidence for Island Structures as the Dominant Architecture of Asphaltenes. *Energy & Fuels* **2011,** *25* (4), 1597-1604.

6.   de Klerk, A.; Gray, M. R.; Zerpa, N., Chapter 5 - Unconventional Oil and Gas: Oilsands. In *Future Energy (Second Edition)*, Letcher, T. M., Ed. Elsevier: Boston, 2014; pp 95-116.

7.   Wang, S. Q.; Liu, J. J.; Zhang, L. Y.; Masliyah, J.; Xu, Z. H., Interaction Forces between Asphaltene Surfaces in Organic Solvents. *Langmuir* **2010,** *26* (1), 183-190.

2 Literature Review

2.1 Introduction

Asphaltenes and cracked naphtha are important components of crude oil and crude oil upgrading. It may seem that these two materials have little in common, except for their relationship to crude oil, but there is a potential synergy that was of interest in this work. Cracked naphtha is a source of olefins that can be used for alkylation. Asphaltenes can potentially be upgraded by alkylation with olefins in a way so that at least part of the asphaltenes becomes more soluble in a paraffin rich matrix.

The compositions and characteristics of asphaltenes and cracked naphtha were studied. Based on the properties of asphaltenes and cracked naphtha, a few catalysts have been identified and discussed as potential catalysts for alkylation of asphaltenes with the olefins in cracked naphtha. The types of alkylation and mechanisms involved are also included.

2.2 Feed materials of interest in this study

2.2.1 Asphaltene

Bitumen can be separated into four parts: saturates, aromatics, resins and asphaltenes (SARA). Asphaltenes are usually the heaviest part of crude oil and are defined as a solubility class of materials that are insoluble in paraffins (usually *n*-pentane or *n*-heptane) but soluble in aromatic solvents such as toluene. Asphaltenes consist of carbon, hydrogen, nitrogen, oxygen, sulphur, as well as trace amounts of vanadium and nickel. The H: C ratio of asphaltenes is approximately (1.1-1.2), depending on the asphaltenes source and the solvent used for precipitation.[1] The compositions of C_7-precipitated asphaltenes from different sources are shown in **Table 2-1**.[2] Heteroatoms such as S, N and O could form intermolecular forces and accelerate asphaltenes aggregation.

The existing forms of S and N in C_7 precipitated asphaltenes are shown in **Table 2-2** and **Table 2-3** respectively.[2] Oxygen has been identified as present in carboxylic acid, phenol, ketone and alcohol functional groups in asphaltenes.

The molar mass of asphaltenes is difficult to determine due to their strong tendency to self-aggregate, but current understanding has determined a distribution in the range of (400 to 2000) g/mol.[1]

Table 2-1. Elemental composition of C_7-asphaltenes

C_7-Asphaltene	Element (wt%)					Metal (ppm)	
	C	H	S	N	O	Ni	V
Campana	87.6	8.2	0.5	1.5	2.2	54	81
Heavy Canadian(Cold Lake)	84.7	7.9	4.5	1.2	1.6	320	697
Lloydminster-Wainwright	80.0	8.0	7.9	1.3	2.7	417	1100
Maya	82.3	7.9	6.6	1.2	1.8	724	1468
Mid-continent US	84.9	8.6	3.8	1.0	1.6	188	309
San Joaquin Valley	84.5	8.3	2.3	2.6	2.3	594	540

Table 2-2. Sulfur functions in C_7-asphaltene

C_7-asphaltene	Total S (wt%)	Aliphatic sulfide S Mol% of total S	Thiophene S Mol% of total S
Campana	0.5	31	69
Heavy Canadian (Cold Lake)	4.5	30	70
Lloydminster-Wainwright	7.9	29	71
Maya	6.6	32	68
Mid-continent US	3.8	16	84
San Joaquin Valley	2.3	37	63

Table 2-3. Nitrogen functions in C_7-asphaltene

C_7-asphaltene	N Wt %	Nitrogen species, mol% of total nitrogen		
		Pyridinic	Free pyrrole	Metal-associated pyrrole
Campana	1.53	28	71	1
Mid-continent US	0.99	28	67	5
San Joaquin Valley	2.56	28	67	5
Lloydminster-Wainwright	1.31	29	59	12
Maya	1.25	24	52	18
Heavy Canadian (Cold Lake)	1.19	26	65	9

2.2.2 Cracked Naphtha

Naphtha is defined by distillation range and it is typically a mixture of C_5 to C_{10} hydrocarbons from the <175 °C distillation fraction of crude oil. Cracked naphtha is the same distillation range product obtained from thermal or catalytic cracking and also contains olefinic hydrocarbons. Such naphtha is typically produced by fluid catalytic cracking, visbreaking and coking processes.

Melpolder et al.[3] studied of the composition of naphtha produced from fluid catalytic cracking. The sample analyzed was the total naphtha from a fluid catalytic cracking unit operating at 480 °C (900°F) on synthetic silica-alumina catalyst and a gas-oil charge stock from a mixed crude source. The compound class analysis of the cracked naphtha is given in Table 4. The non-hydrocarbon compounds present were minor, about 0.002 wt% phenolic compounds and 0.18 wt% sulfur.[3]

Table 2-4. Summary analysis of cracked naphtha.[3]

Hydrocarbon Type	C$_4$ and Lighter	C$_5$	C$_6$	C$_7$	C$_8$	C$_9$ and Heavier	Total
Paraffin	2.26	6.69	4.15	2.31	1.75	7.53	24.69
Monocycloparaffin	..	0.14	1.08	1.25	1.11	5.55	9.13
Dicycloparaffin	..	...	...	...	...	0.85	0.85
Olefin[a]	3.95	10.92	8.48	4.59	2.31	4.75	35.00
Cycloölefin	..	0.40	0.77	2.27	0.87	1.94[a]	6.25
Dicycloölefin	..	...	...	...	...	0.09	0.09
Monocyclic alkyl aromatic	..	...	0.21	2.32	5.41	12.57	20.51
Monocyclic alkenyl aromatic and/or cycloparaffin-aromatic	..	...	...	...	...	2.18	2.18
Dicyclic aromatic	..	...	...	...	...	1.30	1.30
Total	6.21	18.15	14.69	12.74	11.45	36.76	100.00

[a] Includes diolefins and acetylenes.

From the data above it can be seen that the main components in cracked naphtha are olefins, paraffins and monocyclic aromatics. Compared with asphaltenes, the aromatic and heteroatom content in naphtha is much less.

2.3 Catalyst and olefins

Asphaltenes and naphtha contain aromatic rings, hetero-aromatics, hydrocarbons and hetero atoms. To alkylate asphaltenes with naphtha, the catalysts enable such reactions have to be found. In the following four parts, the detailed alkylation reactions with specific catalyst are described.

2.3.1 Phosphoric acid

Phosphoric acid can be used as catalyst for reaction between aromatic rings and olefins. Ipatieff and Pines conducted two reactions with phosphoric acid as catalyst (1) alkylation of benzene, naphthalene and tetrahydronaphthalene with ethylene at 300 °C and (2) the alkylation of naphthalene and fluorine with propene at 200 °C under pressure (from maximum 13 MPa to 2.7 MPa).[4] They found that 85% to 89% ortho-phosphoric acid can be used as a catalyst for the direct alkylation of aromatic hydrocarbons, as depicted in **Figure 2-1**. In this kind of reactions, olefins are used as alkylating agent. However, in the presence of phosphoric acid, the polymerization of olefins could also happen. Ipatieff had suggested the mechanism of olefin polymerization,[5] as depicted in **Figure 2-2**.
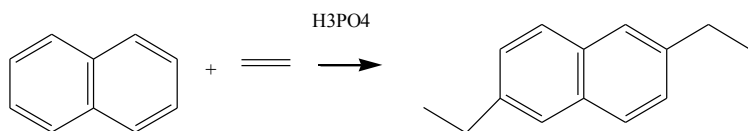
Figure 2-1. Phosphoric acid catalyzed aromatic hydrocarbons alkylation
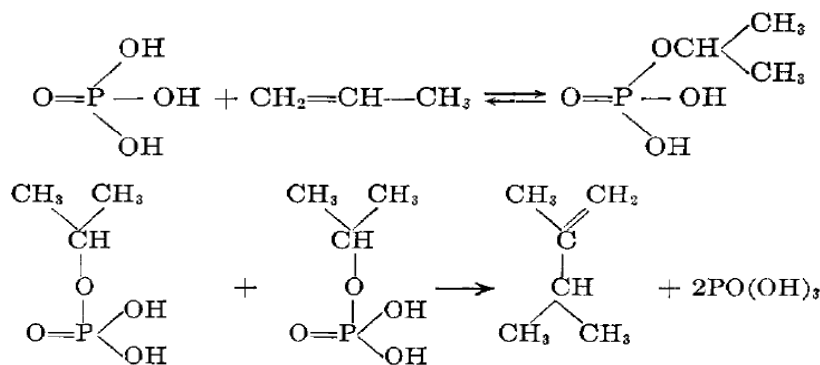
Figure 2-2 olefins polymerization mechanism (from Ipatieff)

Besides aromatics such as benzene and naphthalene, phosphoric acid could catalyze reactions with phenols, thiols and alcohols. Ipatieff and Pines have suggested that phosphoric acid is a catalyst for the alkylation of phenol with olefins including ethylene. The reaction was at 200 °C and yield o-and p-ethylphenol, diethylphenol and higher ethylated phenols, phenetole, o- and p-ethylphenetole, and higher ethylated phenetoles. Ipatieff and Pines also found that propene could react with phenetole in the presence of phosphoric acid and yield nuclear alkylated products.[6] The alkylating agent for phenol could be rings as well as olefins. P-2-Cyclopentenylphenol was identified by Bader[7] as the major product of the condensation of cycopentadiene in the presence of phosphoric acid at room temperature,[7] as shown in **Figure 2-3**.
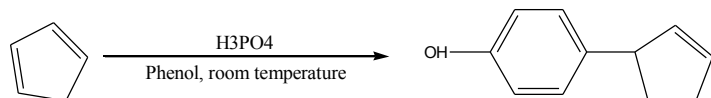
Figure 2-3. alkylation of phenol with cyclopentadiene[7]

Ipatieff and Pines have performed an experiment with 0.2 mol of thiophenol, 0.15 to 0.2 mole of olefin and 0.2 mol of 90% phosphoric acid in a reactor with glass liner. The upper layer of product was consisted of alkyl phenyl sulfide.[8] 85% phosphoric acid was found to catalyze the

reaction between thiophene and olefinic hydrocarbons containing a double bond on a completely substituted carbon atom, such as trimenthylethylene at 70 to 80 °C.[9]

Hart[10] showed the alkylation of alcohol in presence of phosphoric acid as catalyst. Hart found t-butyl alcohol alkylates m-cresol in the position ortho to the hydroxyl and para to the methyl group as shown in **Figure 2-4**.
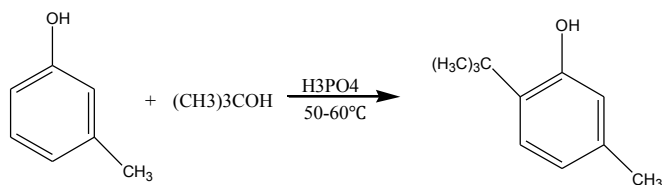
Figure 2-4. Alcohol alkylates phenol[10]

Ipatieff, Komarewsky and Pines found the destructive alkylation of hydrocarbons with phosphoric acid as catalyst. "Destructive alkylation" means under action of a catalyst the hydrocarbons might undergo decomposition and the fragments combine with each other or some other hydrocarbon present, which give rise to the formation of higher boiling alkylated hydrocarbons. The following two reactions were examples for "destructive alkylation" when phosphoric acid was employed as catalyst.[11]

$$(CH_3)_3CCH_2CH(CH_3)_2 + C_6H_6 \xrightarrow{H_3PO_4} (CH_3)_3CH + C_6H_5C(CH_3)_3 \qquad (1)$$

$$2n-C_6H_{14} + 2C_6H_6 \xrightarrow{H_3PO_4} C_8H_8 + C_2H_6 + C_6H_5C_4H_9 + C_6H_5CH(CH_3)_2 \qquad (2)$$
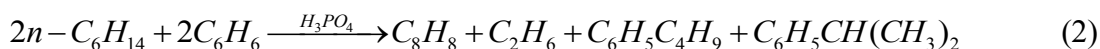
There is consequently ample literature that shows that phosphoric acid can catalyze alkylation reactions targeted at olefins, aromatics, thiols and alcohols. The mechanism in Figure 3 describes how phosphoric acid works as a catalyst. It first attacks the reactant and then a hydrogen on the aromatic is replaced by the reactant as alkylating group. If the second step didn't take place, phosphoric acid would remain connected with the reactant and stay as the intermediate products, the phosphoric acid ester. This kind of situation will be explained in Chapter 3.

2.3.2 Aluminum chloride

Aluminum chloride is a typical active catalyst for Friedel-Crafts alkylation. Under appropriate conditions it can catalyze the alkylation reaction of paraffins and olefins with aromatics.

Ipatieff and Grosse[12] performed reactions of aluminum chloride with paraffins like *n*-butane, *n*-hexane, *n*-heptane and 2,2,4-trimethypentane. It was found that aluminum chloride acts on all these paraffins. However, the presence of hydrogen chloride is necessary for the reaction, and it can be added either directly or indirectly, for instance, through the addition of water. If every trace of hydrogen chloride and water is eliminated, aluminum chloride does not react to any material extent with the hydrocarbons unless the temperature is raised sufficiently high (about 150 to 200 °C). Ipatieff and Grosse[12] also described the mechanism of paraffins alkylation. First, the carbon-carbon bond is broken in the presence of aluminum chloride and hydrogen chloride to form a lower molecular weight paraffin and olefin, i.e. acid catalyzed cracking. Secondly, paraffin and olefins can be added together to form higher molecule weight paraffins. Isomerization of the original paraffin is also possible. This is stated in **Equation 2.3** to **2.6** and **Equation 2.7** embraces the general reaction.[12] Although this was pioneering work at that time, today this is recognized as typical of acid catalyzed reactions where the acid catalyst is strong enough to create a carbonium ion on a paraffin.

$$C_nH_{2n+2} \rightarrow C_{n-x}H_{2(n-x)+2} + C_xH_{2x} \qquad 2.3$$

$$C_nH_{2n+2} + C_xH_{2x} \rightarrow C_{n+x}H_{2(n+x)+2} \qquad 2.4$$

$$CH_3CH_2CH_2CH_2CH_2CH_3 \rightarrow CH_3CH_2CH_2CH_3 + CH_2CH_2 \qquad 2.5$$

2.6

$$zC_nH_{2n+2} \rightarrow aC_{x_1}H_{2x_1+2} + bC_{x_2}H_{2x_2+2} + cC_{x_3}H_{2x_3+2} + ...$$
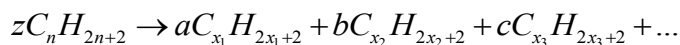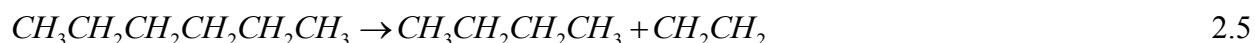
where $zn = ax_1 + bx_2 + cx_3 + ...$ \qquad 2.7

This mechanism is similar to the alkylation of paraffins with olefins. Ipatieff et al.[13] found that both normal and branched paraffins can be alkylated in the presence of aluminum chloride, except methane and ethane. The alkylation of hexane with ethylene and iso-butane with ethylene were discovered. In hexane with ethylene at atmospheric pressure, 75% of the hexane was transformed. In hexane with ethylene under pressure (0.2-0.4 MPa), over 50% of original hexane

reacted and 2.0-2.5 mol of ethylene reacted with 1 mol of hexane generally. In iso-butane with ethylene, all isobutene reacted. On average, one molecule of isobutene condensed with 3 molecules of ethylene. The main reaction of aliphatic alkylation is complicated by side reactions one of which is polymerization of olefins[13]. This polymerization is not true polymers of ethylene. In the presence of hydrogen chloride the product consists of two layers. The upper layer is water-white and consists of paraffins, while the lower layer is dark red-brown and consists of addition compounds of aluminum chloride with unsaturated cyclic hydrocarbons. This polymerization is conjoined with a hydrogenation-dehydrogenation reaction by hydrogen transfer, and products consist of a layer of paraffins and a layer of unsaturated cyclic hydrocarbons, combined with aluminum chloride, which was termed "conjunct polymerization".[14]

Besides of the alkylation on paraffins and olefins, Ipatieff et al.[15] also reported the action of aluminum chloride on benzene and cyclohexane. In the presence of dry hydrogen chloride, the action of aluminum chloride on benzene at 125 °C gave 1.7% of ethylbenzene and 0.84% of diphenyl calculated on the benzene charged. No ethylene was added in this reaction. The mechanism of this reaction was also discussed. Since the main products of action are ethylbenzene and diphenyl, the following reasons are possible 1) two parts of benzene combine to form diphenyl, liberating hydrogen; 2) a destructive hydrogenation of benzene occurs during which benzene decomposes, and the decomposed fragments are hydrogenated to form ethylene; 3) ethylene alkylates the unchanged benzene to form ethylbenzene. The aromatic alkylation takes place by the well-known Friedel-Crafts mechanism. However, it was also demonstrated that it is possible to decompose some benzene and then perform alkylation, which is similar to the decomposition of paraffins instead of benzene. One of the strong proofs is that aluminum chloride and unsaturated ethylene polymers are found in the lower layer of products, as well as that ethylbenzene is formed from benzene only.[15]

Based on the research above, no matter the reactants are paraffins, olefins or aromatics, alkylation could happen in presence of aluminum chloride. Aluminum chloride is a very strong acid catalyst capable also of cracking reactions. The alkylating agents can be olefins, but it is also possible to produce alkylating agents from the decomposition of other reactants.

2.3.3 Amorphous silica alumina

Amorphous silica-alumina (ASA) is widely used as a solid acid catalyst in various chemical reactions including hydrocracking, isomerization and alkylation, which are important in the oil refining and petrochemical industry.[16]Crystalline silica-alumina is better known as zeolites, although not all zeolites are based just on silica-alumina.

In the case of ASA, the activity is attributed to both Lewis- and Bronsted-type acid sites. There is distribution of acid strength on the catalyst surface. The strongest sites are not the most favorable sites for acid catalysis, because the slow rate of desorption can retard the catalytic reactions. The most favorable sites are the acid sites with more moderate strength, but that are still sufficiently strong to accomplish the desired chemical reactions[17].

The first kind of solid acid catalysts used for the alkylation of benzene with ethylene and propylene in the vapor-phase was amorphous silica-alumina gel of the type used in commercial catalytic cracking since 1942.[18] Several studies have been conducted using ASA alone and in combination, and comparisons were made with alumina and zeolites as acid catalysts and acidic catalyst supports.

Reference

1.   De Klerk, A.; Gray, M. R.; Zerpa, N., Chapter 5 - Unconventional Oil and Gas: Oilsands. In *Future Energy (Second Edition)*, Letcher, T. M., Ed. Elsevier: Boston, 2014; pp 95-116.

2.   Siskin, M.; Kelemen, S. R.; Eppig, C. P.; Brown, L. D.; Afeworki, M., Asphaltene molecular structure and chemical influences on the morphology of coke produced in delayed coking. *Energy Fuels* **2006,** *20* (3), 1227-1234.

3.   Melpolder, F. W.; Brown, R. A.; Young, W. S.; Headington, C. E., Composition Of Naphtha From Fluid Catalytic Cracking. *Ind. Eng. Chem.* **1952,** *44* (5), 1142-1146.

4.   Ipatieff, V. N.; Pines, H.; Homarewsky, V. I., Phosphoric acid as the catalyst for alkylation of aromatic hydrocarbons. *Ind. Eng. Chem.* **1936,** *28*, 222-223.

5.   Ipatieff, V. N., Catalytic, polymerization of gaseous olefins by liquid phosphoric, acid I. Propylene. *Ind. Eng. Chem.* **1935,** *27*, 1067-1069.

6.   Ipatieff, V. N.; Pines, H.; Schmerling, L., Phosphoric acid as catalyst in the ethylation of phenol. *J. Am. Chem. Soc.* **1938,** *60*, 1161-1162.

7.   Bader, A. R., Cyclopentenylphenols. *J. Am. Chem. Soc.* **1953,** *75* (23), 5967-5969.

8.   Ipatieff, V. N.; Pines, H.; Friedman, B. S., Reaction of aliphatic olefins with thiophenol. *J. Am. Chem. Soc.* **1938,** *60*, 2731-2734.

9.   Pines, H.; Kvetinskas, B.; Vesely, J. A., Reaction Of Thiophene with Olefinic Compounds. *J. Am. Chem. Soc.* **1950,** *72* (4), 1568-1571.

10.   Harold Hart, E. A. H., Orientation in the phosphoric acid-catalyzed alkylation of ortho-cresol. *J. Org. Chem.* **1950,** *15* (2), 396-399.

11.   Ipatieff, V. N.; Komarewsky, V. I.; Pines, H., Phosphoric acid as a catalyst for the destructive alkylation of hydrocarbons. *J. Am. Chem. Soc.* **1936,** *58*, 918-919.

12.   Ipatieff, V. N.; Grosse, A. V., Action of aluminum chloride on paraffins - Autodestructive alkylation. *Ind. Eng. Chem.* **1936,** *28*, 461-464.

13.   Ipatieff, V. N.; Grosse, A. V.; Pines, H.; Komarewsky, V. I., Alkylation of paraffins with olefins in the presence of aluminum chloride. *J. Am. Chem. Soc.* **1936,** *58*, 913-915.

14.   Ipatieff, V. N.; Grosse, A. V., Polymerization of ethylene with aluminum chloride. *J. Am. Chem. Soc.* **1936,** *58*, 915-917.

15.   Ipatieff, V. N.; Komarewsky, V. I., The action of aluminum chloride on benzene and cyclohexane. *J. Am. Chem. Soc.* **1934,** *56* (7), 1926-1928.

16.   Hensen, E. J. M.; Poduval, D. G.; Magusin, P. C. M. M.; Coumans, A. E.; van Veen, J. A. R., Formation of acid sites in amorphous silica-alumina. *J. Catal.* **2010,** *269* (1), 201-218.

17.   Ali, M. A.; Tatsumi, T.; Masuda, T., Development of heavy oil hydrocracking catalysts using amorphous silica-alumina and zeolites as catalyst supports. *Appl. Catal. A* **2002,** *233* (1-2), 77-90.

18.   Perego, C.; Amarilli, S.; Carati, A.; Flego, C.; Pazzuconi, G.; Rizzo, C.; Bellussi, G., Mesoporous silica-aluminas as catalysts for the alkylation of aromatic hydrocarbons with olefins. *Micropor. Mesopor. Mater.* **1999,** *27* (2-3), 345-354.

3. Asphaltenes behavior in phosphoric acid catalyzed reaction

Abstract

In this chapter phosphoric acid was investigated as alkylation catalyst for the alkylation of asphaltenes with 1-hexene. The behavior and effect of phosphoric acid was discussed.

Key words: phosphoric acid, alkylation, asphaltenes

3.1 Introduction

Asphaltenes has low commercial value. It contains high concentrations of heteroatoms, such as S and N, and it is rich in aromatics, which explains its poor solubility in paraffins. To increase the commercial value of asphaltenes, ways were investigated to convert it into maltene and increase the H/C ratio as much as practicable.

In chapter 2, several typical reactions catalyzed by phosphoric acid have been discussed. As a catalyst, phosphoric acid could alkylate aromatic hydrocarbons, olefins, thiols and alcohols.[1] After reaction, the alkylated product contains side-chains of hydrocarbons. It was postulated that the hydrocarbon side-chains would improve the paraffin solubility of the products.

Though the main structural feature in asphaltenes is aromatic rings, it also has functional groups such as alcohols, olefins and thiols. If the postulate holds true for asphaltenes, the alkylated hydrocarbon side chains will not only increase asphaltenes H/C ratio, but also increase asphaltenes solubility in paraffins. Those alkylated side-chains will coat the asphaltenes to form a "micell"-like structure. On the inside is the paraffin insoluble asphaltenes, while on the outside is paraffin soluble side-chains. Since only the outside is interacting with the matrix, the whole molecule becomes soluble in paraffin. **Figure 3-1** shows the general idea. The goal of this chapter is to see whether phosphoric acid could alkylate asphaltenes, whether the paraffin solubility of the alkylated products was improved and to determine what part of asphaltenes was alkylated.

Hexene was selected as the alkylating agent to simplify experimentation and not because it was believed to be an industrially viable olefin for alkylation. In practice alkylation will more likely be performed using olefins present in cracked naphtha and not by using a single model olefin like 1-hexene.
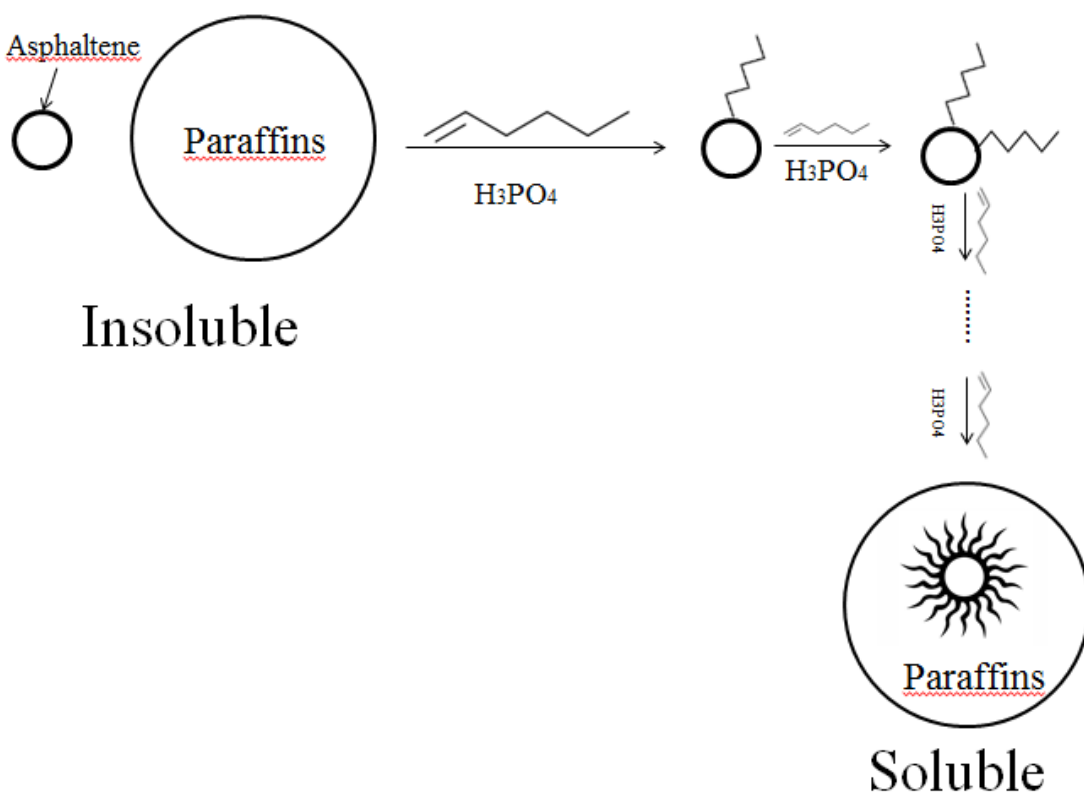
Figure 3-1. Alkylation of an asphaltenes to form a "micell"-like structure to increase solubility in a paraffin matrix.

3.2 Experimental

3.2.1 Materials

The feed material is industrially precipitated asphaltenes from the solvent deasphalting unit at the Nexen Energy ULC Long Lake Upgrader, which employs pentane as solvent. The characterization of the feed material was done in our laboratories. The main properties of the feed are listed in **Table 3-1**.

1-Hexene (97%) was purchased from Sigma-Aldrich. *n*-Pentane (≥98%) was purchased from Fisher Scientific. Ortho-phosphoric acid (85%) was purchased from Fisher Scientific.

Table 3-1. Properties of industrial asphaltenes feed from Nexen Energy ULC

Property	Value [a]
Aliphatic/aromatic hydrogen ratio	7.17 ± 0.18
Micro-Carbon Residue (MCR) value (wt%)	36.0
Chemical analysis (wt%)	
Carbon	82.09 ± 0.12
Hydrogen	8.06 ± 0.07
Nitrogen	1.15 ± 0.01
Sulfur	7.82 ± 0.11
Density at room temperature, ~23 °C (g/mL)	1.087 ± 0.076

[a] Average (x) and sample standard deviation (s) of triplicate analyses given as x ± s.

3.2.2 Experimental procedures

Lab precipitated asphaltenes. The industrial asphaltenes form Nexen was precipitated again in our lab with *n*-pentane. 1 g of feed and 40 mL *n*-pentane were mixed together in flask and stirred for 1 hour at room temperature and then left for another 23 hours. The solution was filtered through a 0.22 µm filter paper and the dry solid was collected. This is called lab precipitated C_5-asphaltenes.

Reaction with phosphoric acid. 5 g of industrial asphaltenes, 10 g of 1- hexene and 5 g of phosphoric acid were added into a flask and heated under reflux for 24 hours. (The heating plate temperature was 140 °C). After reaction, the flask was left in the fume hood for 48 hours to evaporate unconverted 1-hexene and the product was filtered through a 0.22 µm filter paper. *n*-pentane was used as solvent to transport all reactants from flask to filter; the exact amount of pentane was not recorded. 1 g of solid product from filtration was taken and subjected to the lab precipitated asphaltenes procedure. The solid product collected after the lab precipitated asphaltenes procedure was stirred in pure water for 3 hours to remove residual phosphoric acid. Then it was filtered through 0.22 µm filter paper to separate the water from the solid product. The solid part was then washed 3 times with 100 mL pure water per time to remove residual

19

phosphoric acid and purify the product. The number of times that the solid was washed was arbitrarily selected. The solid product was left in a fume hood for two days to dry.

Reaction without phosphoric acid. The procedure is the same as above, except that no phosphoric acid was added. Compared with the experiment above, this blank-reaction was performed to investigate the contribution of phosphoric acid to the reaction.

3.2.3 Analyses

TGA (Thermogravimetric analysis). The instrument is TGA/DSC 1 STAR^e system purchased from Mettler Toledo. This instrument was equipped with an ultra-micro balance cell and two thermocouples. The ultra-micro balance cell has 5 g capacity with 0.1 µg readability. The instrument was capable of measuring simultaneous heat flow and weight change of samples. The sample (5±1 mg) was loaded in open crucibles, which were 70 microns thick made of alumina (Al_2O_3). The procedures for TGA consisted of three steps: 1) staying at 50 °C for 10 min, gas flow N_2 at 50 mL/min. 2) increasing from 50 to 600 °C with rate of 10 °C/min, gas flow N_2 at 50 mL/min. 3) staying at 600 °C for 60 min, gas flow N_2 at 50 mL/min. All micro carbon residue measurements were determined in accordance with the standard test method ASTM D4530.[2]

^{1}HNMR (Proton nuclear magnetic resonance). The ^{1}HNMR spectra were obtained using a Nanalysis 60 MHz NMReady-60 spectrometer. The instrument was pre-calibrated with D-chloroform. 0.2 g of sample was dissolved in 1 ml of D-chloroform, placed in 5 mm NMR tubes and analysed using the following parameters: spectral width 14 ppm; number of scans per sample: 32; scan delay was 20.0 seconds and 4000 points were recorded per scan.

Solid density. The density was measured at room temperature, ~23°C. The density was determined by water displacement. The procedure was as follows. Step 1: put a certain amount of water in a 190 mL A-grade glass cylinder and record volume one. Step 2: take one piece of asphaltenes and weigh its' mass on Mettler Toledo ML 3002E balance and record the mass. Step 3, put this piece of asphaltenes in the cylinder in Step 1 and record volume two. The difference between volume one and volume two is the volume of asphaltenes. This procedure was repeated three times and data was shown in **Table 3-2**.

IR (Infrared spectroscopy). The instrument is MB 3000 purchased from ABB. It is equipped with deuterated triglycine sulfate (DTGS) operating at ambient temperature. The spectral

collection parameters are: detector model 114690-131082; detector gain=27; resolution=4 cm^{-1}; number of scans averaged=120.

CHNS. The Instrument employed is the Thermo Flash 2000 CHNS-O Model. The temperature of pre-packed reactors is 950 °C. Oxygen injection for combustion was set to 5 seconds. Helium carrier gas flow was 140 mL/min. Before each set of run, the equipment was calibrated using a standard material: 2,5-bis(5'-*tert*-butyl-2-benzoxazol-2-yl)thiophene (BBOT), $C_{26}H_{26}N_2O_2S$. Typically 2-4 mg of sample was loaded for analysis.

XRF (X-ray fluorescence). We used AMETEK EDAX (Energy Dispersive) XRF microprobe in this experiment. This XRF Analyzer incorporates fast, simultaneous multi-element X-ray detection with the sensitivity to analyze from parts-per-million to 100% concentrations. It can measure elements from Na to Bk in either air or low-vacuum conditions. It is run under 40 KV, 750 mA. The calibration of the instrument is done by running a standard Al 2024 alloy.

3.2.4 Calculations

a) The precipitation of asphaltenes by an industrial solvent deasphalting process is less rigorous than that of a laboratory precipitation. The actual asphaltenes content (A) of the industrial feed was determined as calculated by:

A = Mass of lab precipitated asphaltenes/Mass of industrial asphaltenes   3.1

where A stands for the mass fraction of laboratory precipitated asphaltenes in the industrial feed.

b) The phosphorus content (P wt %) in alkylated in (H_2PO_3)-O-asphaltenes formation was calculated based on the molar mass and mass of (H_2PO_3)-O- group:

$$\frac{M(P)}{M(H_2PO_4)} = \frac{P(\text{wt}\%)}{H_2PO_4(\text{wt}\%)}$$ 3.2

where M stands for the molar mass.

c) Density of asphaltenes: $Density = \dfrac{Mass}{Volume}$ 3.3

d) To quantify the amount of alkylated phosphoric acid and measure changes in other elements, the content of phosphorus and other elements (Ca, Fe, Ni, Cu, V, Zr, Mo) in the product was measured by XRF. The XRF in not capable of quantifying elements lighter than Na, so that H, C, N and O are not reported in the XRF analysis. In order to obtain a complete elemental analysis, the relative concentration of the Na and heavier elements determined by XRF (that were reported as normalized values) had to be combined with the concentration of the lighter elements determined by CHNS analysis. To convert the elements wt% in XRF to wt% of asphaltenes, the content of S was used as scaling variable. The sulfur content in the XRF analysis was scaled to be equal to the absolute concentration of sulfur determined by CHNS analysis. In this way the relative concentration of the other elements in the XRF analysis could also be scaled to obtain absolute concentration values.

$$\frac{S\left(wt\% \text{ in CHNS}\right)}{S(wt\% \text{ in XRF})} = \frac{Element(wt\% \text{ in CHNS})}{Element(wt\% \text{ in XRF})} \qquad 3.4$$

3.3 Results

3.3.1 Characterization of asphaltenes

The industrial asphaltenes feed material was characterized (Table 3-1) as explained in the experimental section.

The laboratory precipitated asphaltenes fraction of the industrial asphaltenes feed that was obtained by n-pentane precipitation was characterized in a similar way (Table 3-2). The amount of laboratory precipitated asphaltenes recovered was 0.78 g per g of industrial asphaltenes feed, which means 78 wt% of the industrial Nexen asphaltenes feed is C_5-asphaltenes, while 22% is maltene.

Table 3-2. Properties of laboratory precipitated asphaltenes (C_5-asphaltenes)

Property	Value [a]
Aliphatic/aromatic hydrogen ratio	7.21
Micro-Carbon Residue (MCR) value (wt%)	42.0 ± 0.2
Chemical analysis (wt%)	
Carbon	82.54 ± 0.20
Hydrogen	7.66 ± 0.18
Nitrogen	1.14 ± 0.06
Sulfur	7.22 ± 0.39

[a] Average (x) and sample standard deviation (s) of triplicate analyses given as x ± s.

The infrared spectrum of the laboratory precipitated asphaltenes was collected and it is shown in Figure 3-2.
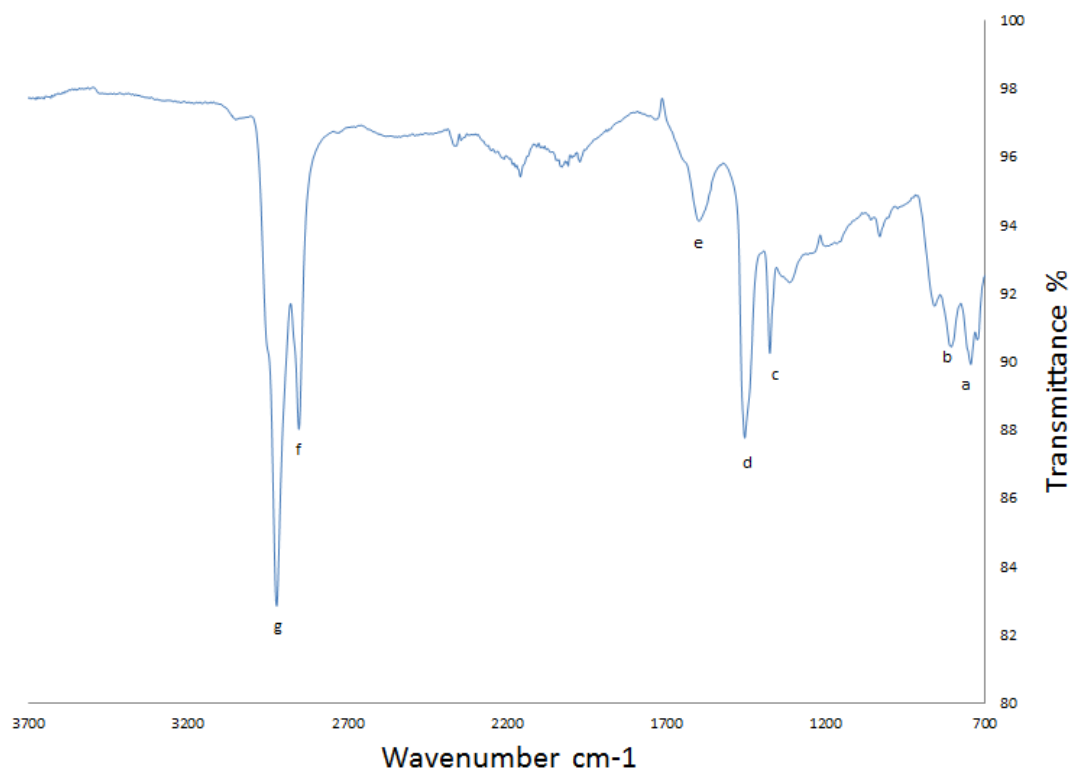
Figure 3-2. IR spectra of laboratory precipitated asphaltenes. The wave numbers of peak (a) to (g) are: (a) 744 cm^{-1}; (b) 808 cm^{-1}; (c) 1375 cm^{-1}; (d) 1454 cm^{-1}; (e) 1596 cm^{-1}; (f) 2852 cm^{-1}; (g) 2923 cm^{-1}.

3.3.2 Reaction yield

In the reaction of the industrial asphaltenes feed with 1-hexene in the presence of phosphoric acid resulted in 4.54 g of solid asphaltenes product from 5.00 g of asphaltenes feed. 1-Hexene and phosphoric acid were evaporated and removed. Organic liquid content washed out by *n*-pentane was discarded.

In the blank reaction of the industrial asphaltenes feed with 1-hexene without phosphoric acid, 4.13 g of solid asphaltenes product was obtained from 5.00 g of asphaltenes feed. 1-Hexene was evaporated and removed. Organic liquid content washed out by *n*-pentane was discarded.

3.3.3 Analysis of solid asphaltenes products after reaction

The research focused on the asphaltenes fraction. The solid asphaltenes products after reaction with/without phosphoric acid were analyzed. The solid asphaltenes product from the reaction in the presence of phosphoric acid will be referred to as "product 1". The solid asphaltenes product from the reaction without phosphoric acid will be referred to as "product 2".

Element analysis. To investigate whether there were any changes in solid asphaltenes product composition after reaction, elemental analysis was performed. If obvious changes in the elemental composition were observed, then it would suggest the possibility of chemical modification.

CHNS analysis could quantitatively determine the concentration of the elements carbon, hydrogen, sulfur and nitrogen, while XRF could analyze the relative concentration of the heavier elements, such as phosphorous. Oxygen cannot accurately be measured directly, so the content was calculated in section 3.4.

The CHNS and XRF analyses of product 1 and product 2 are shown in **Table 3-3** and **Table 3-4** respectively**.**

Table 3-3. CHNS analyses of solid products after reaction with and without H_3PO_4

Product 1 (with H_3PO_4)		Product 2 (without H_3PO_4)	
Element	Value(wt%)	Element	Value(wt%)
Carbon	74.74	Carbon	80.24
Hydrogen	7.53	Hydrogen	7.69
Nitrogen	1.08	Nitrogen	1.18
Sulfur	6.69	Sulfur	7.37

Table 3-4. XRF test of phosphorous and other elements in the solid products after reaction with and without H_3PO_4

Element(wt%)	Product 1 (with H_3PO_4)	Product 2 (without H_3PO_4)
P	17.51	1.57
S	81.93	89.00
Ca	0.15	2.67
Fe	0.08	2.14
Ni	0.06	0.54
Cu	0.03	0.77
V	0.18	1.44
Zr	0.07	1.78
Mo	0.01	0.17
Total	100	100

TGA graph. From the data above (**Table 3-4**), it could be seen that the phosphorous content was quite different between product 1 and product 2. It was postulated that phosphoric acid might alkylate to asphaltenes. If this was the case, a difference might be observed by performing a TGA.

The mass loss due to the release of phosphoric acid could be observed in the TGA of product 1 (**Figure 3-3**) and is highlighted by a circle. This event started at a temperature of around 170 °C

and the mass loss during the event was 4.3 %. Thermal decomposition started at around 320 °C. The final mass remaining after heating to 600 °C is the microcarbon residue and it was 44.6 wt%.
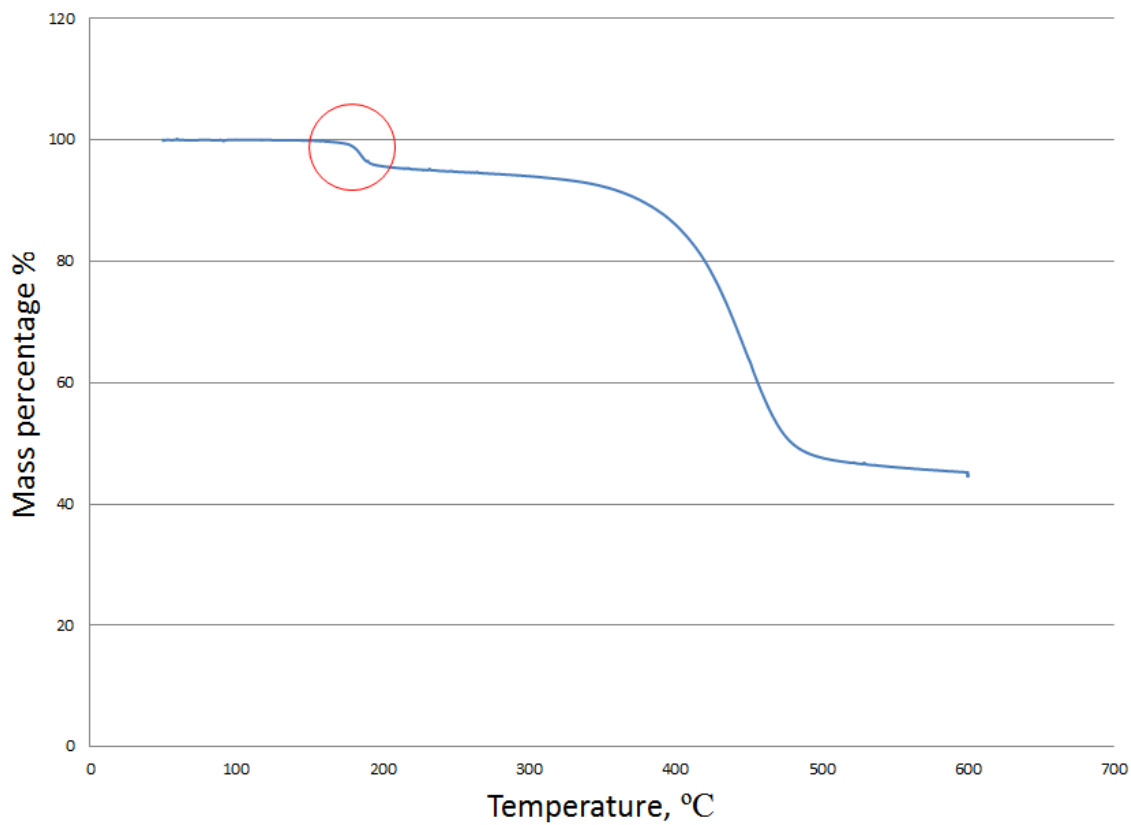
Figure 3-3. TGA of product 1
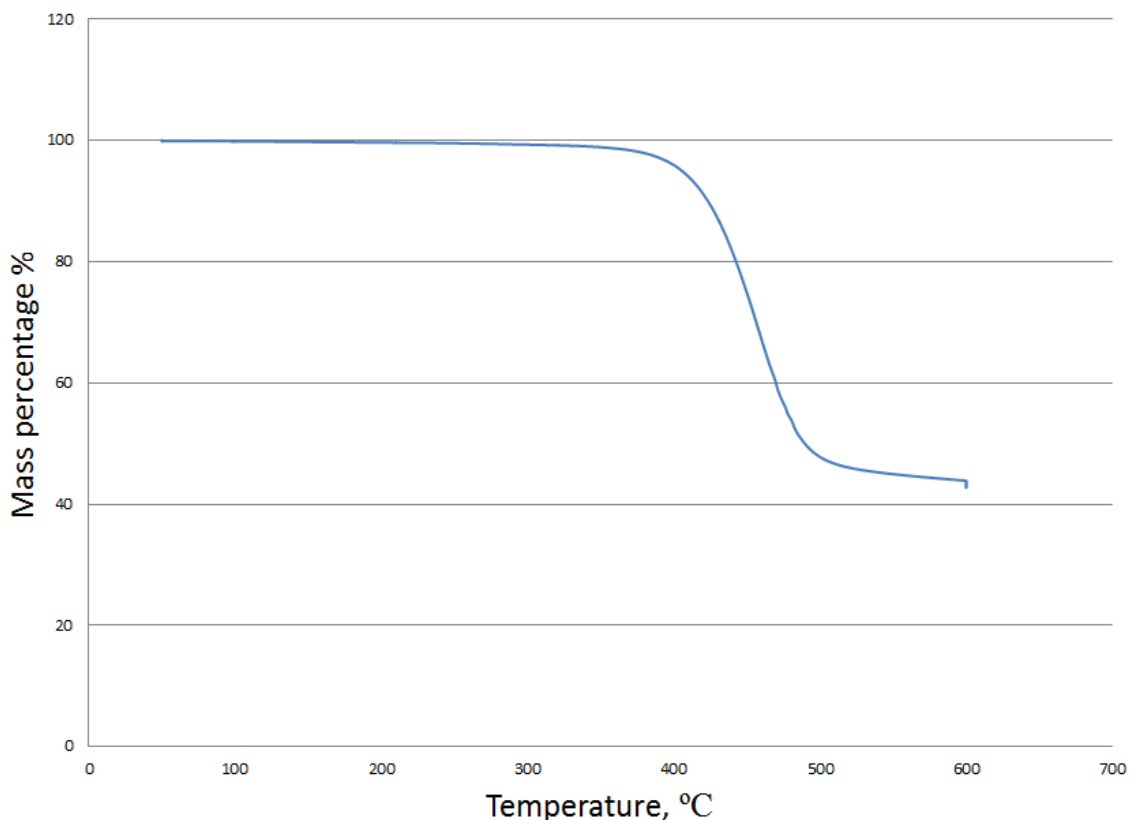
Figure 3-4. TGA of product 2

The TGA of the reaction product from conversion without phosphoric acid is also shown for comparison (**Figure 3-4**). There was no corresponding mass loss due to the release of phosphoric acid. Thermal decomposition started at around 350 °C and the microcarbon residue was 43.6 wt%.

3.4 Discussion

Solid asphaltenes product was heavier after reaction. As mentioned in 3.3.1, The amount of laboratory precipitated asphaltenes recovered was 0.78 g per g of industrial asphaltenes feed. 5g industrial feed were used in both reactions with/without phosphoric acid. So the amount of laboratory precipitated asphaltenes should be 5×0.78=3.9 g if there was no reaction. In this case, product 1 increased 0.79 g while product 2 increased 0.33 g. Also, MCR value of product 1 and product 2 increased 2.2wt% and 1.2wt% respectively compared to the laboratory precipitated asphaltenes. The increase in MCR of product 1 is even more when the data is recalculated taking the 4.3 wt% loss of phosphoric acid into account. In this case, "heavier" not only means increase

in the amount of lab precipitated asphaltenes product mass but also an increase in the MCR value of the asphaltenes. The treatment procedure was not beneficial at all.

Elemental analysis. With the data from CHNS and XRF and the product yield, the mass of each element was calculated as below (**Table 3-5**). The amount of oxygen was calculated by difference

Table 3-5. Mass of elements in product 1 and product 2.

	Product 1 (with H_3PO_4)		Product 2 (without H_3PO_4)	
Element	Wt%	Mass/g	Wt%	Mass/g
C	74.74	3.40	80.24	3.31
H	7.53	0.342	7.69	0.318
N	1.08	0.0490	1.18	$0.04.87 \times 10^{-2}$
S	6.69	0.304	7.37	0.304
P	1.43	0.0649	0.127	5.24×10^{-3}
Ca	0.0122	5.54×10^{-4}	0.221	9.13×10^{-3}
Fe	0.00653	2.96×10^{-4}	0.177	7.31×10^{-3}
Ni	0.005	2.22×10^{-4}	0.0447	1.85×10^{-3}
Cu	0.00245	1.11×10^{-4}	0.0638	2.64×10^{-3}
V	0.0147	6.67×10^{-4}	0.12	4.96×10^{-3}
Zr	0.00572	2.6×10^{-4}	0.147	6.07×10^{-3}
Mo	0.000817	3.71×10^{-5}	0.0141	5.82×10^{-4}
O	8.48	0.385	2.61	0.108
Total	100	4.54	100	4.13

Here are several suggestions for **Table 3-5**. 1) The mass of N and S in both reactions are almost the same which means this reaction either didn't work with nitrogen and sulfur or nitrogen and sulfur was alkylated but couldn't be wash out. 2) In product 1, the molar H/C ratio is 1.21 and in

product 2, the molar H/C ratio is 1.15, the reason of which could be that product 1 has a higher H/C ratio due to hydrogen from alkylated (H_2PO_3)-O- groups and alkylated hexene. 3) The amount of oxygen is calculated by the difference between 100% and all other elements. The alkylated (H_2PO_3)-O- group would bring more oxygen in asphaltenes. Thus, oxygen amount should increase in product 1 which is in correspondence with data in **Table 3-5**. The addition of phosphoric acid alone cannot explain the extent of the increase in oxygen and the oxygen calculated by difference also contains the cumulative error of analysis in this experiment. This suggests oxygen content in product 1 may not be exactly that much in **Table 3-5**.

The H/C mole ratio and aliphatic/aromatic hydrogen ratio are 1.21 and 10.0 respectively in product 1. Compared with laboratory precipitated asphaltenes, which had a H/C mole ratio of 1.11 and aliphatic/aromatic hydrogen ratio of 7.21, both H/C mole ratio and aliphatic/aromatic hydrogen ratio increased. This may be due to alkylation.

Hypothesis for alkylated phosphorous in product 1. As discussed above, the content of phosphorous in product 1 was ten times more than that in product 2 and the results indicated that an alkylated (H_2PO_3)-O- group was introduced into the asphaltenes. By XRF test, phosphorous content in product 1 was 1.43 wt%. By **Equation 3.2** and mass percent drop in **Figure 3-3**, the calculated phosphorous content would be 1.37 wt%, which was only 0.07% less than XRF analysis and within experimental uncertainty. Asphaltenes structure could not be interrogated directly and the way in which the phosphoric acid was connected to asphaltenes could only be inferred. According to the reaction mechanism, the intermediate step is phosphoric acid attack to form a phosphoric acid ester $(R-O-PO_3H_2)$. The most likely explanation is that this intermediate was stable. The inferred stability of the phosphoric acid ester was indirectly confirmed by the TGA (Figure 3-3), which saw the release of phosphoric acid at around 170 °C.

3.5 Conclusion

- Phosphoric acid is alkylated to asphaltenes and promotes hexene alkylation.
- H/C ratio and Aliphatic/aromatic ratio slightly increased

Reference

1.   (a) Ipatieff, V. N.; Pines, H.; Friedman, B. S., Reaction of aliphatic olefins with thiophenol. *J Am Chem Soc* **1938,** *60*, 2731-2734; (b) Pines, H.; Kvetinskas, B.; Vesely, J. A., Reaction Of Thiophene with Olefinic Compounds. *J Am Chem Soc* **1950,** *72* (4), 1568-1571; (c) Ipatieff, V. N.; Pines, H.; Homarewsky, V. I., Phosphoric acid as the catalyst for alkylation of aromatic hydrocarbons. *Ind Eng Chem* **1936,** *28*, 222-223; (d) Ipatieff, V. N.; Komarewsky, V. I.; Pines, H., Phosphoric acid as a catalyst for the destructive alkylation of hydrocarbons. *J Am Chem Soc* **1936,** *58*, 918-919.

2.   ASTM D4530: *Standard test method forDetermination of Carbon Residue (Micro Method);* ASTM: West Conshohocken, PA, 2011.

4. Asphaltenes behavior in aluminum chloride/hydrogen chloride catalyzed reaction

Abstract

Aluminum chloride has been widely used as Friedel-Crafts alkylation catalyst. In this chapter, the reactions between aluminum chloride/hydrochloric acid, hexene and asphaltenes in toluene is investigated.

Key words: aluminum chloride, toluene, alkylation, asphaltenes

4.1 Introduction

Friedel and Crafts demonstrated that benzene would react with alkyl halides in the presence of a Lewis acid (e.g. $AlCl_3$) to produce alkyl benzenes. This reaction became known as Friedel-Crafts alkylation.[1] Aluminum chloride is a typical and strong Friedel-Crafts alkylation catalyst. Ipatieff et al.[2,3] has reported many studies with aluminum chloride, especially in alkylation with aromatics and olefins, which are of interest for the conversion of cracked naphtha and asphaltene.

The steps of alkylation of aromatic hydrocarbons with olefins in the presence of aluminum chloride-hydrogen chloride are depicted in **Figure 4-1**.[4] First, hydrogen aluminum tetrachloride complex is formed, which is a Bronsted acid and then reacts with an olefin to produce an intermediate that can alkylate an aromatic.

Brown et al.[5] reported work with aluminium chloride, hydrogen chloride and toluene at low temperatures. It was found that without hydrogen chloride, aluminum chloride neither interacts with nor dissolves appreciably in toluene. In the presence of excess hydrogen chloride, the aluminum chloride dissolves in toluene to give a clear green solution. The solubility of aluminum chloride in toluene is 0.0135g/1g at 73 °C.

In this chapter, the alkylation of asphaltenes with hexene in toluene was studied with aluminum chloride and hydrochloric acid, individually and in combination. Toluene is not only the solvent

of asphaltenes but also could react with hexene and asphaltenes. However, the reaction will always have two liquid phases present, unlike the work reported by Brown et al.[5] that was conducted in a single phase. It is difficult to exclude water from oilsands derived materials and even when it is rigorously excluded, water can be produced by reaction of the oxygenate functional groups. Thus, it was anticipated that mass transport would influence the reactions. This was an acceptable limitation since the reaction chemistry rather than the kinetics was of interest.

$$AlCl_3 + HCl \rightarrow AlCl_3HCl \quad or \quad \begin{bmatrix} :\ddot{Cl}: \\ :\ddot{Cl}:\ddot{Al}:\ddot{Cl}: \\ :\ddot{Cl}: \end{bmatrix}^{-} H^{+}$$

$$RCH{=}CH_2 + HAlCl_4 \rightarrow RCH{-}CH_3, \quad i.e., \quad \begin{bmatrix} Cl \\ ClAlCl \\ Cl \end{bmatrix}^{-} R^{+}$$
$$\qquad\qquad\qquad\qquad\qquad\quad |$$
$$\qquad\qquad\qquad\qquad\quad ClAlCl_3$$

$$C_6H_6 + RCH{-}CH_3 \rightarrow C_6H_5CH\overset{CH_3}{\underset{R}{<}} + HAlCl_4$$
$$\qquad\qquad\quad |$$
$$\qquad\qquad ClAlCl_3$$

Figure 4-1. Reactions steps of aluminum chloride-hydrogen chloride with olefins[4]

4.2 Experimental

4.2.1 Materials

The feed material is same as chapter 3 section 3.2.1. The characterization of the feed material was done in our lab. See Chapter 3 Table 3-1. *n*-Pentane (≥98%), hydrochloric acid (certified 0.995-1.005 M) and toluene (≥99.5%) were commercially obtained from Fisher Scientific. Aluminum chloride (99.99% pure on trace metals basis) and 1-hexene (97%) were purchased from Sigma-Aldrich. Concentrated hydrochloric acid (12M) was purchased from EMD[TM].

4.2.2 Experimental procedures

In this chapter, the mass was weighed by Mettler Toledo ML 3002 E balance. Volume was measured with a 100 ml glass cylinder.

Reaction with 1-hexene, aluminum chloride, toluene and hydrochloric acid. Solution 1 and solution 2 were prepared as follows. Solution 1: 5.00 g asphaltenes + 10.0 mL toluene + 40.0 mL hexene. Solution 2: 1.81 g aluminum chloride + 20.0 mL 12M hydrochloric acid + 10.0 mL 1M hydrochloric acid solution. The mixed hydrochloric acid in solution 2 was calculated as equal as 30.0 mL 8.3M hydrochloric acid. Solution 1 and Solution 2 were mixed well in a flask under reflux for 20 hours (the heating plate temperature was 75 °C). After reaction, the solution in the flask was transferred to a separating funnel. Then 100mL 1M hydrochloric acid was added to the funnel to wash aluminum chloride and separated the solution into two phases. The upper phase was oil phase. Lower phase was aqueous phase, which contained aluminum chloride. The lower phase was then discarded to remove aluminum chloride. Another two times of 100 mL 1M hydrochloric acid were used to repeat steps above to remove aluminum chloride. The number of washing times was arbitrarily selected. Next, the oil phase was transferred into rotary evaporator (type Heizbad Hei-VAP purchased from Heldolph) under 55 °C 77 mbar for 1 hour to evaporate toluene and 1-hexene. The solid product collected after evaporation was left in a fume hood for 4 days to dry. 1.00 g of dried solid product was randomly selected and subjected to the *lab precipitated asphaltenes procedure* (referred to **Chapter 3 section 3.2.2**).

Reaction with 1-hexene, aluminum chloride and toluene. 5.00 g industrial asphaltenes, 50.0 mL 1-hexene, 0.26 g aluminum chloride and 15.0 mL toluene were mixed well in flask under reflux for 20 hours (the heating plate temperature was 75 °C). The product work-up procedure was the same procedure as above.

Reaction with 1-hexene and hydrochloric acid (12M). 5.00 g industrial asphaltenes, 9.90 g 1-hexene and 5.61 g hydrochloric acid (12M) were mixed together in flask and heater under reflux for 24 hours. The temperature of heating plate was 100 °C. After reaction, the flask was cooled down to room temperature (~23 °C) and left in the fume hood for 48 hours to evaporate unconverted 1-hexene. Then the product was filtered through a 0.22 μm filter paper. *n*-Pentane was used as solvent to transport all reactants from flask to filter; the exact amount of pentane was not recorded. All solid products from filtration were taken and subjected to the *lab precipitated*

asphaltenes procedure (i.e. 1 g asphaltenes mixed with 40 mL *n*-pentane). Maltenes product was collected after precipitation. The solid product collected after the lab precipitated asphaltenes procedure was stirred in pure water for 3 hours to remove residual hydrochloric acid. Then it was filtered through 0.22 μm filter paper to separate the water from the solid product. The solid part was then washed 3 times with 100 mL pure water per time to remove residual hydrochloric acid and purify the product. The number of times that the solid was washed was arbitrarily selected. The solid product was left in a fume hood for two days to dry.

4.2.3 Analyses

TGA (Thermogravimetric analysis), **^{1}HNMR** (Proton nuclear magnetic resonance) and **IR** (Infrared spectroscopy) refer to **Chapter 3 section 3.2.3**.

4.3 Results

4.3.1 Reaction yield

The reaction with hydrochloric acid in presence of aluminum chloride and toluene will be referred to as "reaction 1". The reaction without hydrochloric acid in presence of aluminum chloride and toluene will be referred to as "reaction 2". The reaction with hydrochloric acid (12M) will be referred as "reaction 3".

In each experiment the industrial asphaltenes feed, hexene, toluene and catalyst was heated and after reaction and evaporation of the remaining hexene and solvent, a solid product was obtained. This solid product was then treated by the *lab precipitated asphaltenes* procedure to obtain the asphaltenes fraction of the solid reaction product. The asphaltenes product thus obtained from reaction 1 will be referred as "product 1". In the same way the asphaltenes fraction of the solid reaction product after reaction 2 and 3 will be referred as "product 2" and "product 3" respectively.

In reaction 1, 7.00 g solid product was obtained from 5.00 g asphaltenes feed. The material balance based on solid material was calculated as 7.00/5.00=140%. The extra mass may come from hexene that alkylated with the asphaltenes, residual toluene and/or hexane not removed by evaporation or even some residual aluminium chloride not washed out of the product. In actual fact the material balance on the solids should have contained more solids. When washing the product in separating funnel, the product formed three layers: oil phase, emulsion phase and

water phase. This phenomenon wasn't observed in the reaction without hydrochloric acid. Since only the oil phase was used to perform next procedure; some asphaltenes in the emulsion phase was lost. Furthermore, the product was muddy and sticky to flask after evaporation in the rotary evaporator. So some product couldn't be transferred from the flask.

When 1.00 g of the solid product was subjected to the *lab precipitated asphaltenes* procedure, 0.24 g asphaltenes product was obtained. The maltenes fraction that was washed out by *n*-pentane was discarded. The amount of lab precipitated asphaltenes in the asphaltenes feed, i.e. "A" in Equation 3.1, was 5.00×0.78=3.90 g. Based on the assumptions outlined, the total amount of precipitated asphaltenes after reaction was calculated as 7.00×0.24=1.68 g. This value does not take the potential losses in the emulsion phase and the flask into account. The decreased mass of product 1 did not simply mean that the asphaltenes were converted to maltenes in the reaction.

In the reaction 2, 4.82 g of solid product was obtained from 5.00 g of asphaltenes feed. Material balance was calculated as 4.82/5.00=96.4%. The asphaltenes fraction of the product that was obtained after subjecting 1.00 g solid product to the *lab precipitated asphaltenes* procedure was 0.79 g (product 2). The organic liquid washed out by *n*-pentane was discarded. The amount of lab precipitated asphaltenes in the feed, i.e. "A" in Equation 3.1, was 5.00×0.78=3.90 g. Based on the assumptions outlined the total amount of precipitated asphaltenes after reaction was calculated as 4.82×0.79=3.81 g, which was a slight decrease in asphaltenes content over the feed.

In the reaction 3, 5.04g asphaltenes product was obtained from 5.00 g of asphaltenes feed. The material balance based on the solid product was calculated as 5.04/5.00=101%. 4.24 g product 3 and 0.70 g maltenes was obtained form 5.04 g asphaltenes product after the *lab precipitated asphaltenes* procedure. Since the amount of lab precipitated asphaltenes in the feed, i.e. "A" in Equation 3.1, was 5.00×0.78=3.90 g, there was an increase in asphaltenes content over the feed.

4.3.2 Analysis of asphaltenes fraction from the solid reaction product
The research focused on the asphaltenes fraction. Product 1, 2 and 3 were analyzed.

First, ^{1}HNMR test was done to see changes of aliphatic/aromatic hydrogen ratio after reaction. The results are shown in **Table 4-1**.

Table 4-1. Aliphatic/aromatic hydrogen ratio of product 1, 2 & 3

Product No.	1	2	3
Aliphatic/aromatic hydrogen ratio	8.85	7.55	7.79

Compared with the aliphatic/aromatic hydrogen ratio of 7.21 (**Table 3-2**) of the asphaltenes fraction of the feed, the aliphatic/aromatic hydrogen ratio of all products increased, especially that of product 1. Product 2 has the lowest aliphatic/aromatic hydrogen content of the three products.

The narrow changes in aliphatic/aromatic ratio showed the possibility of alkylation. IR analysis of product 1, 2 & 3 were done for further study. Compared with **Figure 3-2**, if new peaks were found, it suggested changes in asphaltenes. It is found that IR spectrum of product 2 is almost same as **Figure 3-2** while the other two, which reacted with hydrochloric acid have similar IR spectra but were different from **Figure 3-2**.

The comparison between **Figure 3-2** (lab precipitated asphaltenes feed) and product 2 is shown in **Figure 4-2**. IR spectra of product 1 and product 3 were very noisy and it was difficult to ascertain much from them.
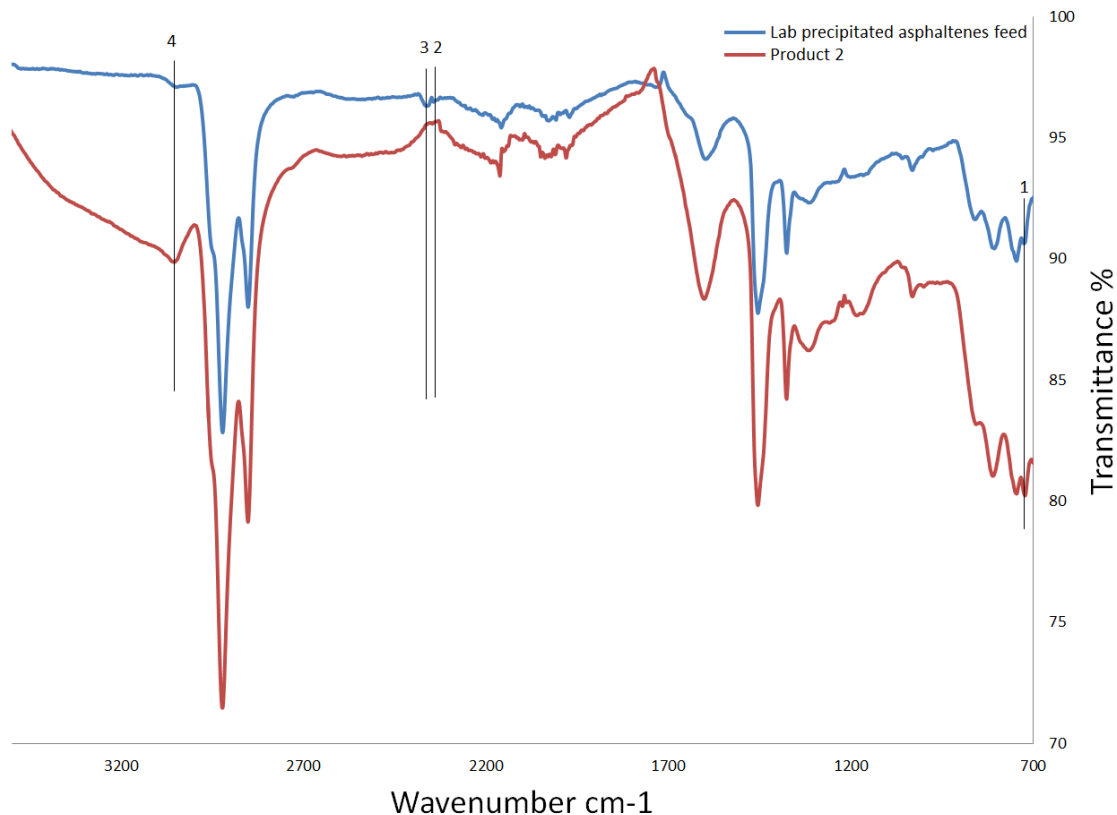
Figure 4-2. IR spectra of product 2 and lab precipitated asphaltenes feed. Peak 1 is at 725 cm^{-1}; peak 2 is at 2356 cm^{-1}; peak 3 is at 2362 cm^{-1}; peak 4 is at 3050 cm^{-1}.

Peak 1 was increased in product 2, which stands for adjacent C-H wag vibration on the aromatics. This means the C-H on the aromatics not only decreased in product 2 but might slightly increased. In this case, alkylation was not succesful on aromatics. Peak 2 and 3 are due to difference in the CO_2 content, which is an unfortunate side-effect of not collecting a background spectrum before each analysis. Peak 4 represents C=C-H vibration.

The microcarbon residue (MCR) value is another indicator of the properties of the asphaltenes. If the MCR value decreases after reaction, it means that the asphaltenes are less prone to form coke. It was anticipated that hexene that alkylated with the feed, but remained in the asphaltenes fraction would cause a decrease in the MCR value. The MCR of the asphaltenes fraction of the feed was 42.0 ± 0.2 wt% (Table 3-2). The MCR of product 1, 2 and 3 is shown in **Table 4-2**.

Table 4-2. MCR value of product 1, 2 and 3

Product No.	1	2	3
MCR value (wt %)	42.8	41.9	41.7

The asphaltenes fraction of the reaction products has similar MCR values as the asphaltenes fraction of the feed. Based on the MCR it appears unlikely that much hexene that alkylated was alkylated to molecules that remained in the asphaltenes fraction.

4.4 Discussion

The increase of aliphatic/ aromatic hydrogen ratio may due to the increase of aliphatic hydrogen or decrease of aromatic hydrogen or both of them. It was tempting to ascribe this to the presence of alkyl groups introduced by the alkylation procedure, but the MCR and IR data did not support such an interpretation.

The most promising outcome of the experiments was possible asphaltenes to maltenes conversion during the reaction catalyzed by aluminium chloride in combination with hydrochloric acid. However, emulsion formation made it difficult to obtain a credible material balance even on the solid materials.

4.5 Conclusion

- The presence of hydrochloric acid has effect on asphaltenes alkylation with aluminum chloride, 1-hexene and toluene. The exact reason is not clear, but the most promising results were obtained by this combination of catalysts.

Reference

1. L. G. Wade, Jr., *Reactions of Aromatic Compounds,* Organic Chemistry, 5th Edition, Prentice-Hall, Upper Saddle River, NJ, 2003.

2. Ipatieff, V. N.; Grosse, A. V.; Pines, H.; Komarewsky, V. I., Alkylation of paraffins with olefins in the presence of aluminum chloride. *J Am Chem Soc* **1936,** *58*, 913-915.

3. Ipatieff, V. N.; Komarewsky, V. I., The action of aluminum chloride on benzene and cyclohexane. *J Am Chem Soc* **1934,** *56* (7), 1926-1928.

4. Ipatieff, V. N.; Pines, H.; Schmerling, L., Isomerization accompanying alkylation. II. The alkylation of benzene with olefins, naphthenes, alcohols and alkyl halides. *J Org Chem* **1940,** *5* (3), 253-263.

5. Brown, H. C.; Pearsall, H. W., The Action Of the Catalyst Couple Aluminum Chloride-Hydrogen Chloride on Toluene at Low Temperatures - the Nature Of Friedel-Crafts Complexes. *J Am Chem Soc* **1952,** *74* (1), 191-195.

5. Asphaltene behavior in silica alumina catalyzed reaction with ethylene

Abstract

An amorphous silica alumina catalyst, Siral40, was employed to catalyze the reaction between asphaltenes and ethylene. After reaction, the reaction products were analyzed and discussed.

Key words: Siral 40, ethylene, alkylation, asphaltene

5.1 Introduction

Solid acid catalysts are widely used in industrial processes and the number of processes employing such materials is likely to increase as mineral acids are replaced by more environmentally appropriate substances.[1] Amorphous silica alumina (ASA) has both Brønsted and Lewis acid sites.[2] The number and strength of the acid sites depend on the alumina content[3] and the distribution of acid sites strengths over the surface is determined by the composition or the existence of short-range interactions on the silica–alumina surface.[1]

The silica-alumina catalyst employed in this chapter is Siral40. Characterization of the catalyst has been performed Xia.[4] The optimal alkylation temperature of Siral40 is 325 °C.[4] ASA has been used in numbers of alkylation reactions such as aromatic and olefins. For example, in the reaction of phenol and 1-octene it was reported that silicated ASA catalysts, such as Siral40, was active for the alkylation and had ~50% selectivity to octyl phenyl ethers and *o*-octylphenol.[5]

In this chapter, asphaltene, as the heaviest part of bitumen, has been studied of the reaction with ethylene in presence of Siral40. Ethylene was selected as alkylation olefins, instead of 1-hexene as in Chapters 3 and 4, to reduce the potential impact of steric bulk of the alkylated asphaltenes in this heterogeneous catalyst, as opposed to the homogeneous catalysts employed in Chapters 3 and 4. The same reaction with propylene instead of ethylene is reported in Chapter 6.

5.2 Experimental

5.2.1Materials

The feed material, industrially precipitated asphaltenes, is the same as characterized in Chapter 3 Section 3.2.1.

Ethylene (>99%) was purchased from Praxair. Methylene chloride (≥99.5%) and *n*-pentane (≥98%) were purchased from Fisher Scientific. Siral 40 (silica-doped silica-alumina, with 40 wt% SiO_2 content) was purchased from SASOL Germany GmbH. Nitrogen (99.999%) gas cylinder was purchased form Praxair.

5.2.2 Experimental procedures

Siral 40 was calcined in Carbolite CWF 11/13 furnace at 550 °C for 6 hours in air before reaction. For the experiment, 5.54 g asphaltene was ground into a powder and mixed with 0.90 g calcined Siral40 in a glass vial. The glass vial was then placed in a micro-batch reactor and sealed. Then nitrogen gas was used to pressurize the reactor to do a leak test. The original air sealed in reactor was not purged before performing the leak test, so that some oxygen may have remained in the reactor. After the leak test, gas was released through the end of tubing to go back to atmosphere pressure and then the reactor was pressurized with ethylene. The mass of ethylene added was 0.34 g. The mass of ethylene was determined by weighing the reactor before and after being pressurized with ethylene.

All weighing operations were performed using a Mettler Toledo ML3002E balance, which has a maximum weighing capacity of 3200 g and readability of 0.01 g.

The reactor was constructed using Swagelok 316 stainless steel tubing and fittings. The inner size of reactor is 5.5 inches long and 1 inch diameter. The experiment setup was depicted in **Figure 5-1**. Reactor was immersed in sand bath heater (fluidised bath SBS-4 from Techne) for 24 hours at 325 °C (temperature of sand bath). The pressure of this reaction was self-generated pressure.

After reaction, the reactor was first cooled down to room temperature (~23ºC). Then the released gas was collected in a pre-vacuumed gas bag and analyzed by gas chromatography (GC). The mass of reactor was weighed after releasing gas. The difference between this mass and weight of

reactor pressurized with ethylene was calculated as mass of released gas. The product in the glass vial was dissolved in methylene chloride. This product contained the catalyst, Siral40, and the asphaltene reaction product. The organic reaction product was soluble in methylene chloride while Siral40 catalyst was insoluble. So the methylene chloride solution became dark and had some solids inside. The solids were separated by filtrating the mixture through a 0.22 μm filter paper. Then solids collected on the filter were mixed with methylene chloride again and the procedure to filter it through 0.22 μm filter paper was repeated until methylene chloride remained colorless. The exact amount of methylene chloride was not recorded. Then the solids were only Siral40 after reaction. All liquids were combined to produce a single asphaltene reaction product in methylene chloride solution. Then methylene chloride was removed in a rotary evaporator, a Heizbad Hei-VAP from Heldolph. The heating medium was water, which was heated to 55 °C and the methylene chloride was evaporated under atmospheric pressure over a period of 1 hour. Both the Siral40 and asphaltene reaction products were left in a fume hood to for 2 days for any remaining methylene chloride to evaporate. 1 g of the dried asphaltene reaction product was subjected to the *lab precipitated asphaltene procedure* (refer to Chapter 3 Section 3.2.2).

1. Sand bath
2. Micro batch reactor
3. Glass vial
4. Reactants and catalyst
5. Pressure gauge
6. Needle valve
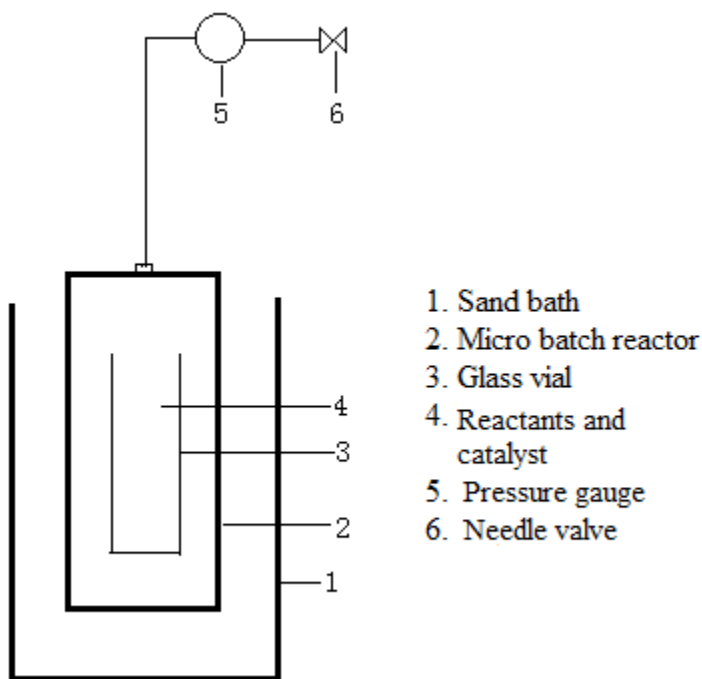
Figure 5-1 Experimental setup

5.2.3 Analysis

GC (Gas chromatography). The instrument used was a 7890A GC system purchased from Agilent Technologies. The method was designed to test olefins containing 1-5 carbons. Helium was the carrier gas and a constant flow of 25mL/min was maintained. The oven program was: (1) 70°C at beginning; (2) from 70°C to 250 °C with rate of 10 °C/min and hold for 2 min; (3) from 250 °C to 70 °C with rate 30 °C/min and hold for 8 min. The instrument was equipped with a flame ionization detector (FID), the front detector, as well as a thermal conductivity detector (TCD), the back detector.

^{1}HNMR (Proton nuclear magnetic resonance), **IR** (Infrared spectroscopy) were described in Chapter 3 Section 3.2.3.

5.3 Results

5.3.1 Product yeild

After reaction, 1.16 g gas was released. After separation, 1.76 g Siral40 and 4.72 g solid reaction product were obtained. Material balance closure was (1.16+1.76+4.72) / (0.34+0.9+5.54) = 113%. It's over 100%. The total mass of Siral40 and asphaltenes before and after reaction were 6.48g and 6.44g respectively. The two values were close and IR spectra of asphaltenes product and catalyst after reaction have proved that no methylene chloride residue was in the product. It was noticed that mass difference between injected ethylene and released gas was huge and this is likely the reason why material balance closure was over 100%.

The Siral40 catalyst was in black in color after reaction, instead of white as it was before the reaction. The catalyst mass after reaction was much higher; it was almost double the mass of the fresh catalyst.

The asphaltenes content in the reaction product was determined using the lab precipitated asphaltenes procedure: 80 wt% asphaltenes and 20 wt% maltenes. The total amount of precipitated asphaltenes after reaction was calculated as 4.72×0.80=3.78 g. The amount of "coke" on the catalyst was 1.76-0.90=0.86g. The amount of lab precipitated asphaltenes in the feed, i.e. "A" in Equation 3.1, was 5.54×0.78=4.32 g. Based on the assumptions outlined the mass of lab precipitated asphaltenes after reaction was 3.78+0.86=4.64 g, which is an increase in asphaltenes content over the feed.

5.3.2 Analysis of asphaltenes products

To see whether ethylene reacted with the asphaltenes and whether new gases were generated during reaction, the gaseous product released from the reactor after reaction was analyzed by GC (**Figure 5-2**).
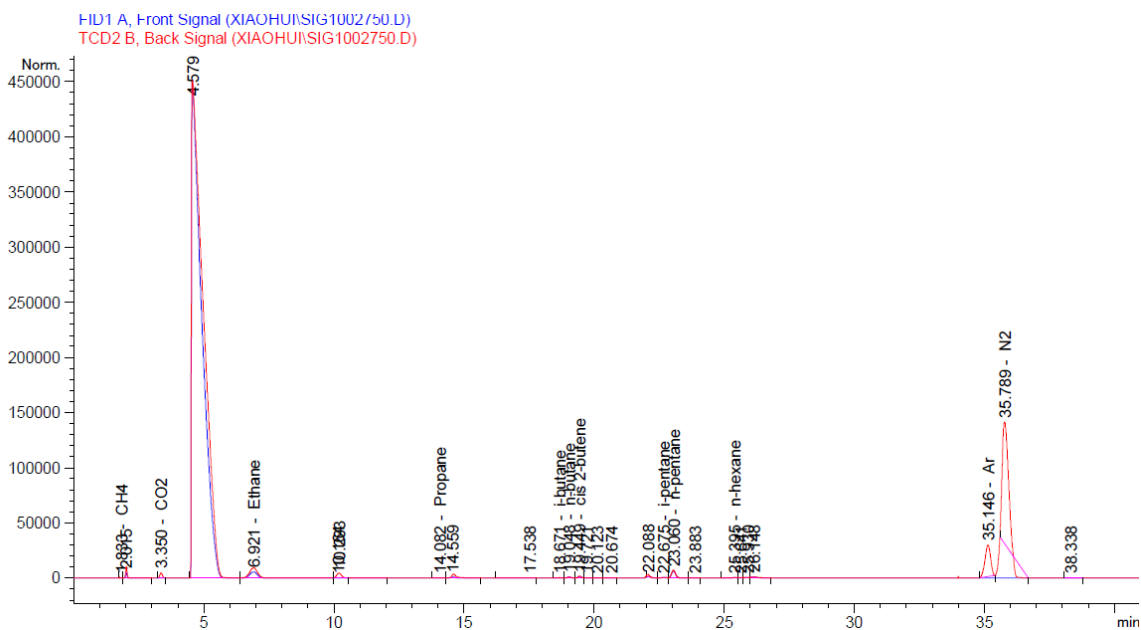
Figure 5-2. GC analysis of gas phase after reaction

From the chromatogram (**Figure 5-2**) it is apparent that ethylene was the dominant product. Nitrogen was the gas used to test air tightness before reaction. In this case, ethylene was actually the only component in released gas. No other gas was generated.

IR and **^{1}HNMR** analyses were done to the asphaltene product after 1g lab precipitated asphaltene procedure.

The IR spectra of lab precipitated asphaltene product (**Figure 5-2**) was very similar to that in **Figure 3-2**, although some differences could be highlighted. The aliphatic/aromatic hydrogen ratio from the ^{1}HNMR analysis was 6.85.

5.4 Discussion

5.4.1 Alkylation of asphaltenes

By comparing IR spectra of industrial asphaltenes feed and asphaltenes product, some peaks were found as new or disappeared peaks in asphaltenes product (see **Figure 5-3**).
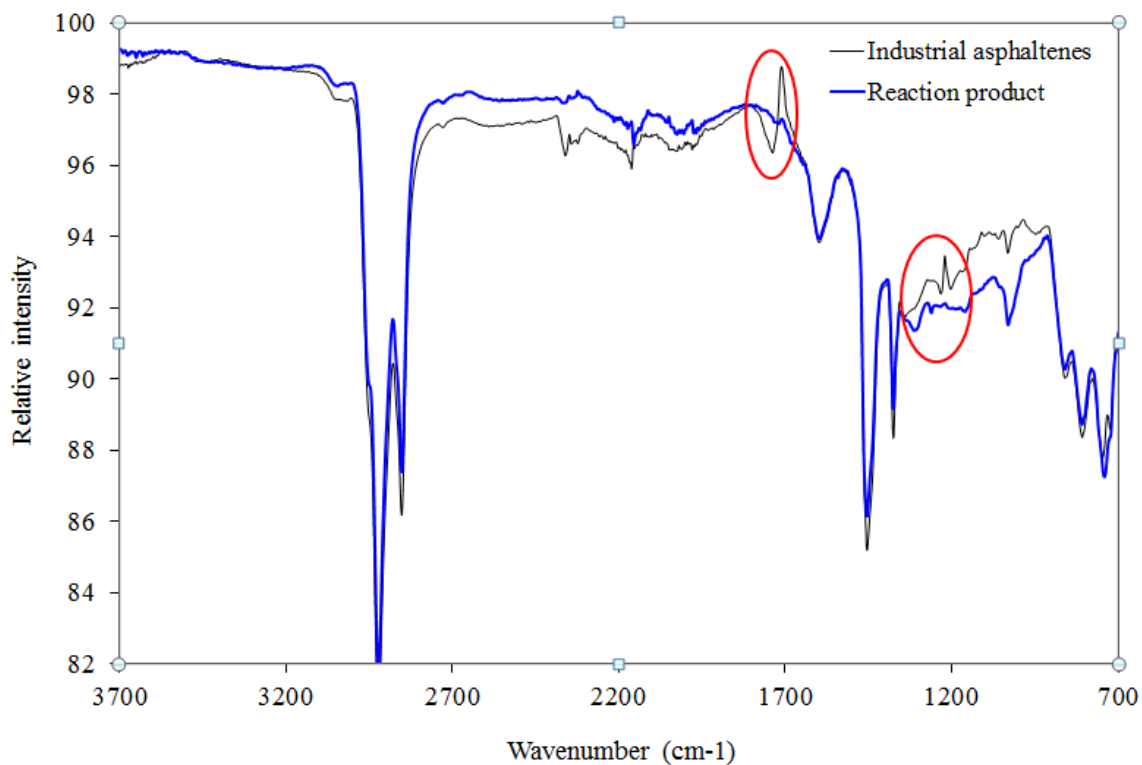
(a)
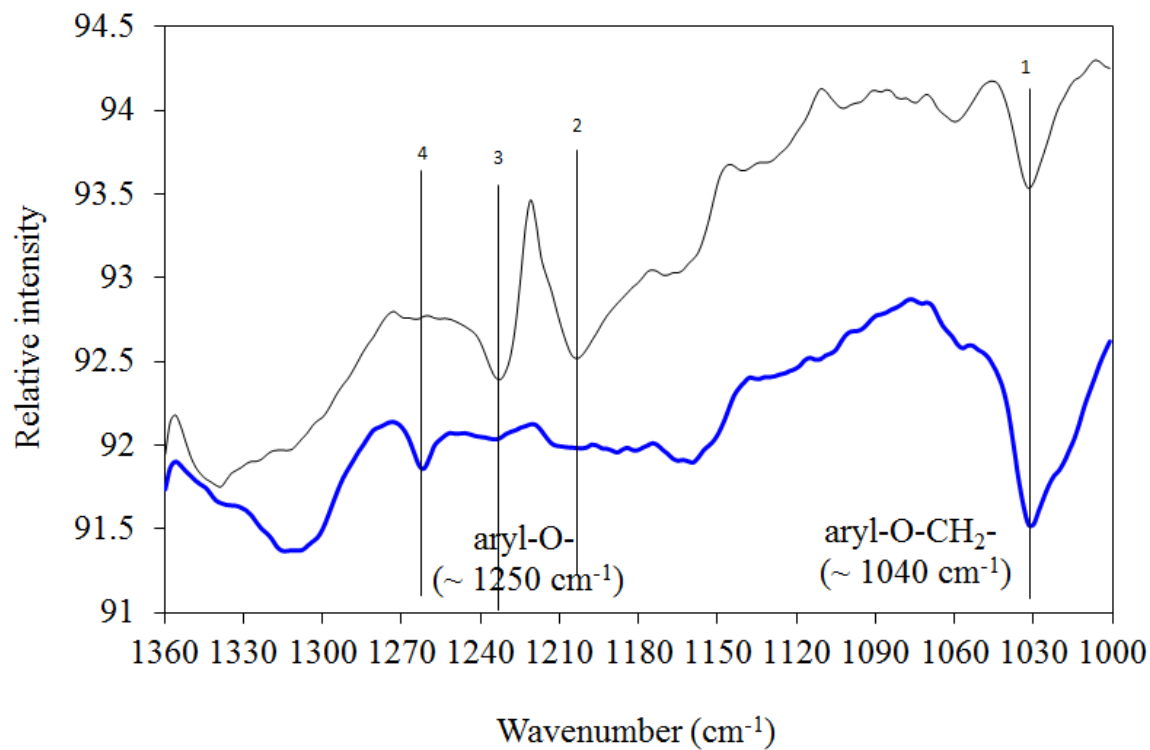
(b)
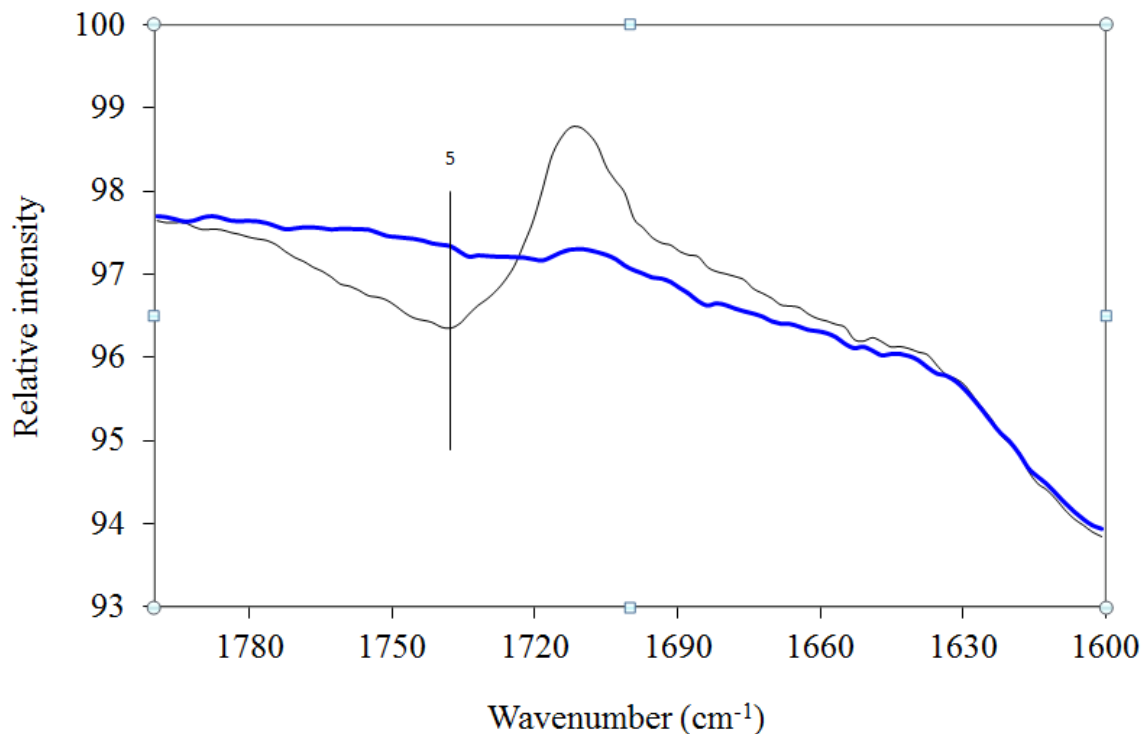
(c)

Figure 5-3. IR spectra of industrial asphaltenes feed and asphaltenes product. (a) full spectra; (b) spectra from 1000cm^{-1} to 1360 cm^{-1} where peak 1 is at 1031 cm^{-1}, peak 2 is at 1203 cm^{-1}, peak 3 is at 1232 cm^{-1} and peak 4 is at 1260 cm^{-1}; (c) spectra from 1600 cm^{-1} to 1800 cm^{-1} where peak 5 is at 1735 cm^{-1}.

The signal in peak 1 is stronger in asphaltenes product. And peak 4 is a new peak. This shows an indirect evidence of aryl-O-ethyl compounds. Also, peak 2 and peak 3 almost disappear in asphaltenes product which stand for aliphatic C-O single bond not aryl(C)-O. Peak 5 disappeared in asphaltenes product stand for C=O double bond. From the discussion above, it is likely that C=O were alkylated to form aryl-O-ethyl groups. C-O may also be alkylated. But C-O-R groups is not obvious to see.

5.4.2 Asphaltenes to maltenes conversion

The lab precipitated asphaltenes content of the feed material was determined and reported in Chapter 3 Section 3.3, namely, 78 wt%. This value was used as blank to compare with the lab

precipitated asphaltene content of the reaction product obtained after the reaction with ethylene over ASA, which was 80 wt%.

Interpretation was complicated by two factors. One is that alkylated ethylene that did not result in asphaltenes to maltenes conversion would increase the mass of asphaltenes. The other is that the catalyst had a high "coke" content, since the Siral40 catalyst mass increased and it turned black. This suggested that some of asphaltenes products may coke or was stuck with Siral40. In this case, the calculated total amount of precipitated asphaltenes after reaction should include the some or all of the carbonaceous products that remained on the catalyst.

5.4.3 Product properties

The aliphatic/aromatic hydrogen ratio was 5% lower than that of lab precipitated asphaltenes (refer to **Table 3-3**). It showed that the aliphatic to aromatic hydrogen ratio decreased a little bit. Since asphaltenes product was split into two parts, one was the precipitated asphaltenes and the remainder was associated with Siral40. It is likely that the product associated with the Siral40 was more carbonaceous, i.e. more aromatic, which implies that there was an overall deterioration in the aliphatic/aromatic hydrogen ratio.

For IR spectra, the hydrocarbon peaks are similar in asphaltenes feed and asphaltenes product generally speaking. However, some changes in the oxygenate composition can be seen and was discussed in section 5.4.1. The alkylation of C=O or C-O group may happen to form a C-O-R structure.

5.5 Conclusions

- Only indirect evidence of ethylene alkylation could be provided based on what appeared to be the appearance of aryl(C)–O–ethyl groups after reaction. The alkylation of asphaltenes is very limited based on all analyses.
- No net asphaltenes to maltenes conversion was found and the H/C ratio of the asphaltenes decreased somewhat during the reaction. Overall no benefit was observed from reacting asphaltenes with ethylene over Siral40.

References

1.	Pieta, I. S.; Ishaq, M.; Wells, R. P. K.; Anderson, J. A., Quantitative determination of acid sites on silica-alumina. *Appl Catal a-Gen* **2010,** *390* (1-2), 127-134.

2.	Trombetta, M.; Busca, G.; Rossini, S.; Piccoli, V.; Cornaro, U.; Guercio, A.; Catani, R.; Willey, R. J., FT-IR studies on light olefin skeletal isomerization catalysis III. Surface acidity and activity of amorphous and crystalline catalysts belonging to the SiO(2)-Al(2)O(3) system. *J Catal* **1998,** *179* (2), 581-596.

3.	Finocchio, E.; Busca, G.; Rossini, S.; Cornaro, U.; Piccoli, V.; Miglio, R., FT-IR characterization of silicated aluminas, active olefin skeletal isomerization catalysts. *Catal Today* **1997,** *33* (1-3), 335-352.

4.	Xia, Y. Acid catalyzed aromatic alkylation in the presence of nitrogen bases. University of Alberta, 2012.

5.	de Klerk, A.; Nel, R. J. J., Phenol alkylation with 1-octene on solid acid catalysts. *Ind Eng Chem Res* **2007,** *46* (22), 7066-7072.

6. Asphaltene behavior in silica alumina catalyzed reaction with propylene

Abstract

In this chapter an alternative alkylating agent, propylene, was employed to react with asphaltenes in presence of Siral40. An obvious improvement has been achieved after reaction. Meaningful conversion of asphaltenes to maltenes was observed and this was tentatively attributed to scission of bringing links in some of the asphaltenes molecules.

Key words: Siral40, propylene, alkylation, asphaltene

6.1 Introduction

In Chapter 2 and Chapter 5 the characteristics of amorphous silica alumina catalyzed reactions were discussed. This chapter is a continuation of the work in Chapter 5. The same silica alumina catalyst (Siral40) is employed, but with a different alkylating agent: propylene instead of ethylene.

To diminish potential steric effects of alkylating asphaltenes in a heterogeneous catalyst, ethylene was employed in Chapter 5. However, reaction over Siral40 did not result in an obvious improvement. Viewed retrospectively, the demanding reaction requirements for ethylene proved to be more detrimental than the anticipated benefit of reduced steric bulk of the alkylated products.

The demanding reaction requirements can be explained in terms of the molecular structure of ethylene. Ethylene has only primary carbons and protonation is more demanding because it would result in the formation of a primary carbocation. Propylene on the other hand has one secondary carbon. A secondary carbocation is more readily formed and alkylation with propylene causes only a single carbon increase in the steric bulk of the alkylated products compared to ethylene. So ethylene is less active than propylene and only somewhat smaller.

Propylene was employed in this chapter as alkylating agent. The reaction products from the reaction of asphaltenes and propylene catalyzed by Siral40 were analyzed and discussed.

6.2 Experimental

6.2.1 Materials

The feed material, industrially precipitated asphaltenes, is the same as characterized in Chapter 3 Section 3.2.1.

Propylene (>99%) was obtained from Praxair. The catalyst, and other chemicals and cylinder gases were the same as listed in Chapter 5 Section 5.2.1.

6.2.2 Experimental procedures

This experiment was performed in triplicate. The amount of reactants employed in each experiment is shown in **Table 6-1**. The equipment, catalyst preparation and all other procedures were the same as described in Chapter 5 Section 5.2.2.

Table 6-1. Amount of reactants and catalyst used in each experiment that was performed at 325 °C, self-generated pressure and 24 hours reaction time.

No.	Asphaltene/g	Calcined Siral40/g	Propylene/g
1	5.01	1.15	1.43
2	5.04	1.01	1.18
3	4.97	1.05	1.20

6.2.3 Analyses

The analytical equipment used for the analysis of reaction products were the same as previously described in Chapter 3 Section 3.2.3 and Chapter 5 Section 5.2.3. The instruments used were: TGA (Thermogravimetric analysis), ^{1}HNMR (Proton nuclear magnetic resonance), CHNS elemental analyser, IR (infrared spectrometer) and GC (Gas chromatograph) equipped with flame ionization detector (FID) and thermal conductivity detector (TCD).

6.2.4 Calculations

a) Mass of component i in released gas was calculated as below.

First, in GC-TCD graph, peak area of a certain compound i is proportional to mole of compound i. In this way, the mole% of compound i can be calculated as

$$\frac{Area(TCD)_i}{\sum Area(TCD)_i} = \frac{Mole_i}{\sum Mole_i} = mol\% \text{ of } i \qquad\qquad 6.1$$

Where i is the compound in GC-TCD analysis.

Then, mass percent of compound i was calculated by multiplying molar mass to mole percent

$$\frac{(mol\% \text{ of } i) \times M_i}{\sum (mol\% \text{ of } i) \times M_i} = mass\% \text{ of } i \qquad\qquad 6.2$$

Where M is the molar mass of compound i.

So, the mass of compound i was calculated based on total mass and mass percent of i.

$$mass \text{ of } i = (mass\% \text{ of } i) \times (mass \text{ of released gas}) \qquad\qquad 6.3$$

b) The mass of reacted propylene was calculated by mass difference between propylene before and after reaction.

$$M_a - M_r = M_p \qquad\qquad 6.4$$

Where M_a is mass of added propylene before reaction; M_r is mass of propylene in released gas after reaction; M_p is mass of reacted propylene.

6.3 Results

6.3.1 Product yields

After reaction, the reactor was cooled down to room temperature (~23°C). The mass of reactor was recorded. Then the reactor was depressurized; the gas was released and stored in a gas bag for GC analysis. The mass of the depressurized reactor was recorded. Mass of released gas was calculated by the mass difference between the reactor after reaction and after releasing gas (**Table 6-2**).

Table 6-2. Mass of released gas

No.	Mass of released gas
1	1.07
2	0.82
3	0.76

The mass of Siral40 catalyst after reaction is shown in **Table 6-3**. In all experiments the mass of the catalyst increased and the color of the catalyst after reaction was black.

Table 6-3. Mass of Siral40 after reaction

No.	Catalyst after reaction/g
1	2.34
2	1.80
3	3.20

The total mass of the Siral40 and asphaltenes product before separation were 5.85 g, 6.08 g and 6.10 g in reactions No.1, No.2, and No.3 respectively. After separation, some of the asphaltenes product from reaction No.2 was lost during transportation due to human error. So its mass was much lower than that in No.1 and No.3. So the mass of asphaltenes product after separation with Siral40 were 3.50 g, 1.40 g and 3.60 g.

If we consider the mass of Siral40 and asphaltenes before separation, the mass balance could be calculated as shown in **Table 6-4**.

Table 6-4. Mass balance based on the mass before Siral40 and asphaltenes product separation.

No.	Mass before reaction/g (asphaltenes feed+propylene+siral 40)	Mass after reaction/g (gas+(siral40+asphalte-nes product))	Balance
1	5.01+1.15+1.43=7.59	1.07+5.85=6.92	6.92/7.59=91.2%
2	5.04+1.01+1.18=7.23	0.82+6.08=6.90	6.90/7.23=95.4%
3	4.97+1.05+1.20=7.22	0.76+6.10=6.86	6.86/7.22=95.0%

The mass of asphaltenes product obtained from performing the *lab precipitated asphaltenes* procedure on 1.00 g of the reaction product is shown in **Table 6-5**.

Table 6-5. The asphaltene and maltene content determined by the Lab precipitated asphaltene analysis procedure using 1.00 g reaction product

No.	1g lab precipitated asphaltenes procedure		
	Asphaltenes/g	Maltenes/g	Asphaltene (wt%)
1	0.66	0.34	66
2	0.51	0.49	51
3	0.64	0.36	64
Average ± Standard deviation			60 ± 8

From **Tables 6-2 to 6-5** several observations were made: (1) The mass of gas decreased after reaction. (2) The mass of Siral40 increased after reaction, but varied significantly from reaction to reaction. (3) The mass percentage of asphaltenes in the reaction product was lower than that in the asphaltenes feed (Chapter 3 section 3.3.1).

6.3.2 Analyses of asphaltenes products

Firstly the composition of the released gas after reaction was determined by gas chromatography and a representative chromatogram is shown in **Figure 6-1**. Propylene was the only major component of the gas, apart from the inert gases. Only minor amounts of other hydrocarbons were detected. In all instances the amount of product gas (**Table 6-2**) was less than the propylene added in the feed (**Table 6-1**). The calculation of propylene converted would be further discussed in Section 6.4.1.
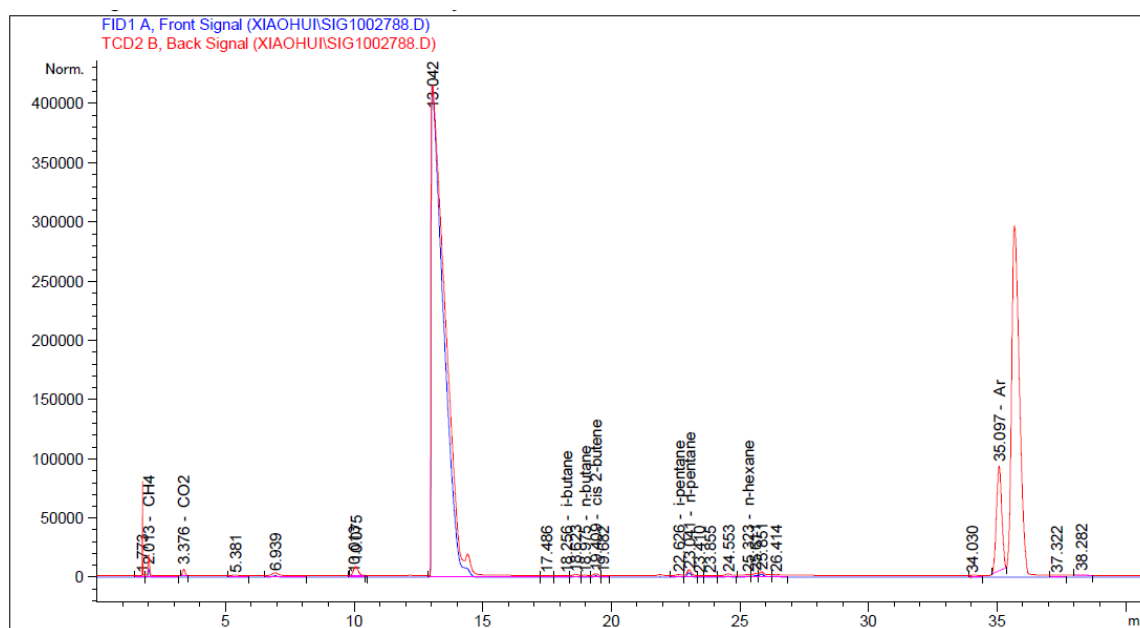
Figure 6-1. GC-FID and GC-TCD chromatogram of the gaseous product after reaction, as illustrated by the released gas in experiment no.3

Secondly, to verify the changes of the Siral40 catalyst, TGA was performed of the calcined siral40 used in the reaction, both before and after reaction (**Figure 6-2**).
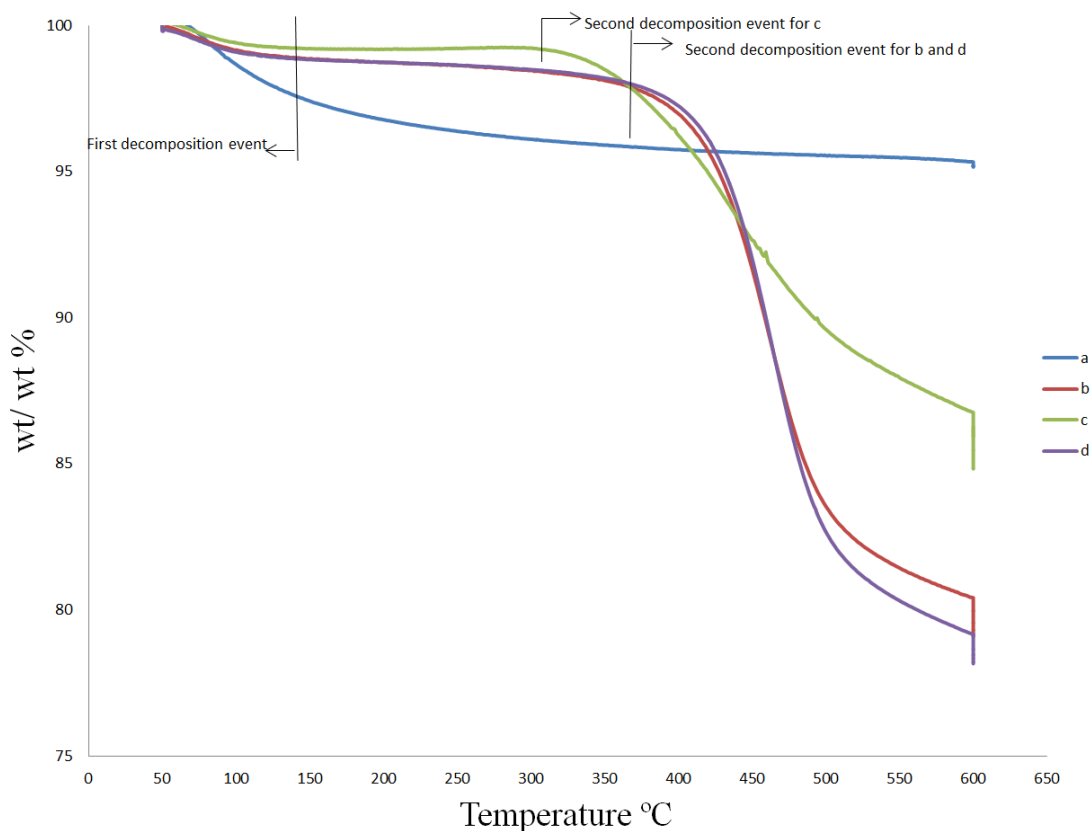
Figure 6-2. (a): pure calcined siral40; (b)(c)(d): calcined siral40 after reaction in No.1, No.2 and No.3 respectively. The TGA anlysis was done under atmosphere of N_2.

For **Figure 6-2** (a), first thermal decomposition started at around 93 °C and the residual mass was 95 wt%. No second decomposition. For **Figure 6-2** (b), the first thermal decomposition event started at around 93 °C and second started at 365 °C, the residual mass was 79 wt%. For **Figure 6-2** (c), the first thermal decomposition event started at around 91 °C and second started at 325 °C, the residual mass was 85 wt%. For **Figure 6-2** (d), the first thermal decomposition

event started at around 95 °C and second started at 370 °C, the residual mass was 78 wt%. In all instances the residual mass was the combined mass of the catalyst and coke.

Thirdly, CHNS analysis was done of the asphaltenes product obtained from the *lab precipitated asphaltenes* procedure to see whether there is any change in the CHNS elemental composition. The results from CHNS analysis are shown in **Table 6-6**. The asphaltenes product from the *lab precipitated asphaltenes* procedure in reaction No.1 will be referred to as "product 1". The same holds for the asphaltenes from the other two reactions, which will be referred to as "product 2" and "product 3".

Table 6-6. CHNS elemental analysis of asphaltenes from the *lab precipitated asphaltenes* procedure (product 1, 2 and 3).

Product	C (wt%)	H (wt%)	N (wt%)	S (wt%)
1	81.65±1.02	8.01±0.53	1.18±0.06	9.38±0.67
2	82.08±0.03	7.70±0.02	1.18±0.00	7.65±0.10
3	82.14±0.41	7.63±0.09	1.16±0.02	7.86±0.12

Compared with CHNS data in **Table 3-2**, the content of elements were in same range except sulfur. Content of sulfur in product 1 was much higher than the other two. For sulfur content in product 2 and product 3, it's about 0.5 wt% higher than that in **Table 3-2**. So, even if some asphaltenes were converted into maltenes, the CHNS elemental composition of the remainder of the asphaltenes was not obviously different from that of the asphaltenes feed.

The reason why sulfur content slightly increased may due to two reasons: 1) the standard deviation of sulfur in product 1 was high, which shows variability in the analyses. In other words, the analysis of the sulfur content of product 1 was not that reliable. The origin of the variability is not known; 2) asphaltenes that contained sulfur were less efficiently converted in this experiment, while the overall conversion was more (**Table 6-5**), so that the total mass of asphaltenes decreased that lead to an increase of sulfur wt%.

C/H ratio in products 1, 2 and 3 were calculated as 1/1.18, 1/1.12 and 1/1.11. The C/H ratio in **Table 3-2** was calculated as 1/1.11. In this case, product 1 and 2 may be slightly alkylated. The alkylation of product 3 cannot be seen from CHNS analysis.

Fourth, aliphatic/aromatic hydrogen ratio was calculated from the ^{1}HNMR spectra. The results were 5.94, 5.33, 5.24 for product 1, 2 and 3. Compared with aliphatic/aromatic hydrogen ratio data in **Table 3-2** that was 7.21, all three products had a decreased aliphatic/aromatic hydrogen ratio. Product 1 had highest ratio while the other two were lower.

Next, IR spectra of product 1, 2 and 3 were compared with IR of lab precipitated asphaltenes from the industrial asphaltenes feed (see **Figure 3-2**). The three products were very similar and the IR analysis is shown in **Figure 6-3** with data from product 2 as representative.
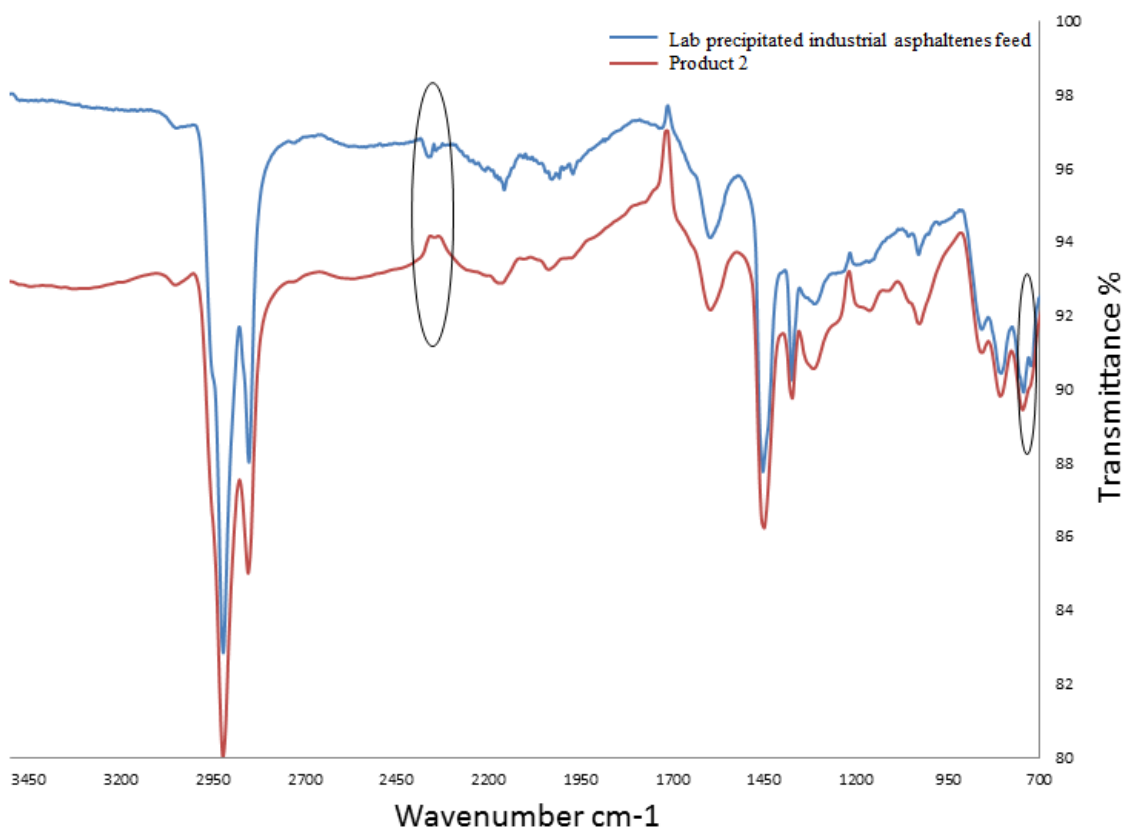
(a)
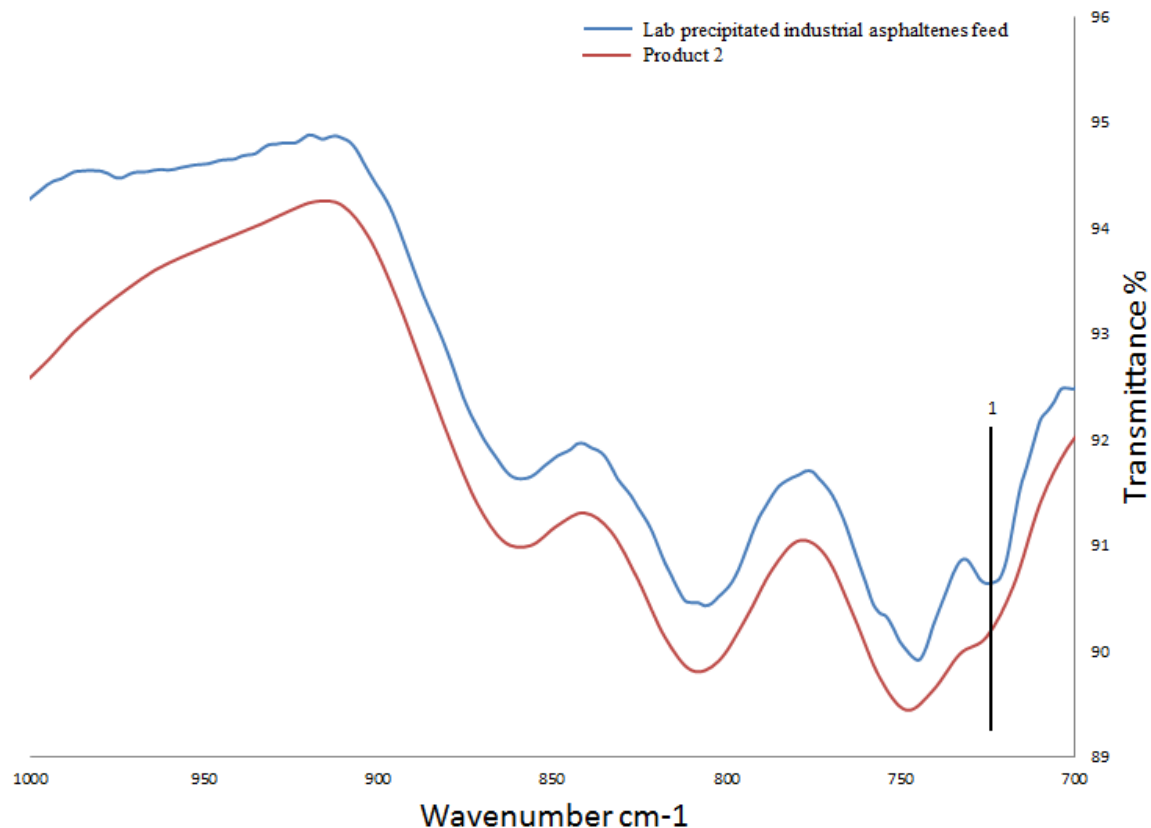
(b)

Figure 6-3. IR spectra of product 2 and lab precipitated industrial asphaltenes feed, (a) whole spectra where the difference were highlighted in black circle; (b) spectra from 700 cm^{-1} to 1000 cm^{-1} where peak 1 is at 723 cm^{-1}.

Peak 1 was diminished in IR spectra of product 2. Peak 1 represents adjacent C–H wag vibrations on the aromatics. If aromatics were alkylated, the number of adjacent of C–H groups in product 2 would be reduced compared to feed. In this case, product 2 was slightly alkylated as same as product 1 and 3. In another word, besides the converted asphaltenes, the rest of asphaltenes were slightly alkylated.

The difference around 2350 cm^{-1} is due to atmospheric CO_2. When the background spectrum is not collected near the time of analysis, minor variations due to CO_2 can often be observed in the infrared spectrum. CO_2 has a strong absorption in the 2350-2340 cm^{-1} range.[2]

6.4 Discussion

6.4.1 Mass of propylene reacted with asphaltenes

Using **Equations 6.1-6.4**, the composition of released gas was calculated from the GC-TCD analysis (**Table 6-7**). The mass of reacted propylene was subsequently calculated in **Table 6-8**, which was also expressed in terms of propylene conversion and conversion relative to the mass of catalyst and mass of asphaltenes feed.

Table 6-7. Mass fraction of hydrocarbon gases in the released gas

Compounds	Mass fraction of hydrocarbons		
	No.1	No.2	No.3
Methane	0.010	0.004	0.003
Propylene	0.933	0.989	0.987
Propane	0.057	0.007	0.010

Table 6-8. Mass of reacted propylene

Description	No.1	No.2	No.3
Mass propylene reacted/g	0.43	0.37	0.45
Propylene converted/(g/g catalyst)	0.18	0.21	0.14
Propylene converted/(g/g asphaltenes)	0.086	0.073	0.091
Conversion of propylene/%	30	31	38

From the data above, we can see that though under the same reaction conditions there was some variation in the results. However, the results also show that both the catalyst and the asphaltenes

content contributed to the observed conversion of propylene. The highest amount of propylene converted per mass of catalyst was also the lowest mass of propylene converted per mass of asphaltenes. Conversely, the least amount of propylene converted per mass of catalyst was also the most mass of propylene converted per mass of asphaltenes. The variation in mass of propylene converted can partly be explained by differences in the relative amounts of materials, although the impact of transport restrictions cannot be ruled out.

6.4.2 Catalyst after reaction

Comparing data in **Table 6-3** and **Table 6-1**, the mass of Siral40 increased after reaction. What has been observed was white Siral40 cannot be seen after reaction. And it stayed black even after washing by methylene chloride and separating from products. The asphaltene might coke or stick to Siral40. This was in agreement with the TGA mass loss. **Figure 6-2 (a)** is pure calcined Siral40 before reaction, the mass residue of which is 95 wt%. Based on the mass residue of **Figure 6-2** (b) to (d), it is that some asphaltenes coked and stuck with catalyst. The calculations of coked asphaltenes shows as below (**Table 6-9**).

Table 6-9. Calculation of mass of coked asphaltenes with catalyst.

No.	Mass of catalyst after TGA if no reaction happened/g	Real mass of catalyst after TGA /g	Mass of coked asphaltenes with catalyst/g
1	1.15×0.95=1.1	2.34*0.79=1.8	1.8-1.1=0.70
2	1.01×0.95=0.96	1.80×0.85=1.5	1.5-0.96=0.54
3	1.05×0.95=1.0	3.2×0.78=2.7	2.7-1.0=1.7
No.	Coked asphaltenes/(g/g catalyst)		
1	0.70/1.15=80%		
2	0.54/1.01=53%		
3	1.7/1.05=160%		

From **Table 6-5**, we can see that the second experiment had lowest asphaltenes wt% which meant highest percentage of converted asphaltenes. One reasonable explanation for that could be catalyst in second experiment had highest catalyzed ability. **Table 6-9** showed the least coke asphatlene/catalyst in second experiment. Anyway, other two groups also suggested that asphaltenes were converted into maltenes.

6.4.3 Alkylation of asphaltenes

Asphaltenes feed were definitely alkylated because it was converted into maltenes and propylene was reacted. Now the questions are 1) what happened to the asphaltenes that not turned into maltenes and 2) which part of asphaltenes were converted into maltenes.

For the first question, the alkylation of rest asphaltenes was very limited. It could be inferred from CHNS and IR test. Besides, the rest asphaltenes part became heavier than before as some parts turned into maltenes by aliphatic/aromatic hydrogen ratio from ^{1}HNMR analysis. And the more maltenes it converted the lower aliphatic/aromatic hydrogen ratio it had. Reaction No.1 generated least maltenes conversion (see **Table 6-5**) and product 1 had highest aliphatic/aromatic hydrogen ratio as well as C/H ratio. The aliphatic/aromatic hydrogen ratio and C/H ratio for product 2 and 3 was almost the same, which was the lowest among three products. And reaction No.2 generated most maltenes conversion while reaction No.3 generated the second most maltenes conversion.

For the second question, it was probably that the parts with higher aliphatic/aromatic hydrogen ratio in asphaltenes feed were converted into maltenes based on the discussion and analyses above. It is speculated that the alkylation resulted in scission of aliphatic bridging heteroatoms, such as sulfides (thioethers). This topic was further investigated in the next chapter.

6.5 Conclusion
- Dark liquid product was directly generated after reaction
- Generally, propylene was proved to react with asphaltenes. Asphaltenes were partly converted into maltenes. The results varied even though reactions were under same conditions. But the trends were same.
- Catalyst activity was affected during reaction.
- The remaining asphaltenes after reaction were heavier than before.

Reference

1. Hensen, E. J. M.; Poduval, D. G.; Magusin, P. C. M. M.; Coumans, A. E.; van Veen, J. A. R., Formation of acid sites in amorphous silica-alumina. J Catal 2010, 269 (1), 201-218.

2. Dolphin, D.; Wick, A. *Tabulation of infrared spectral data*; Wiley: New York, 1977, p. 486.

7. Two model compounds behavior in reaction with silica-alumina catalyst

Abstract

Two model compounds, dibenzyl sulfide and benzyl phenyl sulfide, were alkylated with propylene in presence of Siral40 at the same conditions as in Chapter 6. The function of catalyst and olefins is discussed and cleavage of bridging S-C bonds is suggested as an explanation for the asphaltenes to maltenes conversion observed in Chapter 6.

Key words: Siral 40, propylene, alkylation, dibenzyl sulfide, benzyl phenyl sulfide

7.1 Introduction

In Chapter 5 and Chapter 6, the reaction of ethylene and propyene with asphaltenes catalyzed by Siral40 has been discussed. An obvious asphaltenes to maltene conversion was observed in Chapter 6. This phenomenon was special and differed from all other experiments before. It indicated a modification of the asphaltenes structure. Thus, it became very important to figure out in which way the structure was modified. However, the composition of the asphaltenes fraction is so complex that the investigation of interactions between Siral40, olefins and asphaltenes are affected by multiple factors which cannot be seen clearly from the analysis of the complex product mixtures.

It was speculated that at 325 °C alkylation was accompanied by cracking of sulfur-containing bridges between aromatic "cores". The heteroatom in sulfides (thioethers) can be eliminated as H_2S over an acid catalyst at high temperature in a reaction analogous to the elimination of H_2O from ethers.[1] This reaction does not require propylene, but propylene acts as moderator by reacting with the olefinic fragment from the elimination reaction. The temperature is also high enough for some thermal cracking of aliphatic C–S bonds and propylene may also have played a role in stabilizing the free radical intermediates, either by addition, or by hydrogen transfer to form a resonance stabilized allylic radical derived from the propylene.

Thus, model compounds were selected to interrogate the hypothesis and substitute for asphaltenes. In this chapter, two model compounds have been selected which represent aromatic rings linked by sulfide bridges in asphaltenes. They are dibenzyl sulfide and benzyl phenyl sulfide.

7.2 Experimental

7.2.1 Materials

Dibenzyl sulfide (99%) and benzyl phenyl sulfide (98%) was purchased from Alfa Aesar. Propylene (>99%) in a cylinder was bought from Praxair. Methylene chloride (≥99.5%) and *n*-pentane (>98%) were purchased from Fisher Scientific. Chloroform (99.8%) was purchased from Fisher Scientific. Siral40 (silica-doped silica-alumina, with 40 wt% SiO_2 content) was obtained from SASOL Germany GmbH and calcined for 6 hours in air at 550 °C before use.

7.2.2 Experimental procedures

The same experimental procedure as described in Chapter 5 Section 5.2.2 was followed for these experiments. The main difference was that the asphaltenes were substituted for one of the two model compounds.

Dibenzyl sulfide (DBS). 6.23 g dibenzyl sulfide and 2.91 g calcined Siral40 were mixed well in a glass vial and sealed in micro batch reactor with 1.66 g propylene. The reactor was put in sand bath at 325 °C for 24 hours under self-generated pressure. After reaction, all dibenzyl sulfide was converted into a liquid product. Siral40 (after reaction) was analyzed by TGA and the reaction products were analyzed by gas chromatography coupled with mass spectrometry (GC-MS), flame ionization detector (GC-FID), thermal conductivity detector (GC-TCD) and flame photometric detector (GC-FPD).

Benzyl phenyl sulfide (BPS). 4.80 g benzyl phenyl sulfide and 2.50 g calcined Siral40 were mixed well in a glass vial and sealed in micro batch reactor with 1.36 g propylene. After reaction, all benzyl phenyl sulfide was converted into a liquid product. The same analytical protocol as for dibenzyl sulfide was followed.

Control Experiment 1. The dosage of control experiment 1 was shown in **Table 7-1**. The main difference from the procedure in Chapter 5 Section 5.2.2 were 1) propylene was changed to

nitrogen; 2) asphaltenes were substituted by BPS; 3) The direct generated liquid after reaction was separated from the liquid washed out by methylene chloride.

Control Experiment 2. The dosage of control experiment 2 was shown in **Table 7-1**. The main difference from procedure in Chapter 5 Section 5.2.2 were 1) no siral 40 was added; 2) asphaltenes were substituted by BPS; 3) The direct generated liquid after reaction was separated from the liquid washed out by methylene chloride.

Table 7-1. Dosage of two control experiments.

Control Experiments	BPS/g	Siral 40/g	N_2/g	Propylene/g	Total/g
1	3.88	1.70	1.26	N/A	6.84
2	3.73	N/A	N/A	2.34	6.07

7.2.3 Analyses

The analytical equipment used for the analysis of catalyst and reaction products were the same as previously described in Chapter 3 Section 3.2.3 and Chapter 5 Section 5.2.3. The instruments used were TGA (Thermogravimetric analysis), GC-FID and GC-TCD.

Additionally the compounds in the liquid products were identified using GC-MS. The GC–MS analyses were carried out using an Agilent 7820A GC connected to a 5977E MS detector. The system was equipped with a 30 m × 0.25 mm × 0.25 μm HP-5MS J&W capillary column. Helium was used as the carrier gas at a constant flow rate of 1 mL/min and 1 μL of sample was introduced via split injection mode (split ratio10:1). The oven temperature program was started at 90 °C and held for 2 min; then, the temperature was raised up to 320 ºC at a rate of 5 °C·min^{-1} and held for 1 min. The transfer line was kept at 325 °C. Mass detection was operated at full scan mode (mass to charge ratio range 50-550 m/z) at a rate of 2.5 scans per second. The ion temperature source was set at 230 °C. Compounds were identified by comparing the mass

spectra of the products with those from the National Institute of Standards and Technology (NIST) through the NIST MS Search 2.0 – Mass Spectra Library.

To assist with confirmation of sulfur products, the liquids were also analyzed using GC-FPD. The instrument was a 7890A GC system purchased from Agilent Technologies with column Agilent 19091S-001 50m×200μm×0.5μm. The program was: (1) 90 °C at beginning and hold for 2 min; (2) from 90°C to 320°C at rate 5°C /min and hold for 1 min. Samples were diluted in chloroform before analysis. The injection volume was 0.3μL. The back detector is a dual FPD (Agilent FPD Plus) with photomultipliers for both sulfur and phosphorus, although only the sulfur signal was employed for this study. The parameters for the FPD were 75mL/min H_2 flow, 100mL/min air flow and 60mL/min N_2 flow.

7.3 Results

7.3.1 Product yields

In the reaction with dibenzyl sulfide, 1.58 g of released gas was obtained after reaction. 4.26 g of Siral40 and 4.87 g of product were recovered. Material balance closure for the reaction was (1.58 + 4.26 + 4.87)/(6.23 + 2.91 + 1.66) = 0.99. The product from the reaction in the presence of dibenzyl sulfide will be referred to as "product 1".

In the reaction with benzyl phenyl sulfide, 0.86 g of released gas was obtained after reaction. Some of product was lost due to improper operation; 3.30 g of Siral40 and 2.00 g of product were recovered. The product from the reaction in the presence of benzyl phenyl sulfide will be referred to as "product 2".

In control experiment 1, the material balance was calculated in **Table 7-2**. After washing materials left in the vial by methylene chloride, 2.22 g Siral40 and 2.67 g product were recovered. The direct generated liquid in control experiment 1 will be referred as "direct product 1 (control)". The liquid product washed out by methylene chloride in experiment 1 will be referred as "washed product 1 (control)".

In control experiment 2, the material balance was calculated in **Table 7-2**. After washing materials left in the vial by methylene chloride, 0.01g solids (coke) and 0.10 g product were recovered. The direct generated liquid in control experiment 2 will be referred as "direct product

2 (control)". The liquid product washed out by methylene chloride in experiment 2 will be referred as "washed product 2 (control)".

Table 7-2. Material balance of two control experiments

Control Experiments	Gas/ g	Direct generated liquid product/g	Materials left in vial/g	Total/ g	Material Balance
1	1.52	1.05	3.72	6.29	6.29/6.84=92%
2	2.09	3.51	0.18	5.78	5.78/6.07=95%

7.3.2 Analyses of products

In reaction with DPS and BPS, two model compounds were 100% converted. It's worth noting that dibenzyl sulfide has a symmetric structure, while benzyl phenyl sulfide has an asymmetric structure. If bond cleavage was similar in these compounds, the number of different compounds formed by reaction of benzyl phenyl sulfide would likely be more than that formed by reaction of dibenzyl sulfide.

In the two control experiments, BPS was 100% converted.

First, GC analysis was done to see the components in gas after reaction. A representative chromatogram is shown in **Figure 7-1**. There was a strong smell of hydrogen sulfide in the gas. The retention time of H_2S was 9.465 min and this was also confirmed by analysis of pure H_2S. This retention time may shift a bit when other types of gases were injected together, for example, in **Figure 7-1** the retention time of H_2S was 9.753 min.
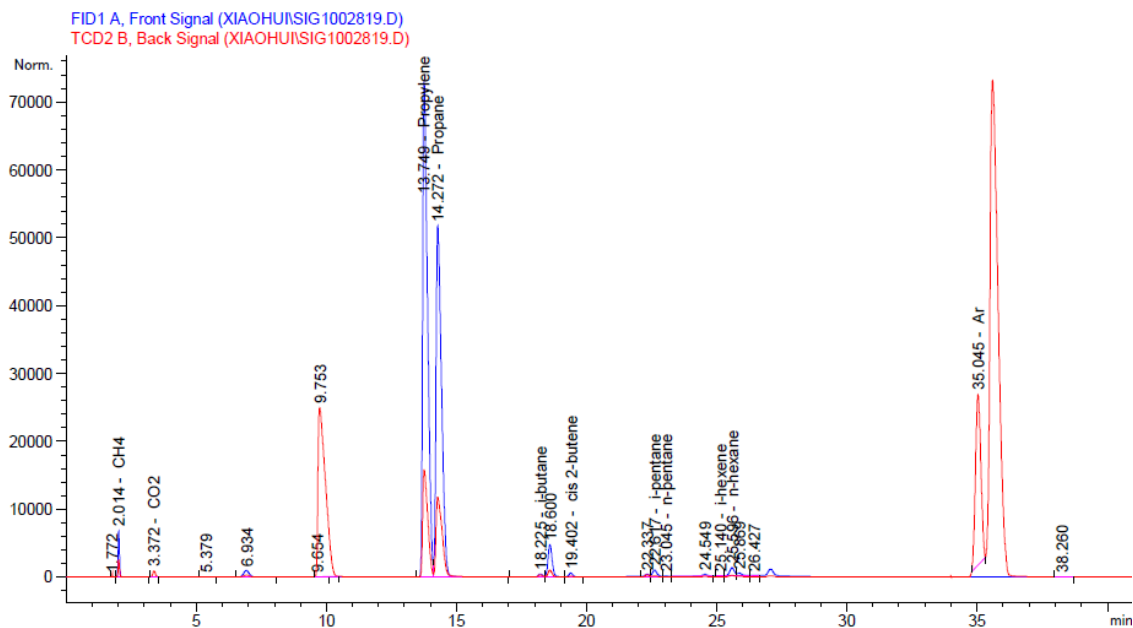
Figure 7-1. GC-FID and GC-TCD analysis of released gas after the reaction of dibenzyl sulfide and propylene over Siral40 at 325 °C for 24 hours.

The composition of the released gas showing only the non-atmospheric sources were calculated by **Equation (1)-(4)** (refer to **Chapter 6 section 6.2.4**). Results were shown in **Table 7-3**. Potential error in this calculation could come from software area integration and the small peaks for other C_1 to C_6 hydrocarbons, which were considered negligible compared to the C_3's and not counted.

Table 7-3. Composition of the released gas.

Released gas in reaction	Propylene		Propane/g		H_2S /g	
	/g	/wt %	/g	/wt%	/g	/wt%
Dibenzyl sulfide	0.15	9.5	0.14	8.9	0.30	19
Benzyl phenyl sulfide	0.23	27	0.24	28	0.23	26

69

Control Experiment 1	N/A	N/A	N/A	N/A	0.16	10
Control Experiment 2	1.86	89	0	0	0.15	7.2

The sulfur release was calculated. In the two model compounds reactions, initially 0.029 mol dibenzyl sulfide and 0.024 mol benzyl phenyl sulfide were present in the reaction mixture. The 0.029 mol dibenzyl sulfide, which contains 0.928 g S, released 0.30 g H_2S. The 0.024 mol benzyl phenyl sulfide, which contains 0.768 g S, released 0.23 g H_2S. Model compounds were the only source of sulfur in this reaction. Therefore, about 30% of S in dibenzyl sulfide and 28.6% of S in benzyl phenyl sulfide was converted into H_2S. 1.51 g propylene was reacted in reaction with dibenzyl sulfide. 1.13 g propylene was reacted in reaction with benzyl phenyl sulfide. In another word, 0.036 mol propylene reacted with 0.029 mol dibenzyl sulfide and 0.024 mol propylene reacted with 0.024 mol benzyl phenyl sulfide.

In the two control experiments, the sulfur conversion (H_2S/BPS wt%) were calculated as 24% and 23% in control experiment 1 and 2 respectively. 0.48 g propylene was reacted in control experiment 2.

Secondly, since the two model compounds contained sulfur and it was shown that only some of the sulfur was released as H_2S, it was worthwhile to check whether any sulfur containing compounds remained in the liquid reaction product. GC-FPD analysis using the sulfur selective photomultiplier was performed. Also, the feed materials, dibenzyl sulfide and benzyl phenyl sulfide, were also analyzed.

From GC-FPD analysis, several points can be found: (1) both dibenzyl sulfide and benzyl phenyl sulfide were 100% converted because no peaks corresponding to the feed was seen in liquid product chromatograms of either products. (2) Besides solvent peaks, only one small peak at 2.04 min retention time was shown in chromatogram of product 1 (chromatogram not included), which was of the same order of the sulfur-containing contaminants in the solvent at ~0.54 min retention time. (3) Besides solvent peaks, three main peaks and five negligible peaks were shown in chromatogram of product 2 (**Figure 7-2**).
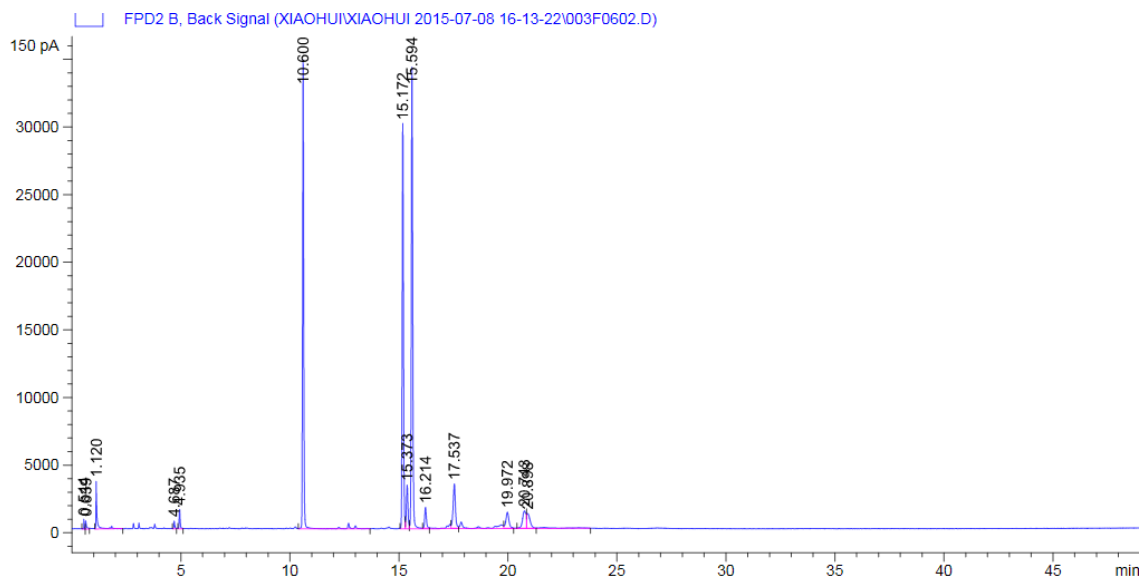
Figure 7-2. GC-FPD analysis of the liquid product (product 2) after the reaction of benzyl phenyl sulfide and propylene over Siral40 at 325 °C for 24 hours.

Based of the GC-FPD analysis only one type of sulfur compound existed in product 1 and was of negligible concentration in the liquid. However, there was more than one type of sulfur compound present in product 2 (**Figure 7-2**) and the sulfur compounds were present in high concentration in the liquid product. These analyses assisted with the GC-MS identification of the products presented at the end of this section.

Thirdly, in two control experiments, the components in direct product 1 (control), washed product 1 (control), direct product 2 (control) and washed product 2 (control) were analyzed by GC-MS and the results can be found in **Table 7- 6**, **Table 7-7**, **Table 7-8** and **Table 7-9**.

Fourth, it was noticed that the mass of Siral40 increased after the reaction. This phenomenon was same as observed in Chapter 5 and 6. So TGA was done to obtain additional information about the organic matter on the catalyst.

For catalyst after reaction of dibenzyl sulfide, the first thermal decomposition started at around 75 °C and second started at 390 °C, the final mass was 88 wt%. For catalyst after reaction of benzyl phenyl sulfide, the first thermal decomposition started at around 75 °C and second started

71

at 385 °C, the final mass was 90 wt%. For catalyst after control experiment 1, the first thermal decomposition started at around 85 °C and second started at 390 °C, the final mass was 93 wt%.

Calcined Siral40 after TGA analysis has 95% mass left. Based on the assumption that all catalyst was recovered after reaction of dibenzyle sulfide, $2.91 \times 0.95 = 2.76$ g catalyst would remain after TGA analysis. The actual remaining mass was calculated as $0.88 \times 4.87 = 4.28$ g. So the increased mass not due to the catalyst was calculated as $4.28 - 2.76 = 1.52$ g, which was the mass of coke. Similarly, based on the assumption that all catalyst was recovered after reaction with benzyl phenyl sulfide, $2.50 \times 0.95 = 2.37$ g catalyst would be remained mass after TGA analysis. The actual remaining mass was calculated as $0.90 \times 3.30 = 2.97$ g. So the increased mass not due to the catalyst was calculated as $2.97 - 2.37 = 0.6$ g, which was the mass of coke.

In control experiment 1, $1.70 \times 0.95 = 1.62$ g catalyst would remain after TGA analysis if there is no reaction. The actual remaining mass was calculated as $0.93 \times 2.22 = 2.06$ g. So the increased mass not due to the catalyst was calculated as $2.06 - 1.62 = 0.44$ g, which was the mass of coke. In control experiment 2, 0.01g coke was generated. Coke comes from reactants that stuck with catalyst in control experiment 1 and were likely addition products of the feed, which could form to a minor extent in the absence of a catalyst, as in control experiment 2.

Table 7-4. GC-MS analysis of product 1.
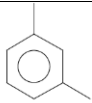
Compound No.	Formula	Structure (example)	Retention time /min	Name	Relative concentration %
1	C_8H_{10}		2.742	Xylene isomers	10.34
2	C_9H_{12}		3.249	Cumene	18.43
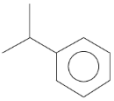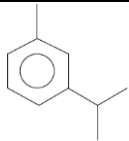
3	$C_{10}H_{14}$		4.519	Cymene isomers	70.50
4	$C_{13}H_{20}$		8.963	Methyl-diisopropyl-benzene isomers	0.38
5	$C_{13}H_{12}$		13.70	Diphenylmethane isomers [a]	0.20
6	$C_{14}H_{14}$		15.80	Bibenzyl	0.14
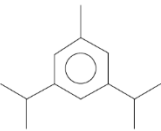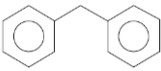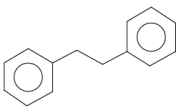
[a] Diphenylmethane and methyl biphenyl isomers.

Last but not least, product 1 and product 2 were analyzed by GC-MS. The results suggested the cleavage of sulfur-carbon bond and alkylation of propylene. Suggested structures in product 1 were shown in **Table 7-4**. No sulfur compounds were identified. Though one sulfur compound was observed in product 1 by GC-FPD it was of such low concentration that it was not seen in the GC-MS chromatogram.

Table 7-5. GC-MS analysis of product 2.

Compound No.	Formula	Structure (example)	Retention time /min	Name	Related Concentration%
1	C_7H_8		2.134	Toluene	25.64
2	C_9H_{12}		3.250	Cumene	47.91
3	$C_{10}H_{14}$		4.519	Cymene isomers	14.59
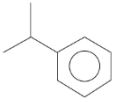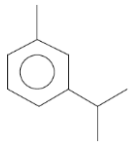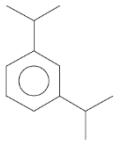
4	$C_{12}H_{18}$		7.005	Diisopropyl-benzene[b]	9.315
5	$C_{13}H_{12}$		13.69	Diphenylmethane isomers [a]	0.2411
6	$C_{12}H_{10}S$		17.34	Diphenyl sulfide	0.5559
7	$C_{13}H_{10}S$		22.33	Thioxanthene	0.7506
8	$C_{12}H_{10}S_2$		22.64	Diphenyl disulfide	0.9881
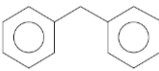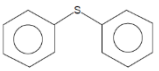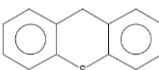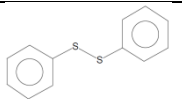
[a] Diphenylmethane and methyl biphenyl isomers.

[b] m-Diisopropyl benzene and p-diisopropyl benzene.

Suggested structures in product 2 were shown in **Table 7-5**. As anticipated from the GC-FPD analysis, some of the compounds in product 2 contained sulfur.

Three sulfur compounds in **Table 7-5** had obvious peaks in MS spectra, which may also be the compounds identified in GC-FPD. The other sulfur compounds identified by GC-FPD were present in low concentration and were not found in the GC-MS chromatogram.

Table 7-6. GC-MS analysis of direct product 1 (control)

Compound No.	Formula	Structure (example)	Retention time /min	Name	Relative concentration %
1	C_8H_{10}		2.742, 2.956	Xylene isomers	2.38
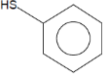
2	C_6H_6S		3.744	Benzenethiol	28.08
3	$C_{13}H_{12}$		13.687	Diphenylmethane	13.49
4	$C_{14}H_{14}$		15.932	Methyldiphenylmethane	1.70
5	$C_{12}H_{10}S$		17.349	Diphenylsulfide	22.89
6	$C_{13}H_{12}S$		22.334	Thioxanthene	22.53
7	$C_{14}H_{12}S$		24.458, 24.672	Dimethyldibenzothiophene	4.46
8	$C_{20}H_{18}$		29.417	Dibenzylbenzene	1.06
9	$C_{20}H_{12}$		38.865	Benzo[k]fluoranthene	3.40
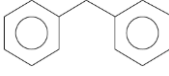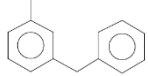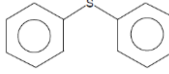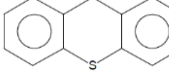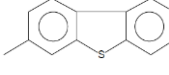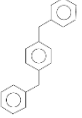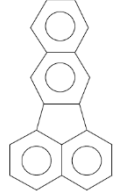
Table 7-7. GC-MS analysis of washes product 1 (control)

Compound No.	Formula	Structure (example)	Retention time /min	Name	Relative concentration %

1	C_6H_6S		3.731	Benzenethiol	12.68
2	$C_{13}H_{12}$		13.667	Diphenylmethane	7.81
3	$C_{14}H_{14}$		15.919	Methyldiphenylm ethane	1.25
4	$C_{12}H_{10}S$		17.322	Diphenylsulfide	20.68
5	$C_{13}H_{12}S$		22.313	Thioxanthene	28.67
6	$C_{14}H_{12}S$		24.665	Dimethyldibenzot hiophene	3.62
7	$C_{20}H_{12}$		38.865	Benzo[k]fluorant hene	25.29
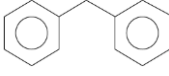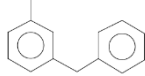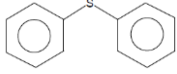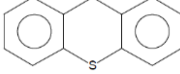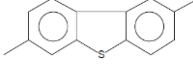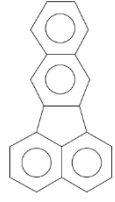
Product 1, 2 in **Table 7-6** and product 1 in **Table 7-7** suggested sulfur-carbon bond cleavage. From the analysis above, it can be seen that direct product has more light component than washed product. The last compound in both tables was considered as a proof of addition reactions.

Table 7-8. GC-MS analysis of direct product 2 (control)
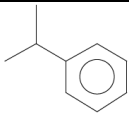
Compound No.	Formula	Structure (example)	Retention time /min	Name	Relative concentration %
1	C_9H_{12}		3.243, 3.577	Cumene	3.74
2	C_6H_6S		3.731	Benzenethiol	8.34
3	$C_{10}H_{14}$		5.087	Butylbenzene isomers	2.71
4	$C_9H_{12}S$		7.499, 9.029	Sulfide, propyl phenyl	22.01
5	C_9H_8S		10.359, 10.713	Methylbenzothiophene	17.05
6	$C_{10}H_8S$		12.958	Phenylthiophene	6.08
7	$C_{13}H_{12}$		13.687	Diphenylmethane	18.53
8	$C_{14}H_{14}$		15.785	Bibenzyl	9.11
9	$C_{12}H_{10}S$		17.456	Diphenyl sulfide	1.19
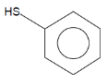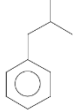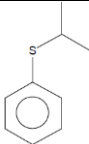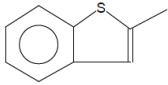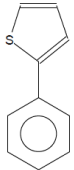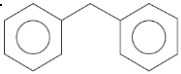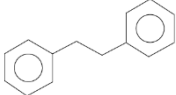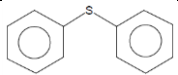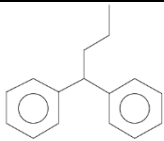
10	$C_{16}H_{18}$		18.718	Diphenylbutane	11.24

In **Table 7-8**, product 1 and 3 showed the cleavage of S-C bond and alkylation of propylene.

Table 7-9. GC-MS analysis of washes product 2 (control)

Compound No.	Formula	Structure (example)	Retention time /min	Name	Relative concentration %
1	$C_9H_{12}S$		7.793, 9.009	Sulfide, propyl phenyl	17.65
2	$C_{13}H_{12}$		13.687	Diphenylmethane	11.35
3	$C_{12}H_{10}S$		17.456	Diphenyl sulfide	71.00
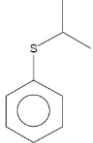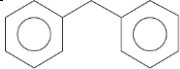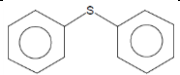
In **Table 7-9**, the number of component was less than **Table 7-8**. Most of compounds existed as direct generated liquid after reaction.

7.4 Discussion

Based on analyses above, the cleavage of S-C bond has been demonstrated. Though model compounds could stand for a simplified situation, the structure of the model compounds are different from the molecules in asphaltenes, which would result in different effects and results. In another word, it cannot be seen as proof that S-C bond cleavage in asphaltenes was responsible for all of the maltenes generated in the previous chapter. To better understand the interactions between asphaltenes, propylene and Siral40 in Chapter 6, it is very important to understand

model reaction deeply and clearly, e.g. figuring out the mechanism (carbon cation or free radical), based on the outcome of the model compound reactions. Thus, two control experiments were designed to compare with the model compound reaction of BPS.

If H_2S is generated in control experiment 1, then the S-C bond cleavage happens, which means propylene would be an unnecessary prerequisite. If H_2S is generated in control experiment 2, then the S-C bond cleavage happens, which means catalyst would be unnecessary prerequisite.

From the results in Table 7-3, it can be seen that propylene and Siral 40 are both unnecessary prerequisites for elimination of H_2S and at least some reaction takes place by a free radical mechanism.

However, since Siral40 was added in the reaction with model compound, there would be carbon cation based reactions besides the free radical reactions. One proof is that no propane was generated in control experiment 2, but in model compound reaction propane was found. The propane formation is due to hydrogen transfer, which could happen in presence of catalyst.

Thus, in reaction with model compounds, free radical and carbon cation mechanisms operated in parallel.

Propylene and Siral 40 are unnecessary prerequisites for S-C bond cleavage. Based on discussions above, **Figure 7-3** and **Figure 7-4** a reaction network for the free radical pathway of sulfur elimination and other reactions was proposed. The contribution of acid catalysis is shown only in step (4).
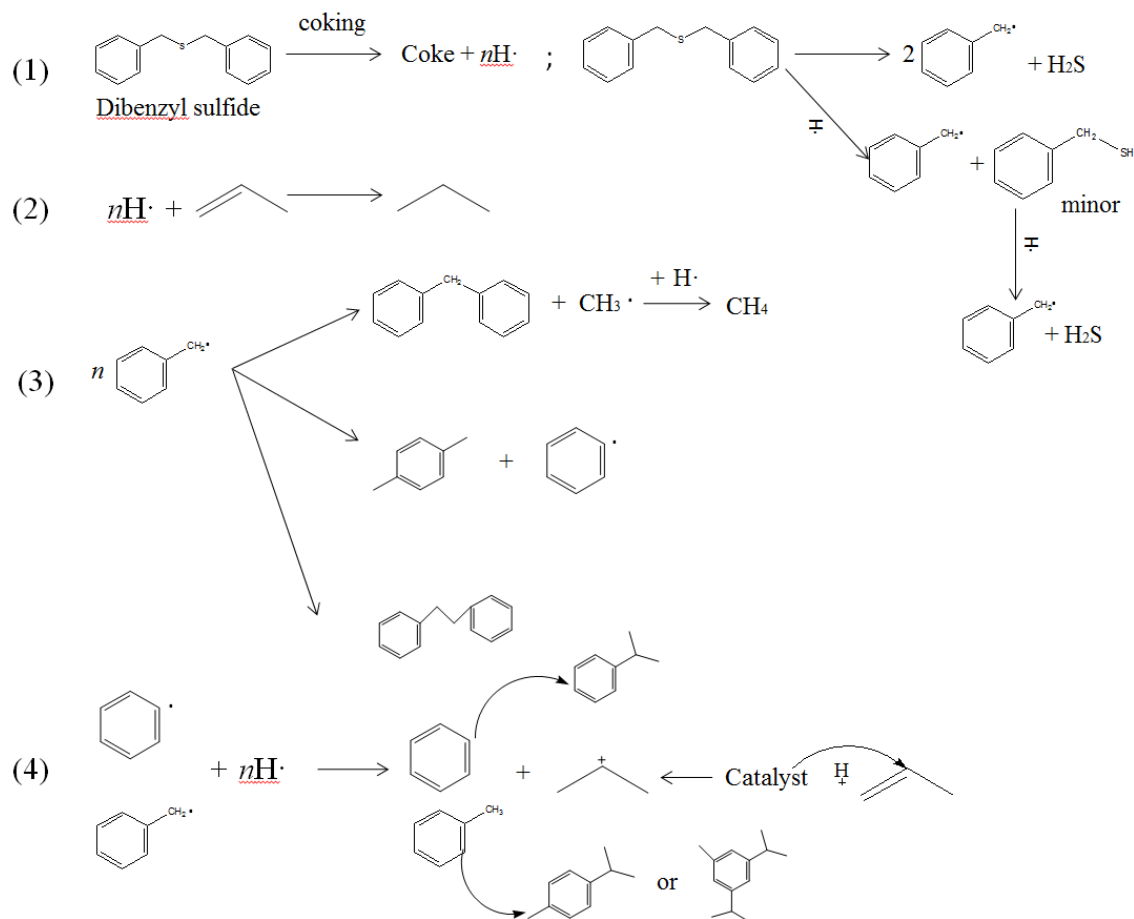
Figure 7-3. Reaction scheme of dibenzyl sulfide

For **Figure 7-3**, the step (1) to (4) may happen simultaneously during reaction. Dibenzyl sulfide facilitates hydrogen transfer, which may transfer hydrogen to propylene to convert it into propane and also change dibenzyl sulfide into coke. More likely the hydrogen transfer takes place on the acid catalyst. The presence of coke on the catalyst has already been verified by TGA. Also, thermal decompositions produces free radicals. Dibenzyl sulfide may also be subject to cracking to give free toluene radicals. Free radicals react with each other or stabilized by other radicals. Propylene was activated by acid sites on catalyst to form a propylene cation. Then it attacked stabilized compounds to do alkylation in the normal way.

Some of the reactions may also have been acid catalyzed. For example, the disproportionation reactions could be acid catalyzed.
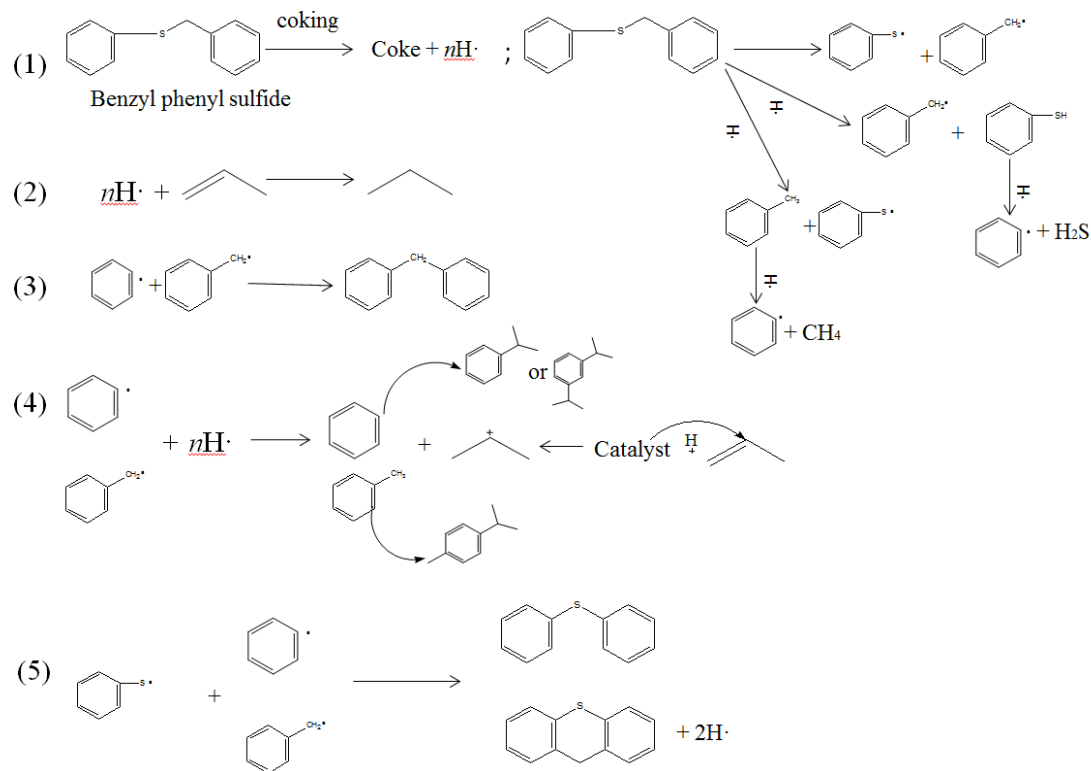
Figure 7-4. Reaction scheme of benzyl phenyl sulfide

In **Figure 7-4**, step (1) to (5) may happen simultaneously during reaction. Most of the reaction steps are similar to that in Figure 7-3. The main difference is that sulfur in benzyl phenyl sulfide is attached to the aromatic to form an aryl(C)–S bond. Eliminating sulfur is more difficult, which explains the presence of sulfur in the products.

Actually, propylene is not necessary based on two figures above. The bond cleavage would still take place without propylene.

7.5 Conclusion

- Two model compounds were 100% converted.

- Some reactants formed coke on the catalyst.

- The cleavage of sulfur-carbon bond was shown. After reaction, sulfur both existed in gas phase as H_2S and liquid phase products.

- Propylene reacted with two model compounds but it appears not to be a necessary prerequisite for C-S bond cleavage.

- Free radical reactions and acid catalysis contributed in parallel to the conversion of C-S bonds at the reaction conditions studied (325 °C).

Reference

1.   Kawai, H.; Kumata, F., Free radical behavior in thermal cracking reaction using petroleum heavy oil and model compounds. *Catal Today* **1998,** *43* (3-4), 281-289.

8. Quantification of aliphatic and aromatic sulfur species in asphaltenes

Abstract

Existence forms of sulfur in asphaltene were analyzed with tetrabutylammonium periodate as oxidant. The content of total sulfur was tested by CNHS. Aliphatic sulfur was converted into sulfoxide and tested by IR. Aromatic sulfur content was calculated.

Key words: sulfur existence, oxidation, asphaltene

8.1 Introduction

Removal of sulfur is important asphaltene upgrading. So knowing the nature of the functional groups of sulfur in asphaltenes becomes important. Generally, sulfur occurs in two major forms in asphaltenes: aliphatic sulfides such as linear and cyclic sulfides (thioethers) and aromatic sulfides such as thiophene and its benzologs.[1] Aliphatic sulfur is easier to be removed. In Chapter 6 and 7, it was suggested that the cleavage of sulfur-carbon bonds took place during acid catalysis and these bonds were likely aliphatic.

To investigate the relative content of aliphatic and aromatic sulfur, an improved method for sulfur characterization reported by Payzant et al.[2] was employed. The method is based on the ability to selectively oxidize only some sulfur groups. This mild oxidation convert most of the aliphatic sulfur without affecting the aromatic sulfur.[1]

Tetrabutylammonium periodate (TBAP) is the selective oxidant. The oxidant oxidizes aliphatic sulfur into sulfoxides, which have a strong IR absorbance near 1040 cm^{-1}, whereas thiols and sulfides have much weaker IR absorbance bands between 2600 to 2400 cm^{-1} and 705 to 570 cm^{-1} respectively. This method was employed with apparent success by Green et al.[3] and Gray et al.[1]

An industrial asphaltenes sample was oxidized using tetrabutylammonium periodate and the amount of aliphatic sulfur that was oxidized was quantified by IR. The total sulfur content of the asphaltenes sample was determined by CHNS analysis. The content of aromatic sulfur was calculated by the difference between total sulfur and aliphatic sulfur.

8.2 Experimental

8.2.1 Materials

The feed material is same as Chapter 3 Section 3.2.1. Methanol (99.8%) and toluene (≥99.5%) was commercially obtained from Fisher Scientific. Tetrabutylammonium periodate (≤100%) was purchased from Sigma-Aldrich. Diphenyl sulfoxide (96%) was purchased from Sigma-Aldrich. Water was obtained from a Millipore Milli-Q apparatus.

8.2.2 Experimental procedures

A Mettler Toledo ML 3002E balance was employed for weighing in this chapter.

Oxidation of asphaltene. 2.00 g asphaltenes was mixed with 36.56 g methanol, 203.32 g toluene and 2.00 g TBAP in flask and heated under reflux conditions for 1 h. Then the flask was cooled down to room temperature (~23ºC). The cooled product was transferred into separating funnel and extracted three times with 100 mL of high purity water per extraction, in order to remove TBAP and methanol. The number of extraction times was arbitrarily selected. After extraction, the oil phase was heated in a rotary evaporator to remove residual toluene and methanol. The instrument was Heizbad Hei-VAP purchased from Heldolph with water as heating medium. The water was heated to 55 °C. The system pressure was controlled at 33 kPa (absolute) for 30 minutes and then changed to 7.7 kPa (absolute) for 1 hour. After evaporation, the asphaltenes product was left in a fume hood for 2 days to dry. CHNS elemental analysis was performed on the dried asphaltenes product to measure the total sulfur content. Then 0.21 g dried product was dissolved in methylene chloride to form a 1 mL solution. The IR spectrum of the solution was recorded.

IR Calibration curve. A series of known concentration diphenyl sulfoxide in methylene chloride solution was tested by IR. The peak at 1041cm^{-1} was chosen to determine the transmittance associated with the sulfoxide. The concentration of diphenyl sulfoxide, experimentally determined transmittance, calculated absorbance, and sulfur (contained in diphenyl sulfoxide) is shown in **Table 8-1**. A linear relationship between the sulfur concentration in diphenyl sulfoxide and the absorbance at 1041 cm^{-1} was found as depicted in **Figure 8-1**.

Table 8-1. IR curve of diphenyl sulfoxide

	Diphenyl sulfoxide [con] g/1 mL	S [con] g/mL	Transmittance	Absorbance
No.1	0.030	0.0046	5.378	1.269
No.2	0.0070	0.0011	33.54	0.4745
No.3	0.049	0.0074	1.963	1.707
No.4	0.015	0.0023	13.51	0.8695

y=186.09x+0.3655
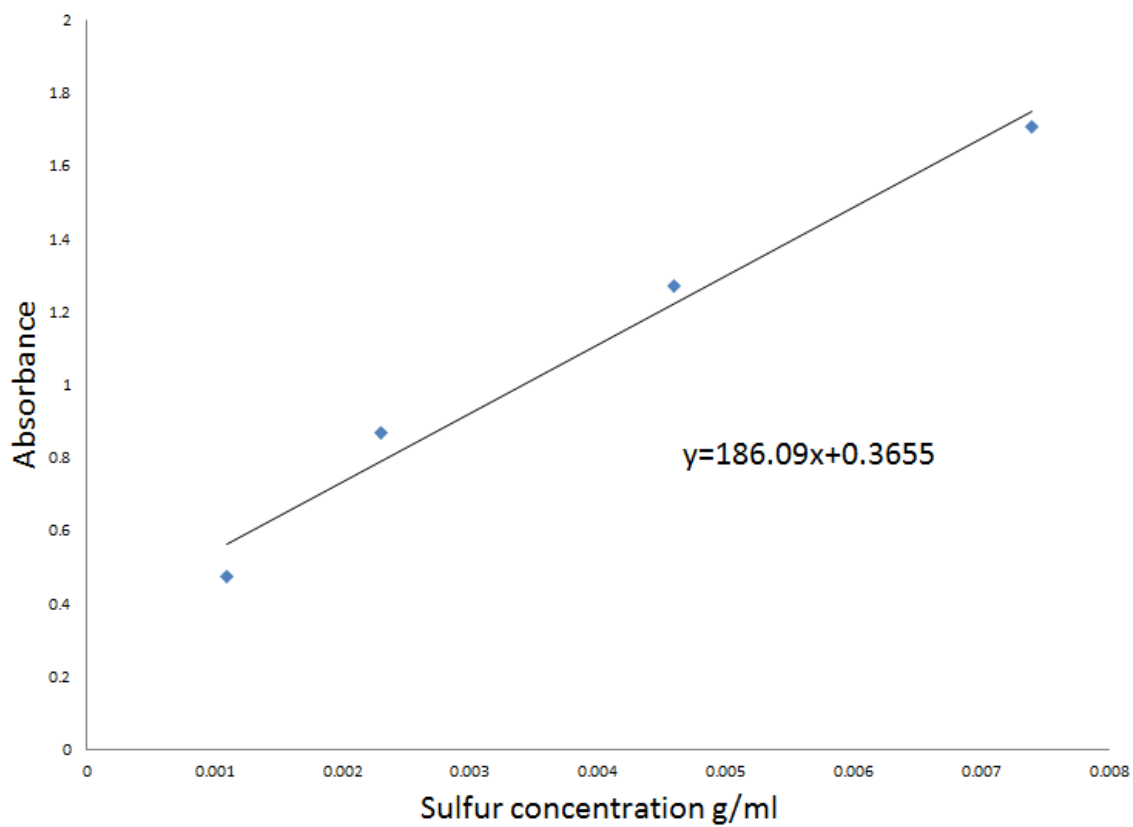
Figure 8-1. Calibration curve based on diphenyl sulfoxide

8.2.3 Analyses

IR(Infrared spectra). The instrument employed was an ABB MB 3000. The analysis parameters used were a resolution of 1 cm^{-1} and the spectrum was the average of 100 scans. The instrument was equipped with a liquid view cell with two Harrick ZnS 13×2mm windows and Harrick 0.63mm spacers (type MSP-630-M13).

8.2.4 Calculations

a) Absorbance is calculated as below by IR measured transmittance

$$Abs = \lg \frac{1}{T} \qquad \qquad \textbf{8.1}$$

where *Abs* is absorbance and T is transmittance

The concentration of S in mg/mL and *Abs* has a relation as below.

$$Abs = \varepsilon *[con]*l + Abs_0 \qquad \qquad \textbf{8.2}$$

Where ε is the coefficient of absorption, $mL*g^{-1}cm^{-1}$; [con] is concentration of sulfur in sulfoxide form, g/mL; l is light path, cm; Abs_0 is a constant absorbance.

8.3 Results and Discussion

The formula shown in **Figure 8-1** represents relationship between sulfur content in diphenyl sulfoxide and absorbance of peak at 1041cm^{-1} in diphenyl sulfoxide. The formula is written as *Abs*= 186.09[*con*] + 0.3655 in the form of **Equation 8.2**, where $\varepsilon*l$ is 186.09 and Abs_0 is 0.3655. So for a sample that contains sulfoxides, the sulfur (in sulfoxide form) concentration could be calculated if *Abs* of peak at 1041cm^{-1} is known.

0.21 g of the oxidized asphaltenes product was dissolved in methylene chloride to form a 0.21 g/mL solution. For the peak at 1041cm^{-1}, transmittance was measured as 1.48%. *Abs* was calculated as 1.83. By **Equation 8.2**, [con] was calculated to be 0.0078 g/mL. This means sulfur (in sulfoxide form) concentration was 0.0078 g/mL. The solution was 1mL. Thus, there was 0.0078 g sulfur in sulfoxide form in 0.21g asphaltenes product. It was aliphatic sulfur that was alkylated to sulfoxide. Thus, the mass percent of aliphatic sulfur was 3.7 wt%. Total sulfur

content was measured by CHNS test was 8.0 wt%. Therefore the aliphatic sulfur content of asphaltenes was about 46 wt% of the total sulfur.

In Chapter 6 it was shown that some asphaltenes to maltenes conversion during alkylation of asphaltenes with propylene over an amorphous silica-alumina catalyst could be explained in terms of scission of bridging C–S bonds. In Chapter 7 is was shown that sulfur bridges in model compounds were indeed severed under such reaction conditions. The work presented here showed that asphaltenes have a high aliphatic sulfur content, 46 wt%, some of which are likely in bridging in nature (i.e. sulfides), which supports the observations in Chapter 6.

8.4 Conclusion

- Aliphatic sulfur content in asphaltene was oxidized into sulfoxide and tested by IR. About 46 wt% aliphatic sulfur was found in the industrial asphaltenes, i.e. 3.7 wt% aliphatic sulfur and 8.0 wt% total sulfur in the asphaltenes.

- The amount of aliphatic sulfur present in the asphaltenes support the explanation of asphaltenes to maltenes conversion during reaction with propylene over an amorphous silica-alumina catalyst that is based on scission of bridging C–S bonds.

Reference

1.   Gray, M. R.; Ayasse, A. R., Kinetics Of Hydrodesulfurization Of Thiophenic And Sulfide Sulfur In Athabasca Bitumen. *Energy & Fuels* **1995,** *9* (3), 500-506.

2.   Payzant, J. D.; Mojelsky, T. W.; Strausz, O. P., Improved Methods for the Selective Isolation Of the Sulfide And Thiophenic Classes Of Compounds From Petroleum. *Energy & Fuels* **1989,** *3* (4), 449-454.

3.   Green, J. B.; Yu, S. K. T.; Pearson, C. D.; Reynolds, J. W., Analysis Of Sulfur Compound Types In Asphalt. *Energy & Fuels* **1993,** *7* (1), 119-126.

9. Hetero atom elimination study of Asphaltenes by ligand formation

Abstract

Zinc perchlorate hexahydrate has been employed in this chapter to form ligand with heteroatoms in asphaltenes. Although this is strictly speaking not alkylation, it builds on the concept of alkylation to effect a solubility transformation in asphaltenes.

Key words: ligand, asphaltene

9.1 Introduction

How to remove hetero atoms is an important topic in asphaltene upgrading. Asphaltenes contain heteroatoms such as sulfur, nitrogen and oxygen which are factors of asphaltene aggregation.

As mentioned in chapter 7, the cleavage of aliphatic S-C bond was suggested as an explanation of asphaltenes to maltenes conversion during alkylation. However, the cleavage of the C–S bond in aromatic forms is much more difficult than aliphatic C–S bonds.

Garner et al.[1] reported the effect of ligands on zinc alkoxide species (see **Figure 9-1**) and how it could interact with heteroatom containing groups. The compound ebnpa, or N-2-(ethylthio)ethyl-N,N-bis(6-neopentylamino-2-pyridylmethyl)amine, contains nitrogen in both aromatic forms and aliphatic forms, and sulfur in aliphatic form. These features are similar to asphaltenes structures. After adding $Zn(ClO_4)_2 \cdot 6H_2O$, ebnpa formed a ligand with Zn. Notably, in presence of water, the product $[(ebnpa)Zn-OCH_3]ClO_4$ forms an equilibrium mixture with the corresponding hydroxide complex. In $[(ebnpa)Zn-OCH_3]ClO_4$, oxygen, nitrogen and sulfur are all connected to Zn to form ligand. Inspired by this idea, if such a ligand form could be achieved in asphaltenes, both aliphatic and aromatic hetero atoms would connect with Zn. It would then in theory be possible to remove very heteroatom rich compounds from asphaltenes by aqueous phase extraction. If these compounds played a role in "binding" aggregates together, it would lead to some material in the asphaltenes becoming less aggregated and potentially maltenes.
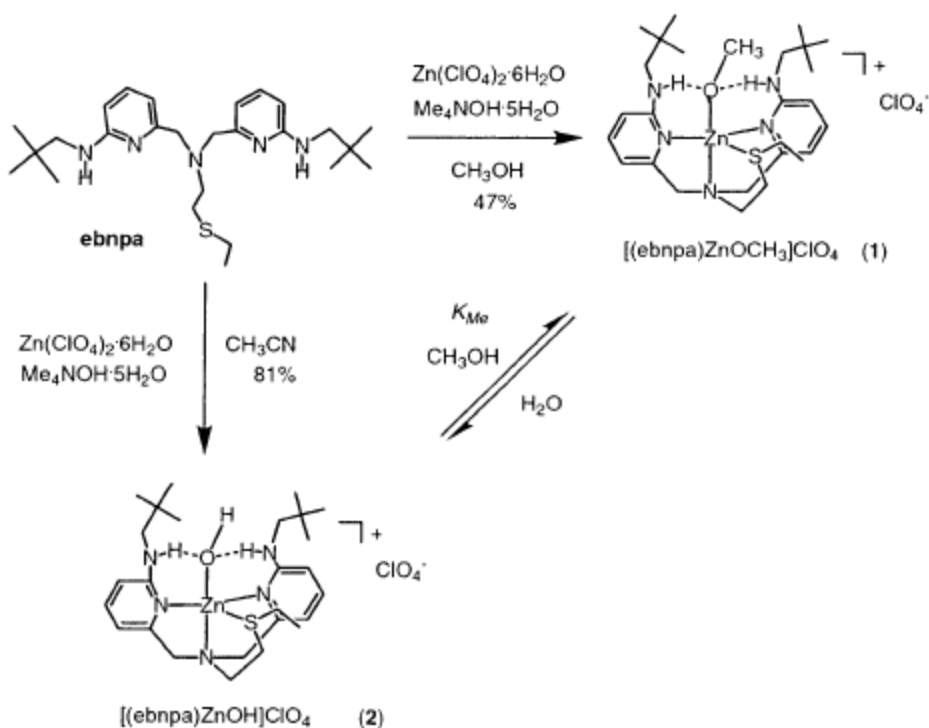
Figure 9-1. Reaction scheme published by Garner et al.[1]

Although metal-ligand interactions are strictly speaking not alkylation, the idea built on the general concept of using alkylation-like chemistry to change asphaltenes solubility behavior.

9.2 Experimental

9.2.1 Materials

The feed material, industrially precipitated asphaltenes, is the same as characterized in Chapter 3 Section 3.2.1.

Acetonitrile (99.9%), zinc perchlorate hexahydrate ($\leq$100%) and tetramethylammonium hydroxide pentahydrate ($\geq$97%) were purchased form Sigma-Aldrich. Water from a Milli-Q apparatus from Millipore was used.

9.2.2 Experimental procedures

All weighing operations were performed using a Mettler Toledo ML3002E balance, which has a maximum weighing capacity of 3200 g and readability of 0.01 g.

2.40 g asphaltene was mixed with 9.15 g $Zn(ClO_4)_2 \cdot 6H_2O$ and 153.40 g CH_3CN in a flask at room temperature (~23°C) while stirring for 30 min. Then 1.20 g $(CH_3)_4N^+(OH)^- \cdot 5H_2O$ was added into the flask and stirring was continued for another 21 hours. After reaction, acetonitrile and water were evaporated by rotary evaporator (type Heizbad Hei-VAP purchased from Heldolph) under 55 °C, 22 kPa and 6.5 kPa for 30 minutes each. The mass of evaporated solvent wasn't recorded. Then methylene chloride was added in the flask to dissolve the asphaltenes product. Next, the whole solution was filtered through a 0.22 μm filter paper. Liquid and solid phases were separated. The solid phase (residue) was the residual $Zn(ClO_4)_2 \cdot 6H_2O$ and $(CH_3)_4N^+(OH)^- \cdot 5H_2O$ after reaction, and potentially Zn-coordinated heteroatom rich asphaltenes (then objective of the treatment). The liquid phase was the asphaltene product in methylene chloride solution. The solid product was washed by methylene chloride again until no asphaltenes product could be washed out. The amount of used methylene chloride was not recorded. Then the methylene chloride was evaporated in rotary evaporator (Heizbad Hei-VAP) under 50 °C and atmospheric pressure to get the asphaltenes product. The asphaltenes product was then left in a fume hood for 2 days to dry. 1 g of the dried asphaltenes product was subjected to do *Lab Precipitated Asphaltene* procedure (refer to Chapter 3 Section 3.2.2).

9.2.3 Analyses

XRF The presence of Zn in the solids was determined by energy dispersive X-ray fluorescence (XRF) analysis with a Bruker S2 Ranger, with a silicon drift detector. The X-ray source uses a Pd target. The analyses were performed at 10 kV with total count rate in the order of 20,000 counts per second; no filters or secondary targets were employed.

CHNS, **IR** refer to Chapter 3 Section 3.2.3.

9.3 Results

9.3.1 Product yields

After reaction, 8.63 g solid residue was obtained. The treated asphaltenes material recovered from the liquid phases after solvent evaporation was 3.65 g. The total mass of products before reaction was 12.75 g and 12.28 g was recovered after reaction. The material balance was 96.3 %. It is likely that the mass loss was due to loss of crystal water.

After performing the *Lab Precipitated Asphaltene* procedure on 1 g of the treated asphaltenes material, 0.10 g maltene and 0.90 g precipitated asphaltenes were generated.

The asphaltene content was 90%, which was 12% higher than that in chapter 3 section 3.3.1. The total amount of precipitated asphaltenes after reaction was calculated as $3.65×0.90 = 3.28$ g. The amount of lab precipitated asphaltenes in the feed, i.e. "A" in Equation 3.1, was $2.40×0.78=1.87$ g. Based on the assumptions outlined the mass of lab precipitated asphaltenes after reaction was 1.41 g more than the asphaltenes content in the feed material.

9.3.2 Elemental analysis of asphaltenes product

Analyses were performed on the precipitated asphaltenes product from the *Lab Precipitated Asphaltene* procedure that was applied to the treated asphaltenes.

First, it was noticed that 2.40 g asphaltenes feed generated 3.65 g asphaltenes product. Following on the chemistry that was outlined (**Figure 9-1**), Zn coordinated with some molecules in the asphaltenes. If Zn was contained in precipitated asphaltenes product, then it would prove that Zn reacted with asphalenes, which would explain the increase in mass.

The presence of Zn was confirmed by XRF analysis. The analysis that was performed was only semi-quantitative and the amount of Zn is calculated as 0.1g by XRF.

Secondly, CHNS test was done to see the content of carbon, hydrogen, nitrogen and sulfur after reaction. The results were shown in **Table 9-1**.

Table 9-1. CHNS test of precipitated asphaltenes product after reaction

Element wt%	C	H	N	S
Precipitated asphaltenes product after treatment	68.17 ± 2.10	6.89 ± 0.14	1.14 ± 0.01	6.41 ± 0.13
Untreated asphaltenes (from Table 3-2)	82.54 ± 0.20	7.66 ± 0.18	1.14 ± 0.06	7.22 ± 0.39

The CHNS data of lab precipitated asphaltenes feed (from **Table 3-2)** was considered as blank to compare with the elemental analysis of the asphaltenes obtained after treatment (**Table 9-1**). The content of CHNS in the asphaltenes after treatment was lower (82.61 %) than the asphaltenes that were not treated (98.56 %), except for the nitrogen content. The mass percent of nitrogen was in the same range.

As mentioned above, the mass increased after reaction and Zn was found in the product. Even if mass of carbon, hydrogen, sulfur and nitrogen did not change or slightly increased after reaction, the mass percent would decrease due to the increased mass of Zn. In this case, the mass of nitrogen should definitely increase after reaction. This suggested asphaltenes gained nitrogen from other compounds. In this experiment, acetonitrile and tetramethylammonium hydroxide pentahydrate contain nitrogen. The source of increased nitrogen cannot be identified currently.

It can also be calculated based on the CHNS mass of the treated product relative to that of the untreated asphaltenes feed (82.62/98.56=0.838) that there was a change in the relative CHNS composition of the asphaltenes after treatment. There was a 1 % relative decrease in C (68.2 % found versus 0.838×82.54=69.2 %), 7 % relative increase in H (6.89 % found versus 0.838×7.66=6.42 %), and 6 % relative increase in S (6.41 % found versus 0.838×7.22=6.05 %).

9.3.3 Infrared analysis of the products

The IR spectra of the treated asphaltenes product is compared with that of the residue (**Figure 9-2**) and the lab precipitated asphaltenes feed (**Figure 9-3**). The lab precipitated asphaltenes feed was previously shown in Figure 3-2.
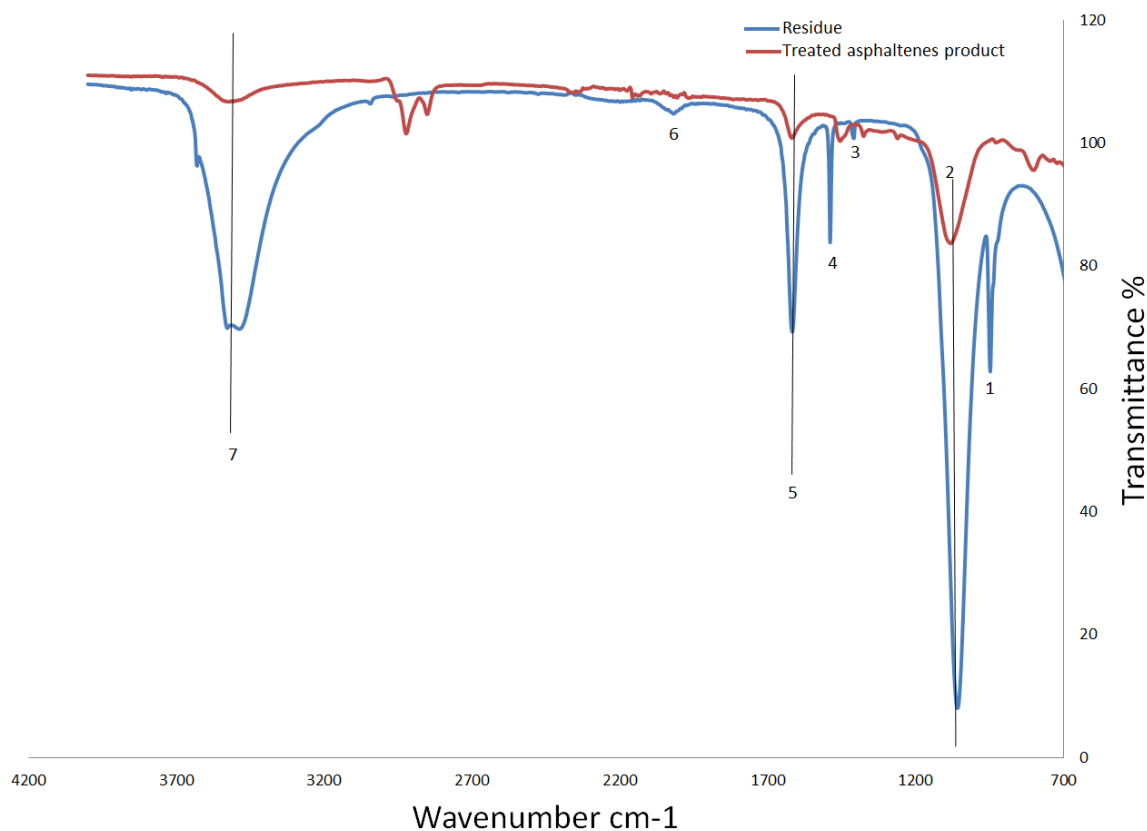
Figure 9-2. IR spectra of residue and treated asphaltenes product. Peak 1 at 945 cm^{-1}; peak 2 at 1065 cm^{-1}; peak 3 at 1434 cm^{-1}; peak 4 at 1500 cm^{-1}; peak 5 at 1618 cm^{-1}; peak 6 at 2020 cm^{-1}; peak 7 at 3540 cm^{-1}.

In **Figure 9-2** the most obvious feature of the residue compare to the treated asphaltenes spectrum, is the complete absence of the characteristic C-H absorptions around 3100 to 2800 cm^{-1}. This makes it unlikely that the residue contains any asphaltenic material. The residue is more inorganic in nature. Peak 2 is C-O vibration and peak 7 is O-H vibration. Specifically, peak 2 has previously been attributed as a tell-tale characteristic of metal–O–C bonds, as is found in metal carbonates for example.[2] It is noticed that the peak 7 in residue seems to be two overlaped small peaks which is different from treated asphaltenes product. This means –NH$_2$ group may also exist in residue. The two small peaks are caused by two N-H vibration.

94
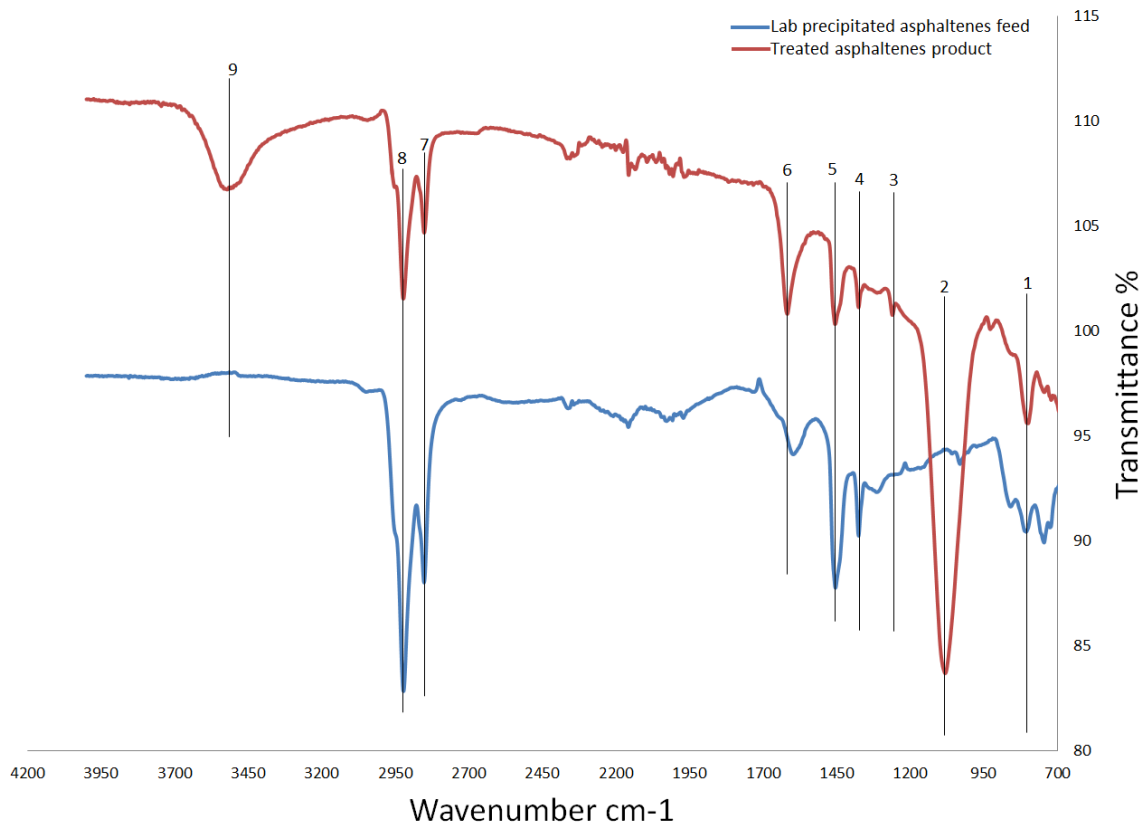
Figure 9-3. IR spectra of treated asphaltenes product and lab precipitated asphaltenes feed. Peak 1 at 808 cm^{-1}; peak 2 at 1065 cm^{-1}; peak 3 at 1263 cm^{-1}; peak 4 at 1373 cm^{-1}; peak 5 at 1450 cm^{-1}; peak 6 at 1614 cm^{-1}; peak 7 at 2852 cm^{-1}; peak 8 at 2923 cm^{-1}; peak 9 at 3540 cm^{-1}.

From 700 cm^{-1} to 900 cm^{-1}, the small peaks stand for aromatic C-H vibration. Less peaks were shown in treated product in range of 700 cm^{-1} to 900 cm^{-1}. In this case, the aromatic C-H bond was diminished after reaction. Peak 2 and 9 shows the difference which has been discussed above. The content of metal–O–C absorption is largely increased in treated asphaltenes product. Peak 4, 5 and 6 stand for aromatics in both asphaltenes samples.

Infrared spectroscopy support the observation by XRF that Zn is present in the treated asphaltenes product. It also indicated that asphaltenes were not detectable in the residue.

9.4 Discussion

The following information was obtained from the results: 1) The mass of asphaltenes in the treated product was more than asphaltenes in the feed; 2) Zn was found in the treated asphaltenes

product; 3) The precipitated asphaltenes content from the treated material was 90%, which was higher than that in the industrial asphaltenes feed.

So we can say that zinc perchlorate hexahydrate reacted with asphaltenes in a way. Based on the chemistry reported in literature,[1] the Zn coordinated to the heteroatom rich molecules in the asphaltenes. The nature of the interaction was not confirmed in this study. Anyway, the procedure neither converted asphaltenes into maltenes, nor washed parts of asphaltenes out.

9.5 Conclusion

- Zinc perchlorate hexahydrate reacted with asphaltenes and Zn was in asphaltenes after reaction.

- No asphaltenes was converted into maltenes or washed out.

References

1.   Garner, D. K.; Fitch, S. B.; McAlexander, L. H.; Bezold, L. M.; Arif, A. M.; Berreau, L. M., Mononuclear nitrogen/sulfur-ligated zinc methoxide and hydroxide complexes: Investigating ligand effects on the hydrolytic stability of zinc alkoxide species. *J Am Chem Soc* **2002,** *124* (34), 9970-9971.

2.   Hair, M. L. *Infrared spectroscopy in surface chemistry*; Marcel Dekker: New York, 1967, p. 207

10. Conclusions and recommendations

10.1 Conclusions

- Phosphoric acid, aluminium chloride, hydrochloric acid and amorphous silica alumina (Siral40) have been employed as acid catalysts for the alkylation of asphaltenes with olefins. Aluminium chloride and hydrochloric acid didn't show obvious alkylation of asphaltenes. Phosphoric acid increased asphaltenes H/C ratio and aliphatic/aromatic ratio after reaction, but in addition to alkylating the asphaltenes, phosphoric acid was also alkylated to the asphaltenes. Siral40 successfully catalyzed alkylation of asphaltenes with propylene, but was not successful in alkylating asphaltenes with ethylene.

- The most successful combination of catalyst and olefin for alkylating asphaltenes was the amorphous silica-alumina catalyst (Siral40) and propylene. Propylene reacted with asphaltenes over Siral40 to generate an increase in maltenes content. Asphaltenes were successfully converted into maltenes.

- All reactions with asphaltenes and olefins over Siral40 resulted in coking of the catalyst.

- Based on the hypothesis that the success of alkylation of asphaltenes by propylene over Siral40 could be attributed to the ability to cause scission of bridging carbon-sulfur bonds, this was further investigated by model compounds reactions. It was found that Siral40 in combination with propylene resulted in complete conversion of dibenzyl sulfide and benzyl phenyl sulfide, as well as near complete desulfurization of the reaction products from dibenzyl sulfide.

- An aliphatic sulfur content of ~40% was found in the industrially precipitated asphaltenes which comes from n-pentane deasphalting unit at the Nexen Energy ULC Long Lake Upgrader. The meaningful aliphatic sulfur content supported the hypothesis that the conversion of asphaltenes to maltenes by propylene over Siral40 could be attributed to scission of aliphatic carbon-sulfur bridges.

- Asphaltenes successfully coordinated with zinc in an attempt to selective removal of the most heteroatom rich compounds from the asphaltenes, but this did not lead to asphaltenes to maltenes conversion, or selective removal of material.

10.2 Recommendations

- The reaction of asphaltenes with hexene using a combination of aluminium chloride and hydrochloric acid appeared to convert some asphaltenes to maltenes, but inadequate material balance prevented firm conclusions to be drawn. This reaction is worthwhile investigating again.

- It would be clearer to understand reaction between asphaltenes and propylene over Siral40 if the directly generated maltenes in Chapter 6 was separated from the maltenes content at the very beginning and analyzed.

- Control experiments, e.g. Siral40, model compounds without propylene; model compounds, propylene without Siral40, are needed for confirming the reaction pathway of model compounds conversion in Chapter 7.

Bibliography

1.   Gray, M. R., *Upgrading oilsands bitumen and heavy oil*. First ed.; The University of Alberta Press Ring House 2: 2015.

2.   Sirota, E. B.; Lin, M. Y., Physical behavior of asphaltenes. *Energy & Fuels* **2007,** *21* (5), 2809-2815.

3.   Wiehe, I. A., A Solvent Resid Phase-Diagram for Tracking Resid Conversion. *Ind Eng Chem Res* **1992,** *31* (2), 530-536.

4.   Alvarez-Ramirez, F.; Ruiz-Morales, Y., Island versus Archipelago Architecture for Asphaltenes: Polycyclic Aromatic Hydrocarbon Dimer Theoretical Studies. *Energy & Fuels* **2013,** *27* (4), 1791-1808.

5.   Sabbah, H.; Morrow, A. L.; Pomerantz, A. E.; Zare, R. N., Evidence for Island Structures as the Dominant Architecture of Asphaltenes. *Energy & Fuels* **2011,** *25* (4), 1597-1604.

6.   de Klerk, A.; Gray, M. R.; Zerpa, N., Chapter 5 - Unconventional Oil and Gas: Oilsands. In *Future Energy (Second Edition)*, Letcher, T. M., Ed. Elsevier: Boston, 2014; pp 95-116.

7.   Wang, S. Q.; Liu, J. J.; Zhang, L. Y.; Masliyah, J.; Xu, Z. H., Interaction Forces between Asphaltene Surfaces in Organic Solvents. *Langmuir* **2010,** *26* (1), 183-190.

8.   Siskin, M.; Kelemen, S. R.; Eppig, C. P.; Brown, L. D.; Afeworki, M., Asphaltene molecular structure and chemical influences on the morphology of coke produced in delayed coking. *Energy Fuels* **2006,** *20* (3), 1227-1234.

9.   Melpolder, F. W.; Brown, R. A.; Young, W. S.; Headington, C. E., Composition Of Naphtha From Fluid Catalytic Cracking. *Ind. Eng. Chem.* **1952,** *44* (5), 1142-1146.

10.   Ipatieff, V. N.; Pines, H.; Homarewsky, V. I., Phosphoric acid as the catalyst for alkylation of aromatic hydrocarbons. *Ind. Eng. Chem.* **1936,** *28*, 222-223.

11.   Ipatieff, V. N., Catalytic, polymerization of gaseous olefins by liquid phosphoric, acid I. Propylene *Ind. Eng. Chem.* **1935,** *27*, 1067-1069.

12.   Ipatieff, V. N.; Pines, H.; Schmerling, L., Phosphoric acid as catalyst in the ethylation of phenol. *J. Am. Chem. Soc.* **1938,** *60*, 1161-1162.

13.   Bader, A. R., Cyclopentenylphenols. *J. Am. Chem. Soc.* **1953,** *75* (23), 5967-5969.

14.   Ipatieff, V. N.; Pines, H.; Friedman, B. S., Reaction of aliphatic olefins with thiophenol. *J. Am. Chem. Soc.* **1938,** *60*, 2731-2734.

15.   Pines, H.; Kvetinskas, B.; Vesely, J. A., Reaction Of Thiophene with Olefinic Compounds. *J. Am. Chem. Soc.* **1950,** *72* (4), 1568-1571.

16.   Harold Hart, E. A. H., Orientation in the phosphoric acid-catalyzed alkylation of ortho-cresol. *J. Org. Chem.* **1950,** *15* (2), 396-399.

17.   Ipatieff, V. N.; Komarewsky, V. I.; Pines, H., Phosphoric acid as a catalyst for the destructive alkylation of hydrocarbons. *J. Am. Chem. Soc.* **1936,** *58*, 918-919.

18.   Ipatieff, V. N.; Grosse, A. V., Action of aluminum chloride on paraffins - Autodestructive alkylation. *Ind. Eng. Chem.* **1936,** *28*, 461-464.

19.   Ipatieff, V. N.; Grosse, A. V.; Pines, H.; Komarewsky, V. I., Alkylation of paraffins with olefins in the presence of aluminum chloride. *J. Am. Chem. Soc.* **1936,** *58*, 913-915.

20.   Ipatieff, V. N.; Grosse, A. V., Polymerization of ethylene with aluminum chloride. *J. Am. Chem. Soc.* **1936,** *58*, 915-917.

21.   Ipatieff, V. N.; Komarewsky, V. I., The action of aluminum chloride on benzene and cyclohexane. *J. Am. Chem. Soc.* **1934,** *56* (7), 1926-1928.

22.   Hensen, E. J. M.; Poduval, D. G.; Magusin, P. C. M. M.; Coumans, A. E.; van Veen, J. A. R., Formation of acid sites in amorphous silica-alumina. *J. Catal.* **2010,** *269* (1), 201-218.

23.   Ali, M. A.; Tatsumi, T.; Masuda, T., Development of heavy oil hydrocracking catalysts using amorphous silica-alumina and zeolites as catalyst supports. *Appl. Catal. A* **2002,** *233* (1-2), 77-90.

24.   Perego, C.; Amarilli, S.; Carati, A.; Flego, C.; Pazzuconi, G.; Rizzo, C.; Bellussi, G., Mesoporous silica-aluminas as catalysts for the alkylation of aromatic hydrocarbons with olefins. *Micropor. Mesopor. Mater.* **1999,** *27* (2-3), 345-354.

25.   (a) Ipatieff, V. N.; Pines, H.; Friedman, B. S., Reaction of aliphatic olefins with thiophenol. *J Am Chem Soc* **1938,** *60*, 2731-2734; (b) Pines, H.; Kvetinskas, B.; Vesely, J. A., Reaction Of Thiophene with Olefinic Compounds. *J Am Chem Soc* **1950,** *72* (4), 1568-1571; (c) Ipatieff, V. N.; Pines, H.; Homarewsky, V. I., Phosphoric acid as the catalyst for alkylation of aromatic hydrocarbons. *Ind Eng Chem* **1936,** *28*, 222-223; (d) Ipatieff, V. N.; Komarewsky, V. I.; Pines, H., Phosphoric acid as a catalyst for the destructive alkylation of hydrocarbons. *J Am Chem Soc* **1936,** *58*, 918-919.

26.   ASTM D4530: *Standard test method forDetermination of Carbon Residue (Micro Method);* ASTM: West Conshohocken, PA, 2011.

27.   L. G. Wade, Jr., *Reactions of Aromatic Compounds,* Organic Chemistry, 5th Edition, Prentice-Hall, Upper Saddle River, NJ, 2003.

28.   Pieta, I. S.; Ishaq, M.; Wells, R. P. K.; Anderson, J. A., Quantitative determination of acid sites on silica-alumina. *Appl Catal a-Gen* **2010,** *390* (1-2), 127-134.

29.   Trombetta, M.; Busca, G.; Rossini, S.; Piccoli, V.; Cornaro, U.; Guercio, A.; Catani, R.; Willey, R. J., FT-IR studies on light olefin skeletal isomerization catalysis III. Surface acidity and activity of amorphous and crystalline catalysts belonging to the SiO(2)-Al(2)O(3) system. *J Catal* **1998,** *179* (2), 581-596.

30.   Finocchio, E.; Busca, G.; Rossini, S.; Cornaro, U.; Piccoli, V.; Miglio, R., FT-IR characterization of silicated aluminas, active olefin skeletal isomerization catalysts. *Catal Today* **1997,** *33* (1-3), 335-352.

31.   Xia, Y. Acid catalyzed aromatic alkylation in the presence of nitrogen bases. University of Alberta, 2012.

32.   de Klerk, A.; Nel, R. J. J., Phenol alkylation with 1-octene on solid acid catalysts. *Ind Eng Chem Res* **2007,** *46* (22), 7066-7072.

33.   Hensen, E. J. M.; Poduval, D. G.; Magusin, P. C. M. M.; Coumans, A. E.; van Veen, J. A. R., Formation of acid sites in amorphous silica-alumina. J Catal 2010, 269 (1), 201-218.

34.   Dolphin, D.; Wick, A. *Tabulation of infrared spectral data*; Wiley: New York, 1977, p. 486.

35.   Kawai, H.; Kumata, F., Free radical behavior in thermal cracking reaction using petroleum heavy oil and model compounds. *Catal Today* **1998,** *43* (3-4), 281-289.

36.   Gray, M. R.; Ayasse, A. R., Kinetics Of Hydrodesulfurization Of Thiophenic And Sulfide Sulfur In Athabasca Bitumen. *Energy & Fuels* **1995,** *9* (3), 500-506.

37.   Payzant, J. D.; Mojelsky, T. W.; Strausz, O. P., Improved Methods for the Selective Isolation Of the Sulfide And Thiophenic Classes Of Compounds From Petroleum. *Energy & Fuels* **1989,** *3* (4), 449-454.

38.   Green, J. B.; Yu, S. K. T.; Pearson, C. D.; Reynolds, J. W., Analysis Of Sulfur Compound Types In Asphalt. *Energy & Fuels* **1993,** *7* (1), 119-126.

39.	Garner, D. K.; Fitch, S. B.; McAlexander, L. H.; Bezold, L. M.; Arif, A. M.; Berreau, L. M., Mononuclear nitrogen/sulfur-ligated zinc methoxide and hydroxide complexes: Investigating ligand effects on the hydrolytic stability of zinc alkoxide species. *J Am Chem Soc* **2002,** *124* (34), 9970-9971.

40.	Hair, M. L. *Infrared spectroscopy in surface chemistry*; Marcel Dekker: New York, 1967, p. 207